universität wien

# DIPLOMARBEIT

Titel der Diplomarbeit

# Development of Novel Methodological Approaches to Detection and Quantitative Monitoring of Point-mutated Clones

angestrebter akademischer Grad

Magistra der Naturwissenschaften (Mag. rer.nat.)


| | |
|---|---|
| Verfasserin: | Sandra Preuner |
| Matrikel-Nummer: | 9520344 |
| Studienrichtung /Studienzweig | Diplomstudium Biologie/<br>Diplomstudium Genetik - Mikrobiologie |
| Diplomarbeit durchgeführt bei: | Prof. DDr. Thomas Lion,<br>Children´s Cancer Research Institute |
| Betreuerin: | Prof. Dr. Angela Witte,<br>Universität Wien |
| Wien, im | Juni 2010 |

# Contents

## Summary

In patients with chronic myeloid leukemia (CML), the occurrence of point mutations within the *BCR-ABL1* tyrosine kinase (TK) domain is currently the most common mechanism of resistance to therapy with TK inhibitors. To date a variety of different techniques to the detection of relevant point mutations is available. This mainly includes methods displaying a limited level of sensitivity e.g. bidirectional sequencing, the standard method of choice, providing a sensitivity of ~ 20%. However, the presence of cells carrying resistant mutations does not necessarily imply imminent disease progression. Mutation analysis by qualitative methods may therefore be insufficient to reliably identify clinically relevant resistant clones. To address this problem, an application permitting the detection of point mutated subclones of clinically relevant size and the additional option for quantitative analysis might be of great benefit. Thus the aim was to establish a technique combining both requirements. The newly developed LD-PCR relies on specific probe hybridization to mutant and wild-type sequences followed by ligation-dependent competitive PCR. Amplicons are detected and quantified via fluorescence-based capillary electrophoresis. Assays have been established for 21 common *BCR-ABL1* TK point mutations including M244V, L248V, V299L-C/T, G250E, Q252H-C/T, Y253F, Y253H, E255K, T315A, T315I, F317C, F317I, F317L-A/G, F317V, M351T, F359V, H396P and H396R. Moreover the technique is adaptive to any kind of point mutation as shown for the detection of V617F point mutation within the JAK2 gene, relevant for several myeloproliferative disorders. The LD-PCR assays display a detection limit of 1-5% and permit quantitative monitoring of mutant clones during the course of treatment. The applicability in CML patients undergoing treatment with TK inhibitors and the existence of kinetic proliferation of mutated cells clones could be demonstrated. Assessment of the size and proliferation kinetics of clones carrying specific mutations could therefore be instrumental in the clinical surveillance and therapeutic management of CML patients.

# Zusammenfassung

Bei Patienten mit chronisch myeloischer Leukämie (CML) ist das Auftreten von Punktmutationen in der *BCR-ABL1* Tyrosinkinasedomäne (TK) die am häufigsten beschriebene Ursache für Resistenzen gegen Tyrosinkinase-Inhibitoren (TKI). Für die Detektion von Punktmutationen ist eine Auswahl an Methoden verfügbar. Diese sind jedoch oft wenig sensitiv, wie zum Beispiel die Standardmethode der bidirektionalen Sequenzierung, mit einer Sensitivität von circa 20%. Das Auftreten von TKI resistenten Zellklonen muss jedoch nicht notwendigerweise mit einer bevorstehenden Progression der Krankheit assoziiert sein. Die Analyse von mutanten Zellklonen mit qualitativen Methoden könnte daher unzureichend sein, um klinisch relevante Klone zu identifizieren. Um diese Problematik bearbeiten zu können, wäre eine Methode von Vorteil, die die Detektion von Punktmutationen in einem klinisch relevanten Bereich mit der Möglichkeit zur Quantifizierung vereint. Solch eine Methode galt es zu entwickeln. Die neu etablierte LD-PCR Methode basiert auf der Hybridisierung spezifischer Sonden an die Wildtyp (WT) bzw. mutierte Sequenz gefolgt von einer ligations-abhängigen kompetitiven PCR. Die generierten Amplikons werden mittels Kapillarelektrophorese detektiert und quantifiziert. LD-PCR Assays wurden für folgende 21 häufig vorkommenden *BCR-ABL1* TK Punktmutationen etabliert: M244V, L248V, V299L-C/T, G250E, Q252H-C/T, Y253F, Y253H, E255K, T315A, T315I, F317C, F317I, F317L-A/G, F317V, M351T, F359V, H396P and H396R. Das Konzept der LD-PCR ist auf jegliche Punktmutation umlegbar, wie am Beispiel der Punktmutation V617V im JAK2 Gen, die bei myeloproliferativen Erkrankungen prognostisch bedeutend ist, gezeigt werden konnte. Die LD-PCR Assays haben eine Sensitivität von 1-5% und ermöglichen eine quantitative Überwachung während des Behandlungsverlaufs.

Die Anwendbarkeit dieser Methode bei CML Patienten unter TKI Behandlung konnte ebenso gezeigt werden wie das Vorhandensein einer Proliferationskinetik mutierter Zellklone. Die Dokumentation der Größe und der Expansion eines mutierten Zellklons könnte die Vorhersage einer

bevorstehenden Resistenz ermöglichen und bei der klinischen Überwachung sowie bei der Therapiesteuerung von CML Patienten hilfreich sein.

# 1 Introduction

## 1.1 Chronic myeloid leukemia (CML)

### 1.1.1 CML- Clinical features

Chronic myeloid leukemia is a clonal myeloproliferative disorder most commonly occurring in middle-aged and elderly patients with an incidence of one or two cases per 100 000 people every year [1]. Untreated, the disease proceeds in three phases: chronic phase (CP), accelerated phase (AP) and, finally, blast crisis (BC). Clinical features of chronic phase CML are often inconspicuous and most patients show only mild symptoms e.g. elevated white blood cell count, malaise, low-grade fever, anemia, thrombocytopenia and increased susceptibility to infections. At diagnosis, about 85% of all patients are in chronic phase CML and the diagnosis is often based on routine blood tests [2,3]. Regarded in detail, granulocytosis occurs and, additionally, is associated with a typical left shift of granulopoiesis [1] including less than 10% blast cells in bone marrow and blood [4]. Depending on the time point of diagnosis and the therapy applied, the chronic phase can last several months to several years.

Progression to accelerated phase is characterized by a blastic transformation [3] accompanied by a variety of clinical features, mainly including increasing myeloblasts up to ~ 20%, increasing white blood cell count and splenomegaly (specified in detail in [5,6].)

The last stage of CML is represented by a blast crisis which is comparable to a phenotype of acute leukemia. Within this phase, leukemic blast cells are present ≥ 30% in bone marrow or peripheral blood [3,5,6]. It can express lymphoid characteristics in about 1/3 of the cases, whereas 2/3 represent as acute myeloblastic or undifferentiated leukemia-like phenotype [3].

### 1.1.2 Molecular characteristics of CML

#### 1.1.2.1 Philadelphia chromosome and rearrangement of *BCR* and *ABL1* gene

CML was the first neoplastic disease associated with a chromosomal aberration. This cytogenetic abnormality results from the reciprocal translocation t(9;22) (q34;q11) [7] of the long arms of chromosome (Chr.) 9 and 22. Following translocation, two derivative chromosomes, an extra-long Chr. 9 and a shortened Chr. 22, the "Philadelphia (Ph) chromosome", are formed [8]. Latter was discovered by Nowell and Hungerford in 1960 [9].

On the molecular level, this translocation results in the rearrangement of two genes, *BCR* (breakpoint cluster region) located on Chr. 22 and *ABL1* (abelson) primarily located on Chr. 9., whereas the disease-relevant fusion gene is present on the Philadelphia chromosome, as depicted in Figure 1.

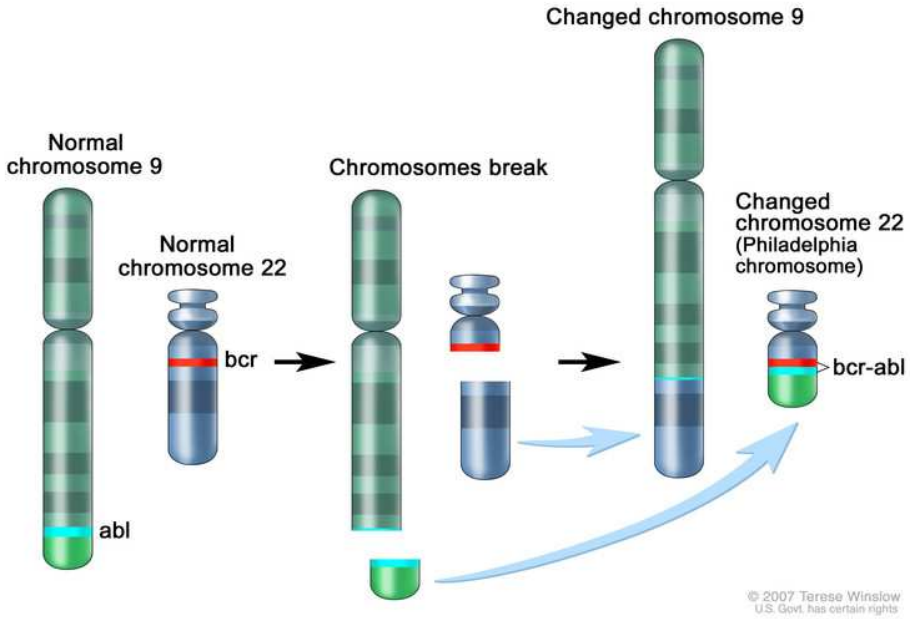


**Figure 1** [10] shows physiological chromosome 9 and 22 as well as the extra-long chromosome 9 and the shortened chromosome 22 (Philadelphia chromosome) present after the reciprocal translocation event.

The physiological *ABL1* gene belongs to the family of nonreceptor tyrosine kinases (TKs) [11-13]. TKs transfer phosphate groups from its donor ATP to tyrosine residues on specific cellular proteins, which are mainly involved in cell proliferation and differentiation [13].
Cellular functions of the *BCR* gene are still ambiguous at the moment. However, a tyrosine residue at amino acid (AA) position 177 (Tyr 177) plays an important role: when phosphorylated in the rearranged *BCR-ABL1* gene, it is a critical anchor for Grb-2, an important adapter molecule within the RAS pathway [13,14], referred to later on.
The juxtaposition of parts of both genes results in fusion transcripts that encode for a constitutively active tyrosine kinase and this mechanism was identified as significant in the pathogenesis of CML [15,16].
Breakpoints within the *ABL1* gene mostly occur in a region of ~ 200 kb between exons 1a and 1b. In case of the *BCR* gene, three prominent breakpoint regions are described: Mbcr (major breakpoint cluster region), a region between exons e12 and e16, mbcr (minor breakpoint cluster region) between exons e1 and e2 and µbcr (µ breakpoint cluster region) located downstream of exon 19 [8].

In either case, *ABL1* exon 2 (a2) represents the fusion partner for the exon acquired from the *BCR* gene. For major *BCR-ABL1*, alternative splicing gives rise to two fusion transcripts: b2a2 or b3a2, both translated into a fusion protein of 210 kDa ($p210^{BCR-ABL1}$) [17] which is found in the great majority (≥ 95%) of CML patients and in about 30% of Ph+ acute lymphoblastic leukemia (ALL) cases [18]. The e1a2 transcript is expressed in case of minor *BCR-ABL1*, resulting in a protein of 190 kDa ($p190^{BCR-ABL1}$) which is present in ~ 70% of Ph+ ALL cases but is only infrequently found in CML. A protein of 230 kDa ($p230^{BCR-ABL1}$) is encoded by the fusion transcript e19a2 which is associated with chronic neutrophilic leukemia, a mild form of CML, but is rarely found in CML and Ph+ ALLs.

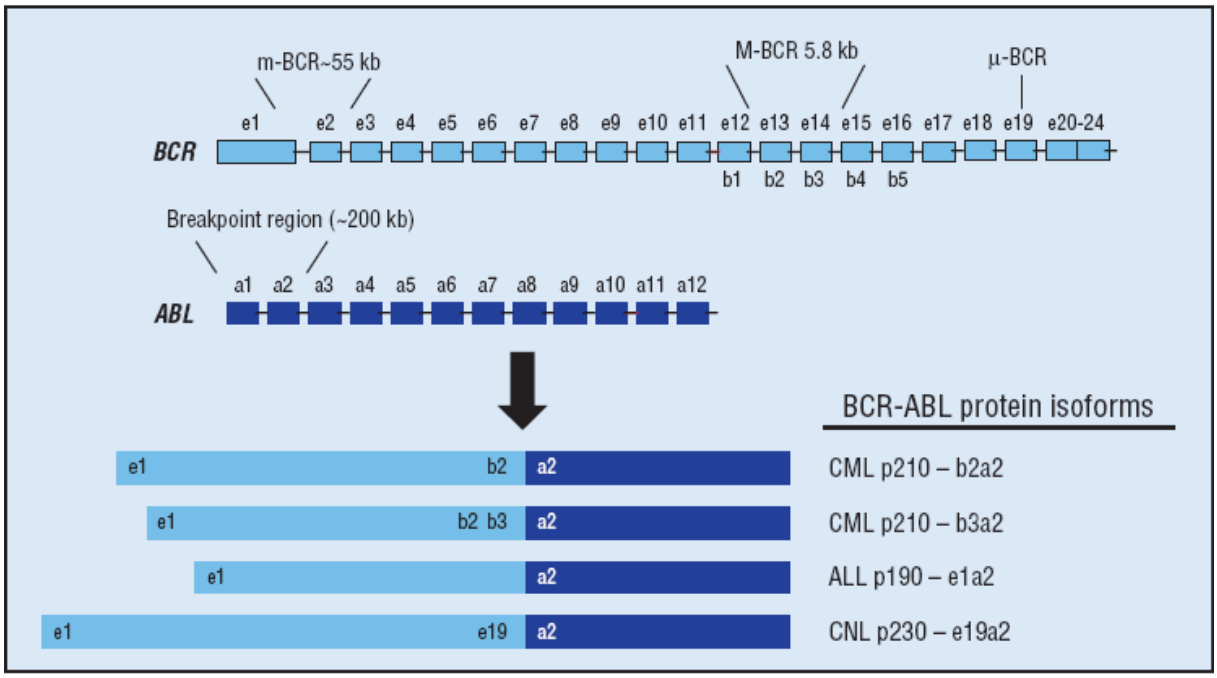


**Figure 2** [8] shows the arrangement of exons within the *BCR* and *ABL1* gene as well as the respective breakpoint regions described above. The predominantly occurring *BCR-ABL1* rearrangements and resulting BCR-ABL1 protein isoforms are depicted below.

#### 1.1.2.2 Functional domains within the BCR-ABL1 protein

As displayed in Figure 3, the rearranged part of the *BCR* gene is located at the N-terminal site of the fusion protein and contributes three important domains: a coiled-coil oligomerization domain, which allows constitutive oligomerization and promotes constitutive trans-phosphorylation [19]; a serine/theronine kinase domain including Tyr 177; and a guanine-nucleotide exchange factor homology domain [8,20]. The adjacent domains are part of the ABL1 protein and contain: a highly conserved Src-homology-2 (SH2) domain, a tyrosine kinase domain (TKD), three prolin-rich domains functioning as binding sites for downstream signalling adapter proteins, three nuclear localizations signals (NLS), a DNA-binding domain, an actin-binding domain and a nuclear export signal (NES) [8,20].

Via its N-terminal oligomerization domain, BCR-ABL1 monomers form an antiparallel dimer that stacks to form a tetramer [20,21]. This altered protein complex has a significant impact on signal transduction and a dramatic effect on the cellular level emerging as CML.

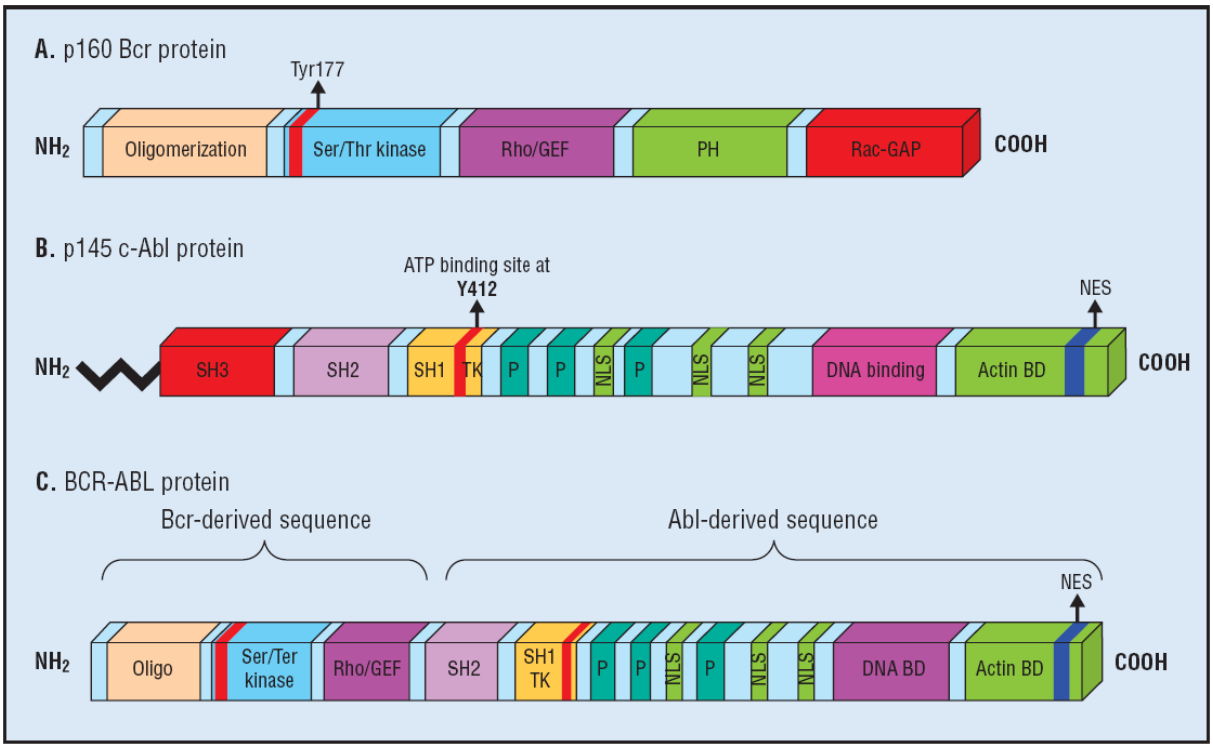


**Figure 3.** [8] (A) The functional domains of the physiological BCR protein include an oligomerization domain at the N-terminal end, a serin/theronine (Ser/Thr) kinase domain containing the critical Tyr residue at AA position 177, a Rho/GEF domain, a pleckstrin homology (PH) domain and a RAS related C3 botulinum toxin substrate (RAC) guanosine triphosphatase-activating protein domain (GAP). (B) As a result of alternative splicing the ABL1 protein shows two alternative exons (1b and 1a) at its N-terminal end. ABL1b is expressed at higher levels and contains a covalently linked C14 myristoyl moiety at the N-terminal position in contrast to ABL1a [20]. This is followed by an SH3 and SH2 domain and the TK domain (SH1 TK) containing the ATP binding site at Y412 and the transautophosphorylation site at Tyr residue 1294 [13]. The second part is assembled by three prolin-rich domains (P), three nuclear localization signals (NLS), a DNA binding domain (DNA BD), and an actin binding domain (Actin BD) including a nuclear export signal (NES). (C) The BCR-ABL1 fusion protein contains parts of the BCR and ABL1 protein.

#### 1.1.2.3 BCR-ABL1 signal transduction

The chimeric BCR-ABL1 fusion protein represents the origin for a network of altered, enhanced or blocked signalling pathways. Many participating/ connecting molecules and proteins have been identified so far, however, the full signalling network might not be elucidated yet. Within this chapter, the focus will be on a limited number of downstream signalling pathways involved.

Oligomerization of BCR-ABL1 proteins is the first important event for the formation of tetramers and facilitates transautophosphorylation at Tyr 1294, which is followed by phosphorylation of Tyr 177 located within the BCR-derived section. The phosphorylated Tyr 177 is an important high-affinity binding site for Grb2 (growth receptor-bound protein 2), which recruits and binds SOS (son of sevenless). SOS activates RAS (rat sarcoma) and its downstream molecules via guanine-nucleotide exchange. This results in the transcription of genes contributing to cell proliferation and transformation [22]. Additionally, Grb2 activates GAB2 (GRB2-associated binding protein 2), which induces a constitutive activation of PI3K (phosphatidylinositol 3-kinase)/AKT [20,23].

Alternatively, BCR-ABL1 directed activation of PI3K/AKT appears to occur via phosphorylation of CRKL (v-crk avian sarcoma virus CT10 oncogene homolog-like), the most abundant phosphorylated protein in CML neutrophils [13] and subsequently via CBL (Casitas B-linage lymphoma).
AKT, a downstream target of Pi3K, activates a plethora of target molecules promoting cell survival [8] which mainly includes FoxO proteins, Bad (BCL2 antagonist of cell death) and GSK3ß (glycogensynthase kinase 3ß). Unphosphorylated, Bad can bind to anti-apoptotic Bcl-2 family members (Bcl-xL), replacing Bax, which subsequently can induce permeabilization of the outer mitochondria membrane and activates caspases and apoptosis. In contrast, phosphorylated Bad is sequestered by 14-3-3 in the cytosol. This prevents the release of Bax and thus lowers the induction of apoptosis [8].

Moreover, activated AKT induces increased transcription of *MYC* and prevents the MYC protein from degradation by inhibiting its degrading enzyme GSK3ß [20].

Other important BCR-ABL1 target proteins are HCK and LYN, members of the SCR kinase family. Phosphorylated via BCR-ABL1, they recruit STAT5 (signal transducer and activation of transcription 5), which enhances cyclin D1 transcription, leading to cell-cycle progression from G1 to S-phase [20]. While anti-apoptotic *BCL-X* genes are activated by STAT5, an additional player ICSBP (interferon consensus sequence binding protein) represses *BCL-X* genes. It is assumed that BCR-ABL1 indirectly inactivates *ICSBP* transcription and thereby contributes to increased survival of myeloid progenitor cells [20].

This summary gives a limited overview of BCR-ABL1 mediated and altered signal transduction processes. Finally, the aberrant signalling cascades mainly result in proliferation, transformation and survival of the *BCR-ABL1* positive leukemic cell, altered adhesion, as well as prevention of apoptosis.

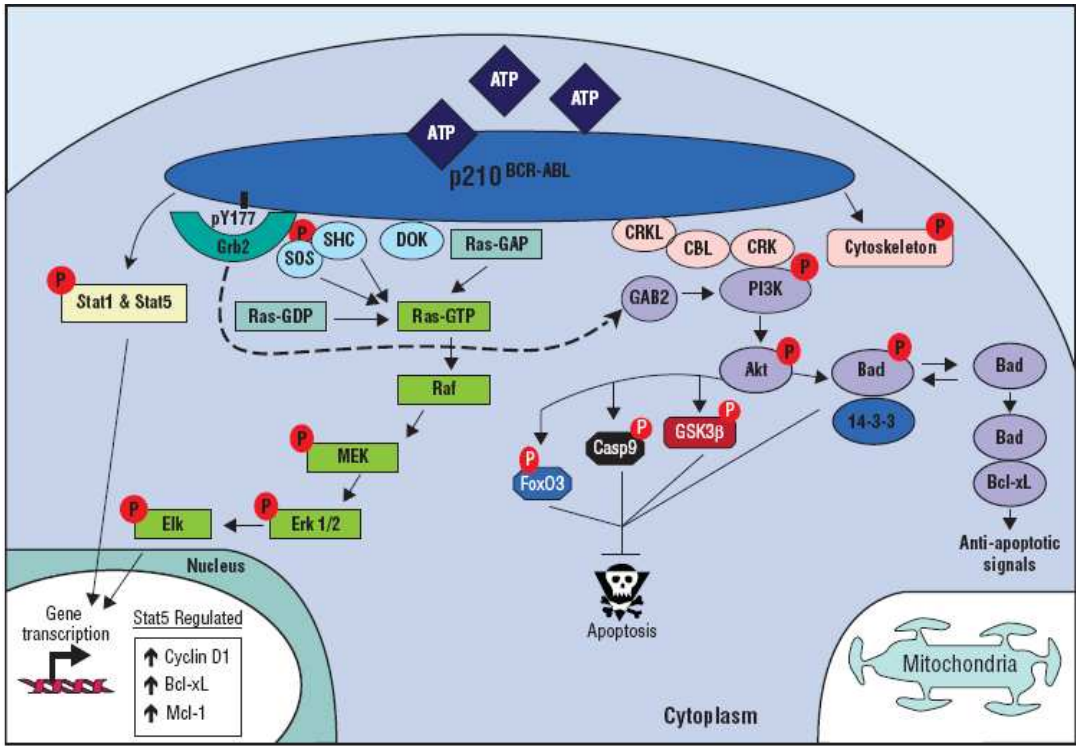


**Figure 4.** [8] **Part of BCR-ABL1 mediated signalling pathways.**

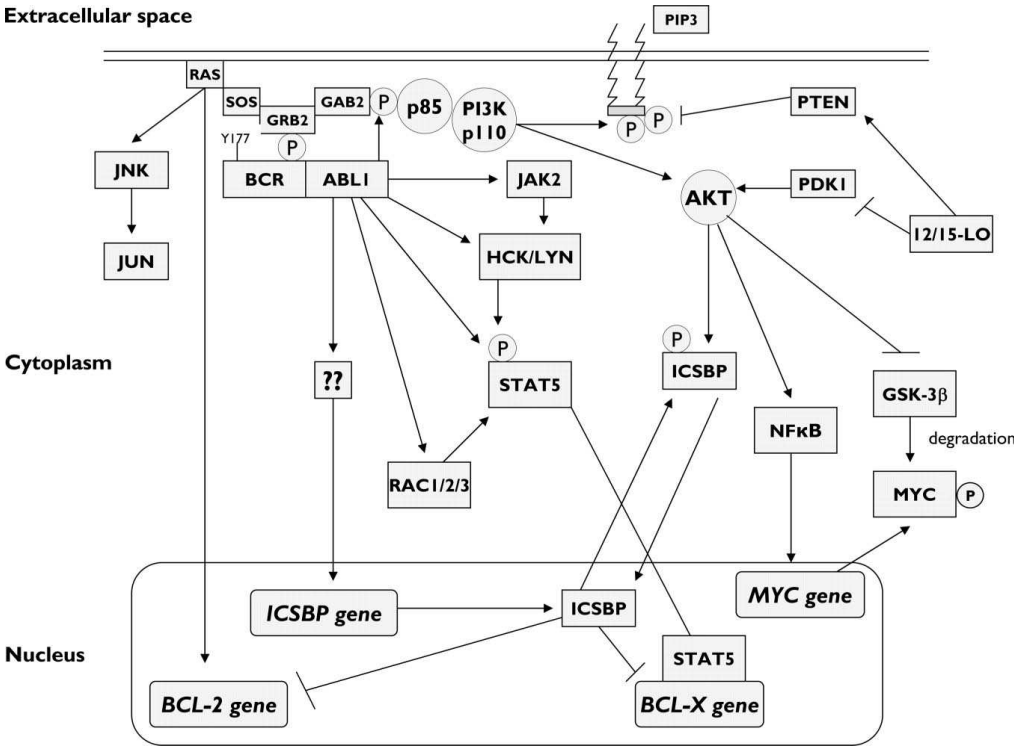


**Figure 5.** [20] **Part of BCR-ABL1 mediated signalling pathways.**

### 1.1.3 CML – evolutional steps

Concerning the issue of CML evolution, many questions are still not answered. However, several observations provide the basis for a rational hypothesis published by Valent et al. in 2008 [24].

Starting at the level of normal hematopoietic stem cells, these cells might be subjected to first mutagenic events, giving rise to premalignant subclones lacking the *BCR-ABL1* rearrangengement. This assumption is based on the findings of *BCR-ABL1* negative, but clonal populations of leukemic subclones in imatinib treated patients with Ph+ CP CML [24-26]. Following hits might introduce the reciprocal translocation event in Chr.9 and Chr.22 attended by the fusion of *BCR* and *ABL1* genes within the premaligant stem cell.

It is discussed whether a *BCR-ABL1* positive but clinically silent phase of CML might follow, since *BCR-ABL1* was already detected in apparently healthy individuals. Accordingly, besides the presence of *BCR-ABL1*, additional genetic events might be necessary for the transformation to the chronic phase (CP) of CML. Within CML CP, the BCR-ABL1 oncoprotein, however, might be the most important parameter providing the basis for proliferation and inhibition of apoptosis via aberrant signalling, as already discussed.

In addition to increased expression of *BCR-ABL1*, progression to blast phase via accelerated phase might require further hits. This includes additional chromosomal abnormalities e.g. trisomy eight, isochromosome 17 or duplication of Ph chromosome; inactivation of tumor suppressor genes e.g. *p53* and *INK4A/ARF*; incorrect DNA repair, and genomic instability and arrest of differentiation by the impairment of appropriate transcription factors [20].

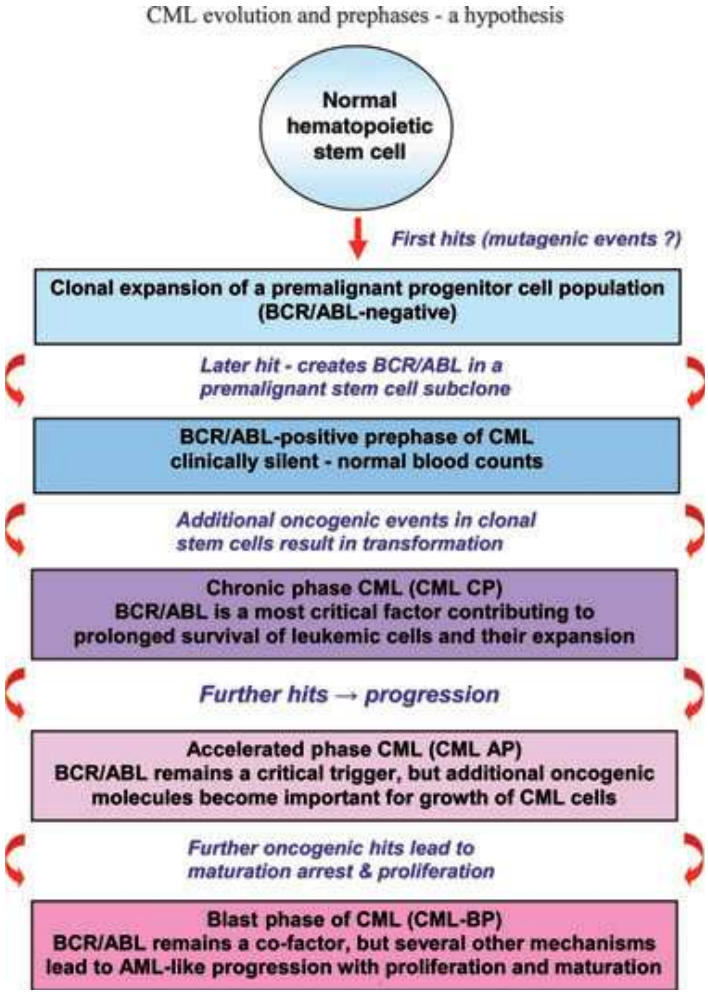


**Figure 6** [24] gives an overview of a potential hypothesis for CML evolution.

### 1.1.4 Therapy concepts in CML

Recombinant interferon-α, which mobilizes the immune system against leukemic cells was regarded as a standard therapy in CML patients prior to the era of tyrosine kinase inhibitors (TKIs). It was shown to be more effective than chemotherapy based on busulfan or hydroxyurea [27]. Interferon-α prolonged life in patients of all ages, however the occurrence of severe side effects e.g. flu-like symptoms, sickness, weight loss and depression were main drawbacks in clinical practice [1].

#### 1.1.4.1 Imatinib mesylate

The development and application of small molecule TKIs was first implemented in CML. This concept of targeted therapy was successful using a compound developed by Novartis Pharmaceuticals: TKI STI571 (imatinib, Gleevec®). The drug inhibits three species of tyrosine kinases: ABL1, PDGFR α and β (platelet derived growth-factor receptor) and KIT. In case of ABL1 TK, the concept relies on the specific binding of imatinib to the ATP-binding pocket of the constitutively active TK. Thus the access of ATP is prevented and phosphate residues required for the activation of downstream target molecules (substrate) are not available.

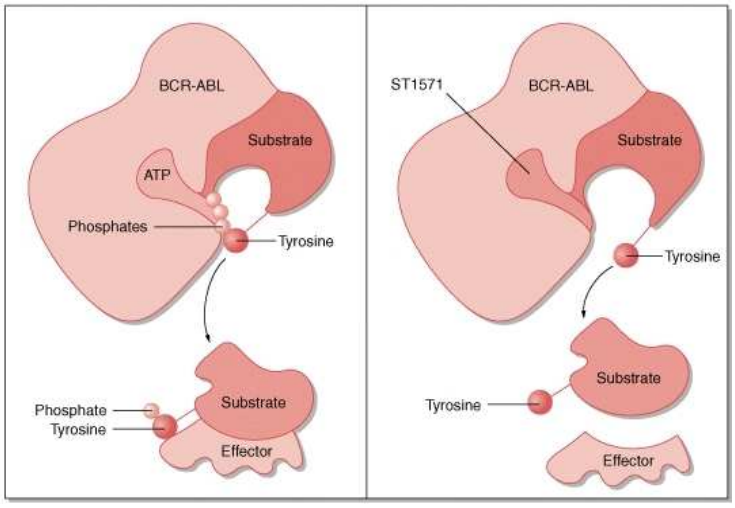


**Figure 7.** [28] Imatinib - mode of action.

The ABL1 kinase three-dimensional structure provides the basis for understanding the underlying imatinib mechanism. The TK consists of different parts: N-terminal lobe, ATP-binding domain (p-loop), activation loop, catalytic loop and C-terminal lobe. Imatinib is designed to bind to the p-loop region, as already mentioned, but only in case of an inactive TK conformation (activation loop is closed). Moreover it has been shown that binding of an imatinib analogue inside ABL1 is only partly superimposable over that of ATP [29]. This observation suggests, that imatinib blocks the kinase activity by stabilizing a unique inactive conformation of ABL1, rather than directly competing with ATP for binding to the active site [29,30]. Overall, imatinib prevents BCR-ABL1 autophosphorylation, interferes with TK activation and blocks downstream signal transduction [31].

The success of imatinib treatment in newly diagnosed CP CML patients was first presented in the Phase III IRIS (International Randomized Study of Interferon and STI571) trial [32]. Within this study, imatinib was compared to INFα- and cytarabine. Results, in summary, showed that after a median follow up of 19 months, imatinib was significantly better than INFα- treatment, with rates of complete hematologic responses (CHR) of 95% and 56%, a major molecular response (CCgR ≤ 35% Ph+ cells) of 85% and 22% and superior results concerning progression-free survival and major molecular response [32]. Based on its superior performance and minor side effects, imatinib is regarded as the standard first-line therapy today [33].

#### 1.1.4.2 Resistance to imatinib

Resistance to imatinib can be defined based on hematologic, cytogenetic or molecular parameters [34,35] and it can occur in primary and secondary instance. Patients with primary resistance show a lack of hematologic or cytogenetic response to initial imatinib therapy whereas patients with secondary resistance lose their initial response during the course of treatment [34].

Several mechanisms responsible for imatinib resistance have been identified and described so far:

**i)** Overexpression of BCR-ABL1 protein is a phenomenon observed in about 18% of CML patients [29,36] and results from *BCR-ABL1* gene amplification. The therapeutic dose of imatinib thus fails to inhibit the increased amount of BCR-ABL1 protein [37].

**ii)** Sufficient imatinib plasma levels are essential for a clinical response to imatinib. In this regard, drug influx and efflux mechanisms play an important role. Overexpression of the *MDR1* encoded glycoprotein, an energy dependent efflux pump, results in decreased imatinib plasma levels and is described to account for imatinib resistance [38]. The same seems to hold true for the drug efflux pump BCRP/ABCG2 [37]. The human organic cation transporter-1 (OCT-1) was described as the influx pump responsible for imatinib transport into the cell. Studies performed in pre-therapy CML patients showed that high OCT-1 activity was associated with an excellent molecular response, independent of the imatinib dosage, whereas response of patients with low OCT-1 activity was highly dose dependent [39].

**iii)** Genomic instability associated with clonal evolution and the activation of additional transformational pathways present further opportunities for imatinib resistance [40]. This is mainly associated with defects of DNA repair mechanisms described to contribute to the progression of CML to advanced stages [20].

**iv)** It has been observed, that imatinib is not able to enter all organ sites. Most importantly this is described for the central nervous system because the drug cannot cross the blood-brain barrier [41,42] It is assumed that this is attributable to the MDR1-mediated efflux of imatinib [43].

**v)** Point mutations within the *BCR-ABL1* TK domain account for the majority of imatinib resistant cases. Since this issue represents the theoretical basis for this diploma thesis, it will be discussed in detail within the next section.

### 1.1.5 Point mutations within the *BCR-ABL1* tyrosine kinase domain

In case of imatinib, resistance is associated with *BCR-ABL1* TK point mutations in 40-90% of cases, dependent on the CML phase, the methodology of detection and the definition of resistance [44]. The substitution of a single base can result in the exchange of an affected amino acid (AA). Referring to the nomenclature, the first letter indicates the AA within the wildtype (WT) sequence, the number shows the affected AA position within the TK domain and the second letter indicates the resulting AA within the point mutated sequence e.g. for T315I , the threonine residue at AA position 325 changes to isoleucine.
Depending on the position of the exchanged nucleotide, *BCR-ABL1* TK point mutations can be clustered into four main groups as comprehensively reviewed [29,45]; an overview is displayed in Figure 8.

Mutations within the imatinib binding site: affected nucleotides are directly interacting with imatinib, either via hydrogen bonds, as in case of T315, or via Van der Waals´ interactions as described for V289, T315 and F317. T315I is considered as the most important point mutation since the AA occurs in the so called, “gatekeeper” position [45]. If T315 is mutated to isoleucine, an important hydrogen bond is lost, preventing the interaction of BCR-ABL1 with imatinib [46]. Additionally, the isoleucine chain is bulkier and sterically hinders imatinib binding [45]. This results in complete insensitivity to imatinib as well as to second generation TK inhibitors. Cortes et al. [47] showed that about 15% of *ABL1* TK point mutations associated with imatinib failure originate from T315I.

Mutations within the ATP-binding loop (P-loop, AA 248-255 of *ABL1* TK domain [48]): G250E, Y253F, Y253H, E255K and E255V are examples for point mutations described within this region and they are described to be associated with higher levels of resistance to imatinib [30,40,49]. Moreover, it is discussed that p-loop mutations are associated with a poorer prognosis [50], however this is still not entirely clear at the moment [51].

Mutations within the activation loop (AA 381-402): prevent the kinase from adopting the inactive conformation to which imatinib can bind [20]. L387M, H396R and H396P are described to show impaired imatinib sensitivity [49].

Mutations outside from the imatinib binding site: include changes within the catalytic domain (AA 350-363) e.g. F359V or M351T and other sites e.g. residue Q459 or F486 [20].

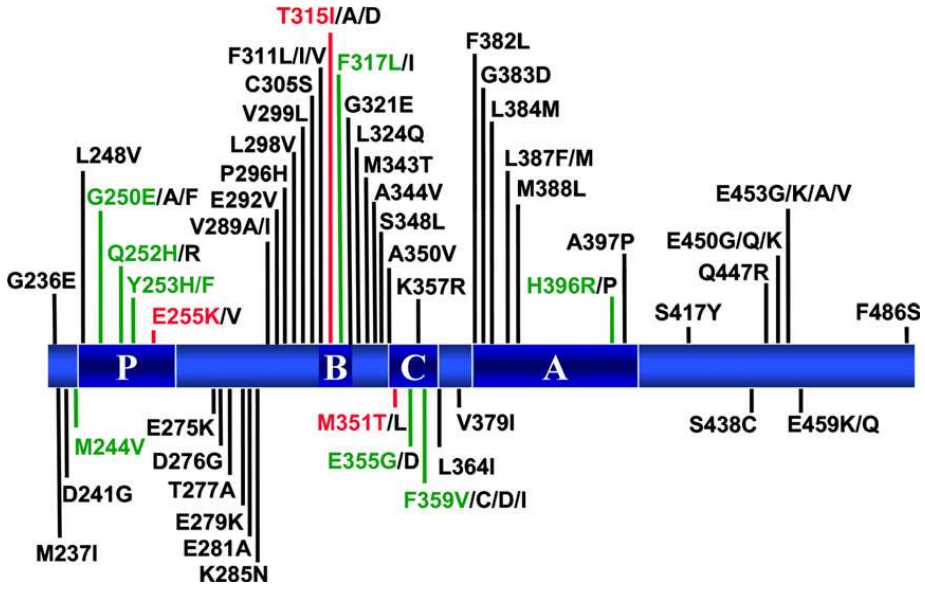


**Figure 8** [37] shows clinically relevant point mutations assigned to their position within the *ABL1* TKD. P = p-loop, B = imatinib binding site, C = catalytic domain, A = activation loop.

### 1.1.5.1 Origin of imatinib resistance and CML stem cells

Since CML is a stem cell disorder, a complete cure of disease requires the eradication of progenitor cells as a source of more differentiated CML cells [52]. CML stem cells are characterized as CD34+, CD 38- Lin- leukemic stem cells (LSCs) and express high levels of *BCR-ABL1* transcripts [20]. Unfortunately, imatinib as well as the second generation TKIs nilotinib and dasatinib do not efficiently target CML stem cells and these cells remain viable [53-55].

The CML stem cell population is hypothesized to be the reason for minimal residual disease detectable over years of therapy [33]. Moreover, it has been shown that discontinuation of TKI treatment, even in patients who achieved a complete molecular response (undetectable *BCR-ABL1* transcripts by real-time and/or nested PCR) results in relapse [56]. This indicates that more undifferentiated CML cells possessing self-renewal capacity, are still present and can re-establish the disease [24].

As described for more mature CML cells, there are several factors inducing resistance in CML stem cells. This again includes overexpression of *BCR-*

*ABL1*, drug transporter-related mechanisms, loss of tumor suppressor gene products and *BCR-ABL1* mutations in stem cell subclones [57]. Additionally, it has been observed that subpopulations of neoplastic stem cells are in a quiescent state of cell cycle, where cell-cycle specific drugs and TKIs are not effective [57]. CML stem cells may also be capable of trans-differentiating microenvironmental cells which, in turn, might render survival and growth of leukemic stem cells possible [57].
Concerning the evolution of point mutations, it has been observed that these mutations already pre-exist in CML stem cells [58]. This observation provided the basis for the hypothesis that the appearance of point mutated clones is comparable to antibiotic resistance in bacteria: imatinib selects for these rare pre-existing cells and induces outgrowth of drug-resistant cells [59].

#### 1.1.5.2 Overcoming *BCR-ABL1* TK point mutation induced resistance

Depending on the type of point mutation and its position within the *BCR-ABL1* sequence, different strategies are available to overcome imatinib resistance. Mutations displaying lower levels of resistance might be overcome by dose-escalation of the drug. This was described to be successful in the presence of e.g. M244V, Q252H, M351T, F359V [24,40,60].

However, there remains the issue of point mutations displaying higher degrees of resistance, where increased doses of imatinib fail. In these instances, the application of second generation TK inhibitors represents a reasonable option. Nilotinib and dasatinib were already tested in a variety of clinical studies, and are important candidate drugs.
Nilotinib (Tasigna®, Novartis Pharmaceuticals) was designed as a derivative of imatinib and allows a better topographic fit to ABL1, thereby overcoming imatinib resistance due to TK point mutations [61]. In-vitro studies showed that the drug selectively inhibits the proliferation of imatinib-resistant BCR-ABL1 expressing cells and the autophosphorylation of imatinib-resistant BCR-ABL1 mutants [62]. It is described to be ~ 20-fold more potent against WT and mutant

BCR-ABL1 expressing cells than imatinib [63]. Similar to imatinib, nilotinib was demonstrated to bind to the ABL1 inactive conformation.

Considering the clinical applicability of the drug, nilotinib was tested in the second-line setting in CP and AP imatinib-resistant CML patients and turned out to be an effective and well tolerated treatment modality [64,65]. Moreover, there are ongoing studies investigating the use of nilotinib in the frontline setting [66-68]. Concerning the performance in case of *BCR-ABL1* TK point mutations, it was observed that patients revealing E255K/V, Y253F/H or F359C/V had a less favorable outcome [66] whereas in case of T315I, complete resistance was observed [62,63].

Dasatinib (Sprycel®, Bristol-Myers Squibb) is a multi-target TKI that inhibits, besides BCR-ABL1 TK, the Src family kinases, Kit, PDGFR and ephrin A receptor kinase [31]. It was described to be ~ 325 fold and ~ 16 fold more potent than imatinib and nilotinib against WT BCR-ABL1, respectively [63]. Dasatinib possesses a different chemical scaffold and can bind to both, the active and inactive ABL1 conformation, in contrast to imatinib and nilotinib [48]. In vitro experiments showed that dasatinib lacks critical interactions with the ABL1 p-loop indicating that imatinib-resistant mutations within this region may not be relevant [48]. However, T315 is an important dasatinib contact residue, implying that mutations occurring at this specific AA position result in dasatinib insensitivity [48]; the same holds true for AA position T317. These experimental data were confirmed in clinical studies, identifying Q252H, E255K/V, V299L and F317L as less sensitive and T315I as completely insensitive to the drug [66]. The successful implementation of dasatinib as a second-line treatment option was demonstrated in a number of clinical studies [66,69]. Two ongoing studies investigate the use of dasatinib in the first-line setting [66].

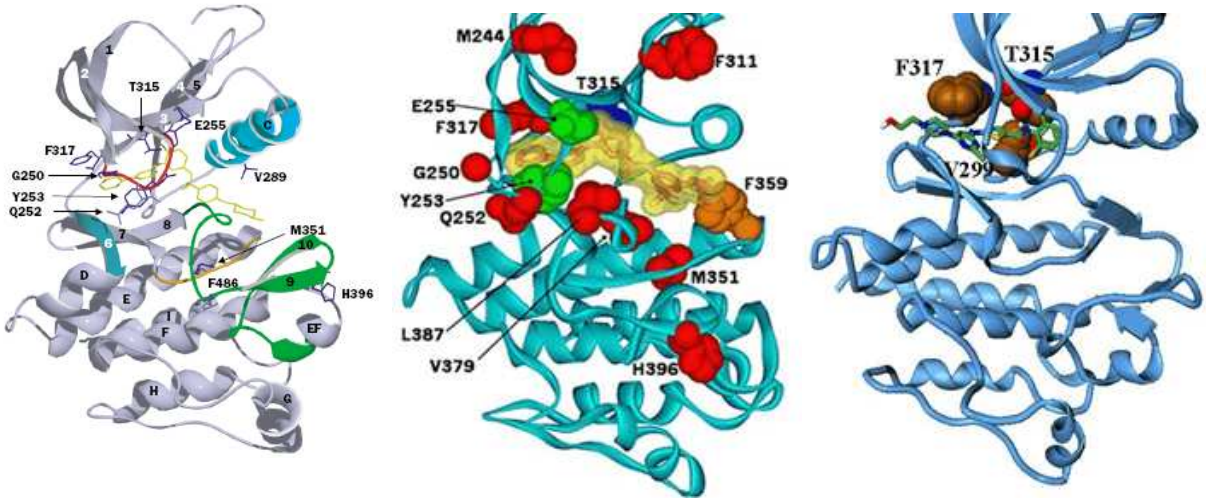


**A) Imatinib** **B) Nilotinib** **C) Dasatinib**

**Figure 9** displays the position of TKI inhibitors imatinib, nilotinib and dasatinib within the ABL1 TK domain. A) Critical residues for *ABL1*-TK point mutations associated with imatinib-insensitivity (e.g. E255, G250, Y253, H396) or resistance (T315) are shown for imatinib [29]. B) AA residues in red indicate the positions of point mutations described to be insensitive to imatinib but sensitive to nilotinib. Mutations at E255 and Y253 (in green) show a intermediate resistance, but those at T315 are completely resistant [70]. C) Critical AA residues for dasatinib associated with insensitivity are shown in brown (e.g. F317 and V299); T315I, displayed in red, is resistant to dasatinib [70].

Despite the success of imatinib, nilotinib and dasatinib for the induction of hematologic, cytogenetic and molecular responses in CML patients, point mutation T315I remains insensitive to all drugs available. To overcome this problem, several alternatives have been pursued as reviewed, for exemple, by Quintás-Cardama and Cortes in 2008 [71]:

This can involve two strategies: a) direct BCR-ABL1 T315I kinase inhibitors and/or b) inhibitors of BCR-ABL1 T315I kinase downstream effectors.

a) Direct BCR-ABL1 T315I inhibitors:

Aurora-A and Aurora-B are two serine/threonine kinases described to be overexpressed or amplified in leukemias. It has been shown that inhibitors of both enzymes target WT and mutants of BCR-ABL1. Several inhibitors were already tested in in-vitro and in-vivo studies including patients with T315I mutation.
ABL1 switch pocket inhibitors regulate conformational changes involved in kinase activity and avoid a steric clash with the T315I-mutated residue. Cross-reaction with other kinases is highly reduced since switch pocket structures are distinct in all kinases [72]. Clinical trials have not been performed yet.
Several other preclinical T315I inhibitors are in development.

b) Inhibitors of BCR-ABL T315 kinase downstream effectors

Targeting BCR-ABL1 downstream signalling molecules is an alternative treatment option that is not influenced by mutations at the gatekeeper residue T315.
BCR-ABL1 activates the RAS/RAF pathway which is therefore a potential target site. It has been shown that the combination of farnesyl transferase inhibitors and imatinib had clinical activity against the T315I mutation [71,73].
The inhibition of RAC GTPases, which are activated in CP CML patients, was demonstrated to be successful in a murine model and in in-vitro experiments using bone marrow cells from BP CML patients. Thus RAC GTPases seem to be an attractive target to prevent BCR-ABL1 signalling [71].
Further approaches include the stabilization of protein phoshatase 2A, a BCR-ABL1 antagonizing tumor suppressor [74] and the activation of apoptotic pathways [71].

Independent of the molecular targeting of T315I-resistant BCR-ABL1 molecules, epigenetic approaches are on the way rendering the induction of cytogenetic and molecular responses even in patients with the highly TKI-resistant T315I mutation possible [71].

Allogeneic stem cell transplantation (SCT) represents a possible treatment option in case of T315I point mutations and it has been shown that it provides long-term disease eradication and prolonged disease-free survival [34,75]. However, SCT is not applicable in all patients due to limitations regarding suitable donors, advanced age of patients and concerns about treatment-related morbidity and mortality (graft-versus-host disease, infection and organ toxicity) [34].

An algorithm of the treatment approach in CML patients including different drugs and their limitations was proposed by Jabbour et al. [66], and is displayed in Figure 10.

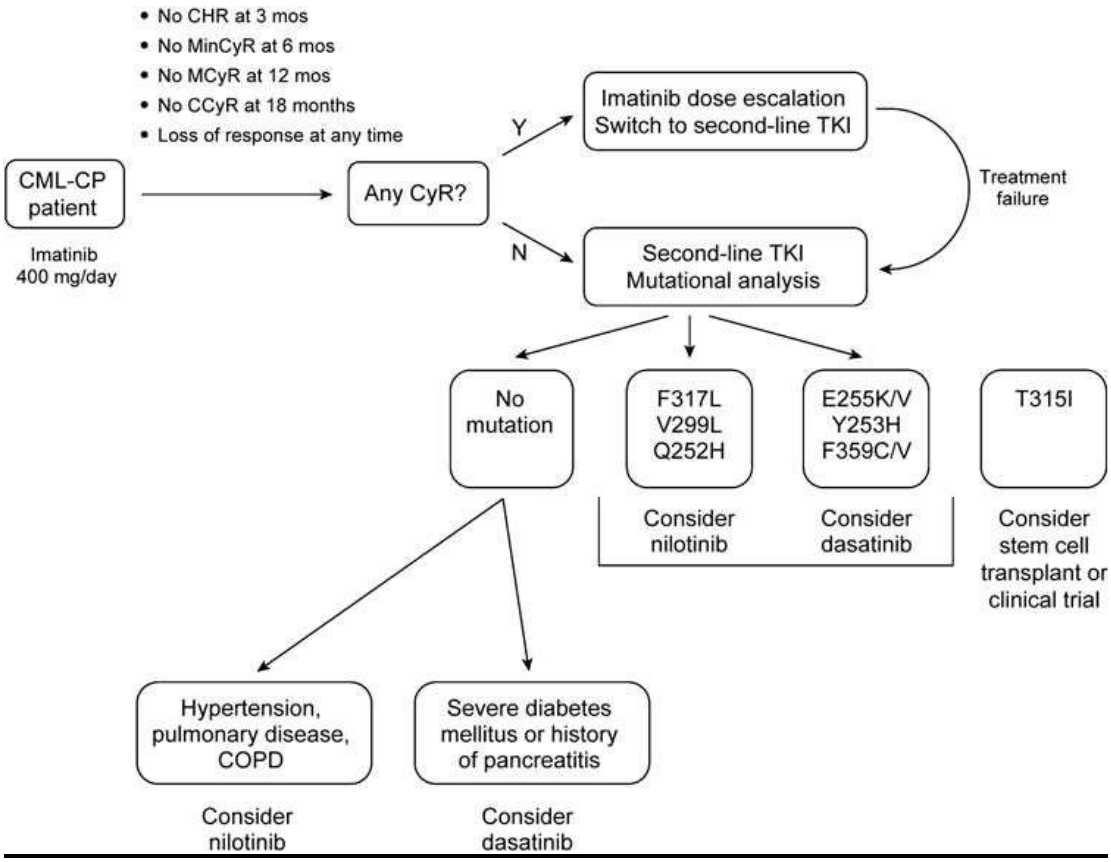


**Figure 10.** [66] Treatment strategy in CML patients. CHR = complete hematologic response; MinCyR = minimal cytogenetic response; MCyr = major cytogenetic response; CCyR = complete cytogenetic response; COPD = chronic obstructive pulmonary disease. Detailed explanations for CHR, MinCyR, MCyr, CCyR are described in Table 1.

## 1.2 Methodologies for CML monitoring and detection /quantification of point mutations

### 1.2.1 Methodological tools for CML monitoring

Initial diagnosis of CML is followed by immediate onset of first-line therapy. To date, imatinib represents the standard first-line drug applied independently of patient-related factors, like age or disease related variables [33]. Imatinib induces response rates superior to earlier treatment approaches [32]. The response is documented by hematologic analysis including blood count and differentials, cytogenetic analysis detecting the percentage of Ph+ positive metaphases in the bone marrow, FISH (fluorescence in-situ hybridization) revealing the percentage of Ph+ positive interphases and quantitative RT-real-time PCR permitting the monitoring of *BCR-ABL1* transcripts [33].

An international group of CML experts established an organization, the ELN (European LeukemiaNet), that develops concepts and management recommendations for CML, defines criteria of response/relapse and provides guidelines for the intervals of diagnostic analysis [35].

Criteria for hematologic, cytogenetic and molecular response are depicted in Table 1.

| Type of response | Definition |
|---|---|
| **Hematologic** | |
| Complete (CHR) | WBC (white blood cell count) < $1x10^9$/L<br>Basophils < 5%<br>No myelocytes, promyelocytes or myelo-blast in the differential<br>Platelet count < $450x\ 10^9$/L<br>Spleen nonpalpable |
| **Cytogenetic** | |
| Complete (CCgR) | No Ph+ metaphases |
| Partial (PCgR) | 1-35% Ph+ metaphases |
| Minor (mCgR) | 35-65% Ph+ metaphases |
| Minimal (minCgR) | 66-95% Ph+ metaphases |
| None (noCgr) | > 95% Ph+ metaphases |
| **Molecular** | |
| Complete (CMolR) | undetectable *BCR-ABL1* mRNA transcripts by real-time quantitative and/or nested-PCR in two consecutive blood samples of adequate quality (sensitivity > $10^4$ ) |
| Major (MMolR) | Ratio of *BCR-ABL1* to *ABL1* (or other house-keeping genes) ≤ 0,1% on the international scale |

**Table 1.** [35] **Definitions of hematologic, cytogenetic and molecular response according to the ELN criteria**. Adapted from Baccarani et al. 2009.

Moreover, the ELN recommends the intervals for hematologic, cytogenetic and molecular analysis after CML diagnosis [35].
Hematologic analysis is to be performed initially at diagnosis and then every 15 days until a complete hematologic response is achieved. Subsequently, the analysis is recommended every three months.
Cytogenetic analysis should be carried out after three and six months, and thereafter every six months until a complete cytogenetic response is documented. Subsequently, cytogenetics is recommended every 12 months if molecular monitoring is not available.
Molecular monitoring should be performed every three months until a complete molecular response is obtained and subsequently at least every six months. If suboptimal response or treatment failure is observed, mutational screening for BCR-*ABL1* TKI point mutations is recommended. Since several point mutations insensitive or resistant to second generation TKIs have been described, mutational analysis must be performed before any change of therapy [35].

### 1.2.2 Techniques for the detection/quantification of point mutations

A number of methods have been employed to detect point mutated clones in CML. This includes, for example, PCR amplification coupled with direct sequencing of the *BCR-ABL1* TK domain [76-78], high-performance liquid chromatography (D-HPLC) [79-81], the SEQUENOM MassARRAY system [82], or allele-specific oligonucleotide (ASO)-PCR amplification [83-85]. These techniques display different detection limits for the identification of mutant clones ranging from 0.01-30%. Detection of a mutation within the *ABL1* TK domain does not necessarily imply impending onset of clinically resistant disease, particularly if the size of a mutant clone is small [85]. Mutant clones have been reported to disappear spontaneously which may, at least in part, be attributable to the occurrence of mutations in cells with restricted proliferative capacity [77,83].

Qualitative methods for mutational analysis may therefore have limited potential to reliably assess the risk of clinically resistant disease, especially if mutant clones present at very low levels are detected [83].
It is currently a matter of discussion whether the detection of small mutant *BCR-ABL1* clones, e.g. below the level of 1%, is clinically useful. The clinical benefit of sensitive techniques for mutational analysis could be increased if the size of mutant clones could be monitored, in order to facilitate timely detection of clonally expanding mutant cells during treatment [83].
Current approaches to assessing the size of mutant clones include e.g. pyrosequencing [77], SEQUENOM MassARRAY analysis [82], or the polymerase colony assay [86]. These techniques, however, have limitations with regard to broad application in clinical diagnosis, such as the requirement of very expensive equipment [82], rather complex and laborious design [86], or the apparent inability to quantify mutant clones in the range below 20% [77].

### 1.2.3 Technical basis for the development of LD-PCR and Hybprobe/PNA assay

MLPA (multiplex ligation-dependent probe amplification) technology was first described by Schouten et al. in 2002 [87]. This technique facilitates relative quantification of up to 40 different DNA sequences within one reaction. For each target region two oligonucleotides are generated, one synthetic and one M13-derived. The M13-derived oligonucleotides possess stuffer-sequences of different lengths rendering the discrimination of different targets within a multiplex reaction possible. Oliogonucleotides adjacently hybridize to the target site followed by a ligation step mediated by a specific ligase (Ligase 65), which is very sensitive to probe-targeted mismatches next to the ligation site [87]. The oligonucleotides have identical end-sequences and serve as a target site for universal forward and reverse primers. Thereafter, amplification by a PCR reaction is performed and amplicons are analyzed by capillary electrophoresis.
To date, hundreds of different MLPA-based detection kits are commercially available and facilitate the assessment of scientific or clinical questions

including congenital and hereditary disorders, tumor and methylation profiling, as well as quantification of mRNA (www.mlpa.com).

In their publication, Schouten et al. described the possibility to use the MLPA technology for SNP (single nucleotide polymorphism) and mutation detection. This provided the basis for the idea to adapt the MPLA technology to assays which facilitate not only the sensitive detection but also the quantification of point mutated subclones.

PNA oligonucleotides used for the PNA/Hybprobe approach consist of nucleotide bases provided with a pseudopeptide backbone instead of a sugar-phosphate backbone [88]. These oligonucleotides were described to form stable structures with complementary DNA and RNA [89] with high affinity and specificity, which is mainly attributable to the uncharged and flexible polyamide backbone [90]. PNA oligos are used for a plethora of technologies, including e.g. FISH and PCR [90].

PNA clamping was first described by Ørum in 1993 [91]: a PNA oligo was designed to bind to its complementary target sequence and thus prevented its amplification within a PCR reaction. This was enabled by either competitive binding to the respective primer sequence, or by physical blocking of the DNA polymerase resulting in the inhibition of the PCR elongation step [92]. Moreover, a combination of PNAs with Hybprobes® (Roche) was described for the specific and sensitive detection of point mutated sequences within the RAS oncogene [93,94].

The LightCycler®Hybprobe format relies on two sequence-specific probes (anchor and sensor probe) which are labelled by different fluorescence dyes. The sensor probe is labelled with a 3´ fluorescein, the anchor with 5´ LightCycler®Red. During the PCR annealing phase, they hybridize adjacently to each other and a FRET (fluorescence resonance energy transfer) reaction takes place. Thereby fluorescein, excited by light from a LED lamp (part of the LightCycler PCR machine), transfers energy to the 5´LightCycler®Red at the anchor probe. The anchor probe thereby emits red fluorescent light, which is subsequently measured. After the PCR amplification reaction is finished, a melting curve program is activated. Starting at about 40℃, the PCR machine

gradually increases the temperature and the double stranded PCR amplicons start to disintegrate. The temperature at which half of the amplicons are present in double stranded form and half are single-stranded is defined as the melting temperature, which is characteristic for each sequence (www.roche-applied-science.com).

## Specific aims

- Development of novel methodological approaches to sensitive detection and/or quantitative monitoring of point-mutated clones in CML patients with known TKI mutations based on the MLPA-related ligase-dependent (LD-)-PCR or the implementation of PNA oligonucleotides
- Proof of feasibility to adapt the LD-PCR technique to the analysis of any point mutation by developing an approach to the detection/quantification of V617F within the *JAK2* gene in patients with myeloproliferative disorders

## Working hypothesis

Point-mutanted subclones may not imply resistance to TKI therapy simply by their presence in peripheral blood or bone marrow samples. Various models suggest that subclones with known TKI resistance might proliferate prior to the onset of clinically detectable resistance. In contrast, point-mutated subclones incapable of inducing TKI-resistance and progression of disease might decrease in size and ultimately disappear or persist on a low level [95].
The technique to be developed (LD-PCR) should provide the basis for sensitive detection and quantitative monitoring of point-mutated subclones to document their proliferation kinetics. The documentation of an expanding mutant subclone is indicative of its resistance to current TKI therapy, and could therefore serve as a basis for timely treatment modification.

# 2 Materials and Methods

## 2.1 PCR amplification of BCR-ABL1 sequences

Semi-nested PCR reactions were performed as described previously [76]. The PCR reaction for the first round of amplification included 0,3 µM forward primer 1 (5'-TGACCAACTCGTGTGTGAAACTC-3'), 0,3 µM reverse primer (5'-TCCACTTCGTCTGAGATACTGGATT-3'), 0,5 mM dNTPs, 0,75 mM $MgCl_2$, 2U Expand Long Template Polymerase, 10 x buffer 3 (Expand Long template PCR system, Hoffmann-La Roche Ltd, Basel, Switzerland), and 150 ng cDNA template in a total volume of 25 µl. In the presence of the e1a2 *BCR-ABL* fusion, the same concentration of a different forward primer (5'-ACCGCATGTTCCGGGACAAAAG-3') was used. The first PCR round was performed according to the following protocol: preheating to 94°C, followed by 2 min at 94°C, 10 cycles with the profile of 94°C for 20 sec, 60°C for 30 sec, 68°C for 2 min, 25 cycles with the profile of 94°C for 2 0 sec, 60°C for 30 sec, 68°C for 2 min + 20sec/cycle, a final extension step at 68°C for 7 min with subsequent cooling to 10°C. For the second round of amplificat ion, 1 µl of the first-round PCR product was added to a reaction mix identical to the above indicated, a nested forward primer (5'-CGCAACAAGCCCACTGTCT-3') at 0,3 µM being the only difference. The second round of PCR was performed according to the following protocol: preheating to 94°C, 2 min at 94 °C, 10 cycles with 94°C for 20 sec, 60°C for 30 sec, 68°C for 1 min, 25 cycles wit h 94°C for 20 sec, 60°C for 30 sec, 68°C for 1 min + 20sec/cycle, a final exten sion step of 68°C for 7 min followed by cooling to 10°C.

## 2.2 LD-PCR approaches

For LD-PCR analysis, reaction mixes were prepared on ice. All reagents were components of the Salsa® MPLA® reagents kit (MRC Holland, Amsterdam, The Netherlands), containing basic reagents except ligation and hybridization oligos. For the first step, 0,5 µl probe mix [containing 0,8 µl from 1µM concentrations of each Lig-WT probe, Lig-Mut probe and Hyb probe (Sigma, Steinheim, Germany) in 200 µl $H_2O$], 1,5 µl of MLPA buffer and 50 ng of the *BCR-ABL1* PCR product (determined by photometric measurement) were mixed and immediately subjected to a hot-start at the ABI 9600 thermocycler (Applied Biosystems (AB), Foster City, USA) for 5 min at 98°C in order to prevent the formation of secondary structures. For hybridization of Lig-WT, Lig-Mut and Hyb-oligonucleotide, the reaction mix was cooled down to the appropriate hybridization temperature listed in Table 3, and incubated for 1 min. For ligation procedure performed at 54℃ for 15 min., 32 µl of a ligation-mix containing 3 µl Ligase-65 buffer A, 3 µl Ligase-65 buffer B, 1 µl Ligase 65 and 25 µl water were added and mixed properly. This step was followed by enzyme inactivation for 5 min at 98℃ and cooling of the samples to 4℃. A mi xture of 4 µl 10x SALSA PCR buffer and 26µl sterile water was added to 10 µl of the ligation reaction heating to 60℃ to prevent non-specific primer anne aling, and supplemented with 10 µl of the PCR-mix containing 2 µl FAM-labelled SALSA PCR primers, 2 µl SALSA enzyme dilution buffer, 0,5 µl SALSA polymerase and 5,5 µl sterile water. The LD-PCR program was started according to the following protocol: 95℃ for 30 sec, 60℃ for 60 sec, 72℃ for 60 sec f or 35 cycles, 72℃ for 20 min, and cooling to 4℃.

## 2.3 Capillary electrophoresis

Analysis of LD-PCR products was performed on the ABI PRISM® 3100-Avant Genetic Analyzer (Applied Biosystems (AB) Foster City, USA). The set up of the instrument was done according to the manufacturer´s instructions. Due to the FAM label of the SALSA fw primer, DS-01 Matrix Standard Set for the 3100 and 3100-Avant Systems (AB) was used to establish a matrix file (dyset D). A 36 cm capillary column containing the high performance polymer POP-4™ (AB) was used for PCR product separation. The LD-PCR product was diluted 1:50 using Aqua bidestillata (Mayerhofer Pharmazeutics, Linz, Austria). To identify the PCR products according to their lengths in bp, a reaction mix containing 0,3 µl GeneScan™-500 ROX™ Size Standard (AB) and 9 µl Hi-Di™ Formamide (AB) was prepared and 1 µl of the diluted PCR product was added. The reaction was denatured at 94℃ for 3 min, and cooled to 4℃. Amplicon separation on the ABI PRISM® 3100-Avant was performed using an injection time of 10 s, injection voltage of 1 kV, electrophoresis voltage of 10 kV, and an oven temperature of 60℃. In case of off-scale results, the injection was repeated using lower injection time and voltage.

### 2.3.1 Analyses of capillary electrophoresis results

The ABI PRISM® GeneScan® Analysis software 3.7 (AB) was used to analyze the results obtained by capillary electrophoresis. Due to the stuffer sequence inserted within the MUT Lig-oligo, the PCR product amplified from the MUT sequence was six base pairs longer than the WT product. Peak heights of WT and MUT amplicons were used for the calculation of relative amounts. This ratio was calculated using the following formula: % Mut = (peak height of Mut product/ $\sum$ peak heights of Mut + WT products) x 100.

## 2.4 Patient material

### 2.4.1 RNA extraction and cDNA synthesis

Peripheral blood anticoagulated with EDTA was collected from CML patients revealing suboptimal response to imatinib and control patients with adequate response to treatment. Leukocyte counts were determined using the Sysmex KX-21N system (Sysmex Austria GmbH, Vienna, Austria). Erythrocytes were lysed by red cell lysis buffer ([10 mM Tris (pH 7,6), 5 mM $MgCl_2$, 10 mM NaCl] (Sigma, Steinheim, Germany)), and the leukocytes were pelleted by centrifugation for 10 min at 1 300 rpm. Total RNA was extracted from $2x10^7$ leukocytes using the QIAamp® RNA Blood Mini Kit (Qiagen, Hilden, Germany) according to the manufacturer´s instructions.
cDNA synthesis was performed using 10 µl of reverse transcriptase mix including MMLV-RT 5x buffer, 0,2 mM dNTPs, 0,25 µg random primers, 20 U RNAsin, 100 U MMLV Reverse Transcriptase (all Promega, Mannheim, Germany) and 10 µl of total RNA. The reaction was incubated for 1 h at 37℃. Assessment of cDNA concentration was performed by Nanodrop measurement.

#### 2.4.1.1 RNA extraction from methanol/acetic acid-fixed cells

200-500 µl of the cell suspension from methanol/acetic acid-fixed cells were pelleted at 13 000 rpm for 5 min. The supernatant was removed completely and 1 ml 96% ethanol was added without agitating. Again, the cells were pelleted as described and the supernatant was removed. Cells were resuspended in 350 µl RLT-buffer provided with the QIAamp® RNA Blood Mini Kit (Qiagen) and further steps were performed as described by the manufacturer.

### 2.4.2 Real-time PCR analysis of *BCR-ABL1* and control gene

To determine the quantity of *BCR-ABL1* transcripts in relation to the control gene *ABL1*, quantitative real-time PCR analysis was performed as already described [96]: for *major BCR-ABL1* (Mbcr) 300 nM Mbcr fw primer (5´ TCCGCTGACCATCAAYAAGGA 3´), 200 nM Mbcr probe (5´ Fam-CCCTTCAGCGGCCAGTAGCATCTGA-Tamra 3´), 300 nM Mbcr rev primer (5´ CACTCAGACCCTGAGGCTCAA 3´), 2 x LC-480 probes mastermix and 0,5 U Uracil-DNA Glycosylase (Roche Diagnostics, Penzberg, Germany) were used. For *minor BCR-ABL1* (mbcr) and *ABL1* (abl) the reaction components remained the same with the exception of primers and probes: i) mbcr: 300 nM mbcr fw primer (5´ CTGGCCCAACGATGGCGA 3´), 200 nM mbcr probe (5´ Fam-CCCTTCAGCGGCCAGTAGCATCTGA-Tamra 3´), 300 nM mcbr rev primer (5´ CACTCAGACCCTGAGGCTCAA 3´) and ii) abl: 300 nM abl fw primer (5´ TGGAGATAACACTCTAAGCATAACTAAAGGT 3´), 200 nM abl probe (5´ Fam-CCATTTTTGGTTTGGGCTTCACACCATT-Tamra 5´), 300 nM abl rev primer (5´ GATGTAGTTGCTTGGGACCCA 3´). The RT-PCR reactions were amplified according to the LightCycler standard program: pre-amplification for 10 sec. at 95℃; 50 amplification cyles for 10 sec. at 95℃, 3 0 sec. at 60℃, 10 sec. 72℃; followed by cooling to 4℃.

For calculation, results obtained for the rearranged transcripts were correlated to 1x $10^5$ ABL1 molecules [(1x $10^5$ * *BCR/ABL1* molecules)/*ABL* molecules], additionally the *BCR-ABL1/ABL1* (%) ratio was indicated: (*BCR-ABL1/ABL1*)*100.

### 2.4.3 Detection of point mutated sub-clones via bidirectional sequencing

The presence of *ABL1* TK point mutations was verified by bidirectional sequencing of the *BCR-ABL1 TK* domain prior to LD-PCR analysis. Initially, the first round of semi-nested PCR was prepared as described above. In case of low starting amount of *BCR-ABL1*, a second round of PCR amplification had to be performed. The PCR product was analyzed on a 1,5% agarose gel and the respective band [first round products b2a2 (Mbcr): 1504 bp; b3a2 (Mbcr): 1579 bp; e1a2 (mbcr): 1641 bp; second round product: 863 bp] was eluted from the gel using the QIAquick PCR Purification Kit (Qiagen) according to the manufacturer's instructions. PCR products were subjected to bidirectional sequencing (VBC Genomics, Vienna, Austria) using the primers NTBP+ (5´ AAGCGCAACAAGCCCACTGTCTAT 3´) and NTBP- (5´ CTTCGTCTGAGATACTGGATTCCTG 3´). The presence of point mutations was determined by comparing the patient sequence, with the reference sequence (>gi|62362413:4-3396 Homo sapiens v-abl Abelson murine leukemia viral oncogene homolog 1 (ABL1), transcript variant a, mRNA) using the BLAST program (http://www.ncbi.nlm.nih.gov/blast/bl2seq/wblast2.cgi).

# 3 Results

## 3.1 LD-PCR

### 3.1.1 Design of LD-PCR oligonucleotides

#### 3.1.1.1 Methodological principle of LD-PCR approaches

The principle of LD-PCR relies on a ligation-dependent competitive PCR approach. This newly developed technique is a modification of the MLPA technique described by Schouten et al in 2002 [87]. Competitive hybridization of WT/MUT specific ligation (Lig) oligonucleotides and a common hybridization (Hyb) oligonucleotide is followed by a ligation step. Thereby adjacent Lig- and Hyb-oligonucleotides are conjugated to form a continuous template for the subsequent PCR amplification applying universal primers. The amplification products are separated and detected by capillary electrophoresis.

Probe sets required for each LD-PCR approach consist of two Lig- and one Hyb-oligonucleotide. Lig-oligonucleotides bind specifically to the 5´ region of the particular point mutation. While one oligonucleotide hybridizes to the WT sequence (Lig-WT), the other one is specific for the mutated sequence (Lig-MUT). Lig-WT and Lig-MUT oligonucleotides differ in a single nucleotide located at their 3´terminal position. An additional “stuffer” sequence is attached at the 5´ site of the Lig-MUT oligonucleotide, and consists of six nucleotides not complementary to the DNA target sequence. Hence, the Mut-PCR product is six bp longer than the WT product and this renders the discrimination of Mut- and WT-specific LD-PCR products by capillary electrophoresis possible. A universal template sequence facilitating the binding of a universal forward primer is attached at the 3´ terminal end of the Lig-oligonucleotide. The Hyb-oligonucleotide is located adjacently to the 3´ end of the Lig-oligonucleotides and as a prerequisite for ligation, the 5´ end is phosphorylated.

Accordingly, the universal template sequence, facilitating the annealing of a universal reverse primer is attached at the 3´ terminal end of the Hyb-oligonucleotide. The arrangement of Lig-WT, Lig-MUT and Hyb-oligonucleotide and the principle of the LD-PCR approach are displayed in detail in Figure 11.

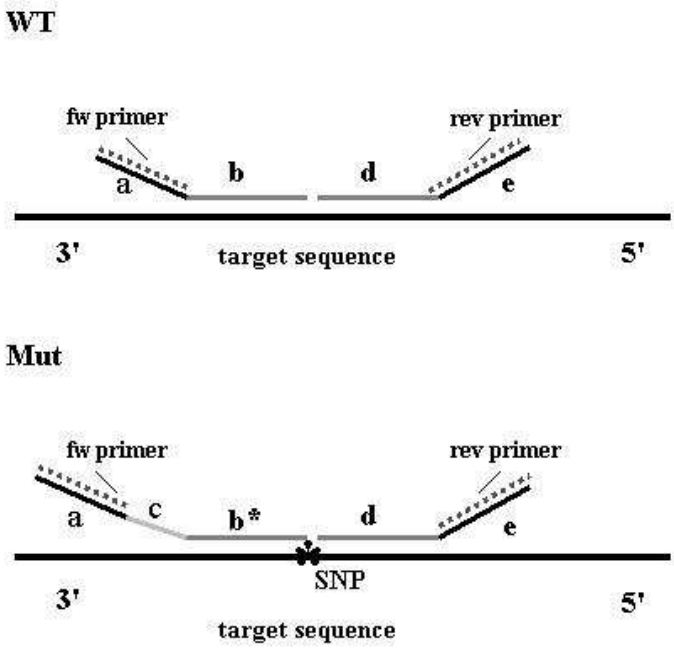


**Figure 11. LD-PCR assay for the sensitive detection and quantification of wild-type (WT) and point-mutated (MUT) sequences.** The principle of LD-PCR is a modification of the MLPA technology [87]. The LD-PCR reaction contains three different probes: 1) The wild-type ligation probe (Lig-WT) contains a section complementary to the WT target sequence [**b**] and a tag sequence for the forward primer [**a**]. 2) The ligation probe for the mutant sequence (Lig-MUT) [**b***] differs from the Lig-WT probe by a nucleotide at the 3´ terminal position complementary to a specific point mutation. This probe carries the same tag sequence [**a**] for the forward primer, but contains an additional stuffer sequence of 6 non-homologous nucleotides [**c**]. 3) The common hybridization (Hyb) probe contains a section complementary to its target sequence directly adjacent to that of the ligation probes [**d**] and a tag sequence for the reverse primer [**e**]. Upon specific hybridization to the target sequence, the probes are fused under conditions described in Materials and Methods, permitting the ligation only in the presence of perfect match to the target sequence. In a subsequent step, the ligated probes are amplified competitively in a PCR reaction with a single set of primers binding to the tag sequences **a+e**. Due to the difference in length between the WT- and MUT-derived products, the amplicons can be readily separated and quantified by fluorescent capillary electrophoresis (see Fig.2).

### 3.1.2 Rules for oligonucleotide design

For the design of Lig- and Hyb- oligonucleotides, a number of criteria have to be considered. Probes must never overlap, the length of each oligonucleotide has to be more than 21 nucleotides, the melting temperature ≥ 70℃, the G/C content should be around 50% and the two hybridizing sequences have to be immediately adjacent. A specific program, available at www.mlpa.com, permits the verification of the design according to the criteria described. The forward primer (5'-GGGTTCCCTAAGGGTTGGA-3') is designed to be complementary to the tag sequence at the 5' end of the Lig probe, and the reverse primer (5'-GTGCCAGCAAGATCCAATCTAGA-3') to the tag sequence at the 3' end of the Hyb probe, as indicated.

In some instances, the above rules for probe design had to be modified due to the base composition around the site of mutation in order to provide optimal performance of individual probe systems. This was mainly attributable to the phenomenon of hybridization of unrelated bases, which is well documented (Table 2).

| Base | Base on complementary strand | Ligation between the bases |
|---|---|---|
| G | C | no |
| | T | no |
| | A | 25% |
| T | A | no |
| | G | no |
| | C | 25% |
| C | A | no |
| | G | no |
| | T | possible |
| A | T | no |
| | G | no |
| | C | no |

**Table 2. Ligation of unrelated bases**. Displayed are the options for ligation reactions between the normal nucleotide and the nucleotide of the polymorphic sequence on the complementary strand as described by MRC Holland (www.mlpa.com).

Primarily, the oligonucleotides were designed in a sense-orientated fashion, and the assays were tested for functionality, using synthetic templates containing the target region of interest (data not shown.) In case of high cross-reactivity with the WT sequence, the systems were re-designed in an antisense-complementary fashion. This was necessary for some LD-PCR systems for the following mutations: Q252H-T, Q252H-C, F359V, H396R and H396 P.

To exclude the formation of secondary structures close to the hybridization temperature, each oligonucleotide/universal template construct was controlled using the program http://frontend.bioinfo.rpi.edu/applications/mfold/cgi-bin/dna-form1.cgi. Default analysis parameters were used except for ionic concentration, ([Na+] was set at 0,35M) and the folding temperature, which was set at the appropriate hybridization temperature of the Lig- and Hyb-oligonucleotides.

In general, the WT and MUT Lig-oligonucleotides, as well as hybridization oligonucleotides were designed to hybridize at a temperature of 70°C. However, due to the high G/C content of surrounding DNA regions, the hybridization temperature had to be increased to 75°C in some instances. This was mainly necessary for several point mutations located within the P-loop of the *ABL1 TK* domain (E255K, Y253F, Y253H, Q252H-C and Q252H-T) or within the activation loop (H396P and H396R).

The final LD-PCR oligonucleotide sequences, the calculated and employed hybridization temperature, G/C content and lengths are depicted in Table 3.

| LD-System | Primer *Stuffer* **Oligo** | Hybridizationtemperature C° | Lig/Hyb oligo properties | | |
|---|---|---|---|---|---|
| **E255K** | | | lengths (bp) | G/C content (%) | TM (°C) |
| Lig Oligo WT | gggttccctaagggttgga**cgggggccagtacgggg** | 75 | 17 | 82 | 76 |
| Lig Oligo Mut | gggttccctaagggttgga*ttcaat***cgggggccagtacggga** | | 17 | 76 | 74 |
| Hyb Oligo | 5´Phos **aggtgtacgagggcgtgtggaag**tctagattggatcttgctggcac | | 23 | 61 | 74 |
| **Y253F** | | | | | |
| Lig Oligo WT | gggttccctaagggttgga**gctgggcgggggccagta** | 75 | 18 | 78 | 76,6 |
| Lig Oligo Mut | gggttcccgaagggttgga*tagtcc***gctgggcgggggccagtt** | | 18 | 78 | 77,5 |
| Hyb Oligo | 5'Phos **cggggaggtgtacgagggcg**tctagattggatcttgctggcac | | 20 | 75 | 77,5 |
| **Y253H** | | | | | |
| Lig Oligo WT | gggttccctaagggttgga**ctgggcgggggccagt** | 75 | 16 | 81 | 74,4 |
| Lig Oligo Mut | gggttccctaagggttgga*tgtggt***ctgggcgggggccagc** | | 16 | 88 | 77,4 |
| Hybr Oligo | 5'Phos **acggggaggtgtacgagggcg**tctagattggatcttgctggcac | | 21 | 71 | 75,9 |
| **F317L-A** | | | | | |
| Lig Oligo WT | gggttccctaagggttgga**gcccccgttctatatcatcactgagttc** | 70 | 28 | 50 | 72,8 |
| Lig Oligo Mut | gggttccctaagggttgga*cttatc***gcccccgttctatatcatcactgagtta** | | 28 | 46 | 71 |
| Hyb Oligo | 5'Phos **atgacctacgggaacctcctgga**tctagattggatcttgctggcac | | 23 | 57 | 71,2 |
| **F317L-G** | | | | | |
| Lig Oligo WT | gggttccctaagggttgga**cccccgttctatatcatcactgagttc** | 70 | 27 | 48 | 70,6 |
| Lig Oligo Mut | gggttccctaagggttgga*cttatc***ccccgttctatatcatcactgagttg** | | 27 | 48 | 71,1 |
| Hyb Oligo | 5'Phos **atgacctacgggaacctcctgga**tctagattggatcttgctggcac | | 23 | 57 | 71,2 |
| **F317-C** | | | | | |
| Lig Oligo WT | gggttccctaagggttgga**ccccccgttctatatcatcactgagtt** | 70 | 26 | 46 | 69,1 |
| Lig Oligo Mut | gggttccctaagggttgga*ttatct***ccccgttctatatcatcactgagtg** | | 26 | 50 | 70,7 |
| Hyb Oligo | 5'Phos **catgacctacgggaacctcctg**tctagattggatcttgctggcac | | 22 | 59 | 71,1 |

| | | | | | |
|---|---|---|---|---|---|
| **F317-I** | | | | | |
| Lig Oligo WT | gggttccctaagggttgga**gcccccgttctatatcatcactgagt** | 70 | 26 | 50 | 71 |
| Lig Oligo Mut | gggttccctaagggttgga*ttattg***gcccccgttctatatcatcactgaga** | | 26 | 50 | 70,7 |
| Hyb Oligo | 5'Phos **tcatgacctacgggaacctcctg**tctagattggatcttgctggcac | | 23 | 57 | 70,8 |
| **F317-V** | | | | | |
| Lig Oligo WT | **gggttccctaagggttggagcccccgttctatatcatcactgagt** | | 26 | 50 | 71 |
| Lig Oligo Mut | gggttccctaagggttgga*ttattg***gcccccgttctatatcatcactgagg** | 70 | 26 | 54 | 73,1 |
| Hyb Oligo | 5'Phos **tcatgacctacgggaacctcctg**tctagattggatcttgctggcac | | 23 | 57 | 70,8 |
| **V299L-T** | | | | | |
| Lig Oligo WT | gggttccctaagggttgga**catgaaagagatcaaacaccctaacctgg** | | 29 | 45 | 72,2 |
| Lig Oligo Mut | gggttccctaagggttgga*gttgtg***catgaaagagatcaaacaccctaacctgt** | 70 | 29 | 41 | 71,1 |
| Hyb Oligo | 5'Phos **tgcagctcctttgggtctg**tctagattggatcttgctggcac | | 19 | 63 | 69,1 |
| **V299L-C** | | | | | |
| Lig Oligo WT | gggttccctaagggttgga**catgaaagagatcaaacaccctaacctgg** | 70 | 29 | 45 | 72,2 |
| Lig Oligo Mut | gggttccctaagggttgga*gttgtg***catgaaagagatcaaacaccctaacctgc** | | 29 | 45 | 72,2 |
| Hyb Oligo | 5'Phos **tgcagctcctttgggtctg**tctagattggatcttgctggcac | | 19 | 63 | 69,1 |
| **M244V** | | | | | |
| Lig Oligo WT | gggttccctaagggttgga**gaacgcacggacatcacca** | 70 | 19 | 58 | 69,1 |
| Lig Oligo Mut | gggttccctaagggttgga*tgacct***gaacgcacggacatcaccg** | | 19 | 63 | 71 |
| Hyb Oligo | 5'Phos **tgaagcacaagctgggcgg**tctagattggatcttgctggcac | | 19 | 63 | 71 |
| **L248V** | | | | | |
| Lig Oligo WT | gggttccctaagggttgga**ggacatcaccatgaagcacaagc** | 70 | 23 | 52 | 70,7 |
| Lig Oligo Mut | gggttccctaagggttgga*taatct***ggacatcaccatgaagcacaagg** | | 23 | 52 | 70,4 |
| Hyb Oligo | 5'Phos **tgggcgggggccagt**tctagattggatcttgctggcac | | 15 | 80 | 71,2 |
| **G250E** | | | | | |
| Lig Oligo WT | gggttccctaagggttgga**tgaagcacaagctgggcgg** | 70 | 19 | 63 | 70,9 |
| Lig Oligo Mut | gggttccctaagggttgga*gtgttg***tgaagcacaagctgggcga** | | 19 | 58 | 68,9 |
| Hyb Oligo | 5'Phos **gggccagtacggggaggt**ctagattggatcttgctggcac | | 17 | 76 | 71,4 |
| **Q252H-T*** | | | | | |
| Lig Oligo WT | gggttccctaagggttgga**gccctcgtacacctccccgtac** | 75 | 22 | 68 | 74,8 |
| Lig Oligo Mut | gggttccctaagggttgga*tacaga***gccctcgtacacctccccgtaa** | | 22 | 64 | 74 |
| Hyb Oligo | 5'Phos **tggcccccgcccagctt**tctagattggatcttgctggcac | | 17 | 76 | 74,8 |
| **Q252H-C*** | | | | | |
| Lig Oligo WT | gggttccctaagggttgga**agctgggcgggggccag** | 75 | 22 | 68 | 74,8 |
| Lig Oligo Mut | gggttccctaagggttgga*tatctc***agctgggcgggggccac** | | 22 | 68 | 74,7 |
| Hyb Oligo | 5'Phos **tacggggaggtgtacgagggcg**tctagattggatcttgctggcac | | 17 | 76 | 74,8 |

| | | | | | |
|---|---|---|---|---|---|
| **T315A** | | | | | |
| Lig Oligo WT | gggttccctaagggttgga**ggagcccccgttctatatcatca** | 70 | 23 | 52 | 69,7 |
| Lig Oligo Mut | gggttccctaagggttgga*tcttat***ggagcccccgttctatatcatcg** | | 23 | 57 | 71,4 |
| Hyb Oligo | 5'Phos **ctgagttcatgacctacgggaacctc**tctagattggatcttgctggcac | | 25 | 52 | 70,3 |
| **T315I** | | | | | |
| Lig Oligo WT | gggttccctaagggttgga**ggagcccccgttctatatcatcac** | 70 | 24 | 54 | 70,9 |
| Lig Oligo Mut | gggttccctaagggttgga*tcattt***ggagcccccgttctatatcatcat** | | 24 | 50 | 69,5 |
| Hyb Oligo | 5'Phos **tgagttcatgacctacgggaacctc**tctagattggatcttgctggcac | | 25 | 52 | 70,7 |
| **M351T** | | | | | |
| Lig Oligo WT | gggttccctaagggttgga**ccactcagatctcgtcagccat** | 70 | 22 | 55 | 69,3 |
| Lig Oligo Mut | gggttccctaagggttgga*gatgtt***ccactcagatctcgtcagccac** | | 22 | 59 | 70,8 |
| Hyb Oligo | 5'Phos **ggagtacctggagaagaaaaacttcatcc**tctagattggatcttgctggcac | | 29 | 45 | 71,1 |
| **F359V*** | | | | | |
| Lig Oligo WT | gggttccctaagggttgga**ggcagcaagatctctgtggatgaa** | | 24 | 50 | 70,9 |
| Lig Oligo Mut | gggttccctaagggttgga*acgcat***ggcagcaagatctctgtggatgac** | 70 | 24 | 54 | 71,6 |
| Hyb Oligo | 5'Phos **gtttttcttctccaggtactccatggc**tctagattggatcttgctggcac | | 27 | 48 | 71,7 |
| **H396P*** | | | | | |
| Lig Oligo WT | gggttccctaagggttgga**ttgatggggaacttggctccagcat** | | 25 | 52 | 74,05 |
| Lig Oligo Mut | gggttccctaagggttgga*tgaagg***ttgatggggaacttggctccagcag** | 75 | 25 | 56 | 75,3 |
| Hyb Oligo | 5'Phos **gggctgtgtaagtgtcccctgtc**tctagattggatcttgctggcac | | 23 | 65 | 75,15 |
| **H396R*** | | | | | |
| Lig Oligo WT | gggttccctaagggttgga**ttgatggggaacttggctccagcat** | | 25 | 50 | 74,05 |
| Lig Oligo Mut | gggttccctaagggttgga*tgaagg***ttgatggggaacttggctccagcac** | 75 | 25 | 56 | 75,37 |
| Hyb Oligo | 5'Phos **gggctgtgtaagtgtcccctgtc**tctagattggatcttgctggcac | | 23 | 65 | 75,15 |

* LD-System reverse complementary

**Table 3.** LD-PCR detection systems for 21 mutations in the *BCR-ABL* TK domain.

*LD-PCR system designed in a reverse complementary fashion. The table includes information on the constitution of each LD-PCR system including WT-and Mut-ligation oligonucleotides and Hyb oligonucleotide, the hybridization temperature, lengths (in bp), G/C content (%) and calculated melting temperature (TM).

### 3.1.3 Establishment of positive controls/calibrator samples

#### 3.1.3.1 Cloning of the WT *BCR-ABL1* TK domain

In vitro mutagenesis was performed to establish positive controls for LD-PCR assays. The WT *ABL1* TK domain (~ 1kB) was amplified as a template from the K562 cell line using 400 mM B2A fw (5'-TTCAGAAGCTTCTCCCTGACAT-3') primer targeting the *BCR* exon 13, 400 nM JAMR rev (5'-GTACTCACAGCCCCACGGA-3') targeting *ABL1* exon 10, 10 x ABI buffer, 2,5 U AmpliTaq® DNA Polymerase, 0,5 mM dNTPs and 5 mM $MgCl_2$ in a total volume of 25 µl. The following amplification conditions were used [77]: 10 min. at 95℃ for initial denaturation; 30 sec. at 95℃, 45 sec. at 50℃, 1 min 20 sec. at 72℃ for 35 cycles, 10 min. at 72℃, cooling to 4℃. The PCR product was analyzed on a 1,5% agarose gel and subsequently eluted from the gel using the QIAquick PCR Purification Kit (Qiagen) according to the manufacturer's instructions.

The purified PCR product was cloned into a pGEMt vector (Promega, Mannheim, Germany). To introduce the PCR product into the vector, a ligation reaction was performed containing 2 x buffer, 1 µl pGEMt, 1 µl Liagase (all Promega) and 3 µl purified PCR product. The ligation reaction was performed for 1 h at room temperature.

For transformation purposes, E. coli chemically competent cells (One Shot® Top 10, Invitrogen, Lofer, Austria) were used and thawed on ice for ~ 10 min; ligation products were kept on ice. 50 µl One Shot® Top 10 cells were applied to the ligation product and incubated on ice for 30 min. The reaction was heated to 42℃ for 45 sec, cooled on ice for 2 min, adjusted with 500 µl SOC medium and incubated for 30 min at 37℃. Transformed cells were plated on two LB amp plates (100 µg/ml) containing 80 µg/ml X-GAL and 0,5 M IPTG and incubated overnight at 37℃. Single white colonies were selected and applied to 4 ml of liquid LB amp medium and grown overnight at 37℃. The QIAprep ®Spin Miniprep Kit (Qiagen) was used to obtain the *ABL1* TK domain-containing

plasmid by applying the cell pellet from 2 x 1,5 ml bacterial suspension, according to the manufacturer´s instructions. The plasmid concentration was determined by photometric measurement using the Nandrop instrument ND-1000.
The presence of the *ABL1* TK domain was confirmed by direct sequencing in both directions (as explained in 2.4.3.) using the primers B2A fw and JAMR rev (see above).

#### 3.1.3.2 Mutagenesis assays

To generate 21 different *ABL1* TK point-mutated plasmids, mutagenesis assays were performed using the QuikChange® II Site-Directed Mutagenesis Kit (Stratagene, CA, USA). Fw and rev primers required were designed using a program provided on the Stratagene website applying the *ABL1* TK reference sequence (accession number: >gi|62362413:4-3396 [Homo sapiens v-abl Abelson murine leukemia viral oncogene homolog 1 (ABL1), transcript variant a, mRNA]).
Primer sequences designed for each *ABL1* TK point mutation are listed in Table 4. Primers were required to be PAGE-purified. The amount of primers necessary for mutagenesis PCR reaction was 125 ng each and had to be calculated according to the following formula: x pmol primer = [125/(330 x number of nucleotides)] x 1000. In addition to fw and rev primers the PCR reaction contained: 5 µl of 10 x reaction buffer, 1 µl of dNTP mix, 1 µl of *PfuUltra* HF DNA polymerase (2,5 U) (all Stratagene) and 1 µl of the 1: 100 diluted WT *ABL1* TK plasmid. Amplification was performed according to the Stratagene protocol: 30 sec. 95℃; followed by 12 cycles of 30 sec. 95℃, 1 min. 55℃, 5 min. 68℃; and cooling to 10℃. To digest the amplification products with *Dpn1*, the total amount of PCR product was incubated with 10 U *DpnI* for 1 h at 37℃, 10 min at 65℃ and subsequently cooled on ice. For transformation purposes, XL1-Blue supercompetent cells (Stratagene) were thawed on ice for 10 min. Each 50 µl were mixed with 1 µl of digestion-product, incubated on ice for 30 min, 45 sec at 42℃, cooled on ice for 2 min, mixed with 500 µl SOC

medium and incubated for 30 min at 37℃. Transformed cells were subsequently plated on LB amp plates and incubated overnight at 37℃. Single colonies were taken and incubated in 4 ml LB liquid medium overnight at 37℃.

Plasmid preparation was performed using the QIAprep®Spin Miniprep Kit (Qiagen), using the pellet of 2 x 1,5 ml bacterial suspension, according to the manufacturer´s instructions. The plasmid concentration was determined by photometric measurement using the Nandrop instrument ND-1000.

To control for the success of nucleotide exchange, direct sequencing in both directions was performed (VBC Genomics, Vienna, Austria) using the NTBP+ fw primer (5´ AAGCGCAACAAGCCCACTGTCTAT 3´) [77]. Depending on the position of the point mutation within the *ABL1* TK sequence the following reverse primers were used: AA position 237 – 351 rev primer abl mid rev (5´ GCAGTTTCGGGCAGCAAGATC 3´); AA position 351 – end, rev primer NTBP-rev (5´ CTTCGTCTGAGATACTGGATTCCTG 3´) [77]. The sequence obtained after sequencing reaction was compared to the WT *ABL1 TK* sequence using the “bl2seq” within the BLAST program (http://blast.ncbi.nlm.nih.gov/Blast.cgi). In case of successful mutation reaction, the chromatogram was analyzed using the freely available “Chromas lite” program for additional verification.

For storage purposes the remaining bacterial suspension (+ 80% glycerine) was frozen on -80℃.

| Mutation | Base exchange | Fw primer (5´-3´) | Rev primer (5´-3´) |
|---|---|---|---|
| **E255K** | GAG → **A**AG | gggccagtacgggaaggtgtacgaggg | ccctcgtacaccttcccgtactggccc |
| **Y253F** | TAC → T**T**C | tgggcgggggccagttcggggagg | cctccccgaactggcccccgccca |
| **Y253H** | TAC → **C**AC | gcgggggccagcacggggaggtg | cacctccccgtgctggcccccgc |
| **F317L-A** | TTC → TT**A** | cccgttctatatcatcactgagttaatgacctacggga | tcccgtaggtcattaactcagtgatgatatagaacggg |
| **F317L-G** | TTC → TT**G** | cgttctatatcatcactgagttgatgacctacggg | cccgtaggtcatcaactcagtgatgatatagaacg |
| **F317C** | TTC → T**G**C | ctatatcatcactgagtgcatgacctacgggaacc | ggttcccgtaggtcatgcactcagtgatgatatag |
| **F317I** | TTC → **A**TC | ttctatatcatcactgagatcatgacctacgggaacc | ggttcccgtaggtcatgatctcagtgatgatatagaa |
| **F317V** | TTC → **G**TC | ttctatatcatcactgaggtcatgacctacgggaacc | ggttcccgtaggtcatgacctcagtgatgatatagaa |
| **V299L-T** | GTG → **T**TG | aaacaccctaacctgttgcagctccttgggg | ccccaaggagctgcaacaggttagggtgttt |
| **V299L-C** | GTG → **C**TG | aacaccctaacctgctgcagctccttggg | cccaaggagctgcagcaggttagggtgtt |
| **M244V** | ATG → **G**TG | cgcacggacatcaccgtgaagcacaagctgg | ccagcttgtgcttcacggtgatgtccgtgcg |
| **L248V** | CTG → **G**TG | atgaagcacaaggtgggcgggggcc | ggcccccgcccaccttgtgcttcat |
| **G250E** | GGG → G**A**G | acaagctgggcgagggccagtacgg | ccgtactggccctcgcccagcttgt |
| **Q252H-T** | CAG → CA**T** | ggcgggggccattacggggaggt | acctccccgtaatggcccccgcc |
| **Q252H-C** | CAG → CA**C** | ggcgggggccactacggggaggt | acctccccgtagtggcccccgcc |
| **T315A** | ACT → GCT | ccccgttctatatcatcgctgagttcatgacctac | gtaggtcatgaactcagcgatgatatagaacgggg |
| **T315I** | ACT → A**T**T | agcccccgttctatatcatcattgagttcatgacc | ggtcatgaactcaatgatgatatagaacgggggct |
| **M351T** | ATG → A**C**G | cagatctcgtcagccacggagtacctggaga | tctccaggtactccgtggctgacgagatctg |
| **F359V** | TTC → **G**TC | gagtacctggagaagaaaaacgtcatccacagagatc | gatctctgtggatgacgtttttcttctccaggtactc |
| **H396P** | CAT → C**C**T | cacctacacagcccctgctggagccaagt | acttggctccagcaggggctgtgtaggtg |
| **H396R** | CAT → C**G**T | cacctacacagcccgtgctggagccaagt | acttggctccagcacgggctgtgtaggtg |

**Table 4. Primer pairs designed for mutagenesis assays.** Indicated are the type of mutation, the resulting base exchange and the sequences of fw and rev primers required for mutagenesis assays using the QuikChange® II Site–Directed Mutagenesis Kit (Stratagene, CA, USA).

### 3.1.4 Testing for sensitivity, divergence and specificity

To determine the lowest size of mutated cell clones detectable by the LD-PCR approach (limit of detection or sensitivity of the assays), dilution series in a range of 0% to 100% (0%, 1%, 5%, 10%, 20%, 30%, 40%, 50%, 60%, 70%, 80%, 90%, and 100%) were established. For this purpose, DNA from mutated plasmids was mixed with WT plasmids resulting in a total amount of 10 ng/µl for each dilution step. The dilution series for each individual LD-PCR system was tested in a minimum of triplicate reactions. The lowest reproducibly detected dilution step lacking any cross-reactivity with the WT sequence was regarded as the limit of detection.

Since mutant and WT ABL1 TK sequences only differ by a single base, cross-reactions between WT and MUT Lig-oligonucleotide can occur. Thus, data calculated directly from the results of capillary electrophoresis were shown not to reflect the actual proportions of WT and mutated cell clones. To account for this problem resulting from the occurrence of cross-reactivity, calibration curves were established by preparing dilution series of quantified plasmids containing WT and Mut sequences for each mutation. Standard curves were used to convert values measured by LD-PCR into percentages of cells displaying a specific mutation, in order to account for the differences between measured and true values. A statistical program specifically designed for the present study was employed for the evaluation of measurements in CML patients.

To test for possible cross-reactions between different LD-PCR assays for adjacent *ABL1* TK point mutations, a series of experiments was performed. Dilution steps of 5%, 10%, 50% and 100% of plasmids representing the potentially cross-reacting LD-PCR system(s) were tested as described above and no relevant cross-reactivity was observed (data not shown).

#### 3.1.4.1 Statistical analysis

Statistical evaluation was performed by an external statistician. Initial assessment of confidence intervals was based on independent analysis of LD-PCR detection systems for three different mutations (T315I, E250G, Y253F). For each detection system, three dilution series $d_k$ were produced at levels x = 0,0.1,0.2,0.3,0.4,0.5,0.6,0.7,0.8,0.9,0.95 and 1. For each dilution series, three semi-nested PCR approaches were performed. Three independent LD-PCR analyses $l_{j(k)}$ were conducted independently, and each LD-PCR assay was subjected to two independent measurements by fluorescent capillary electrophoresis $a_{i(j(k))}$. Denoting the measurements with y, the following model was applied: $y_{ijk} = f(x) + d_k + l_{j(k)} + a_{i(j(k))} + \varepsilon_{ijk}$, where f(x) is a non-linear function, the factors $d_k$ , $l_{j(k)}$, and $a_{i(j(k))}$ are nested, and $\varepsilon_{ijk}$ is the error term. Analysis was restricted to polynomial regression, where f(x) is a polynomial of maximal

degree four. To assess the effects of the three factors, analysis of covariance was performed using SAS PROC GLM (SAS Institute Inc., SAS 9.1.3 Help and Documentation, Cary, NC: SAS Institute Inc., 2000-2004). After ensuring that neither the dilution series $d_k$ nor the fragment analysis $a_{i(j(k))}$ exert significant effects, the average over measurements by fluorescent capillary electrophoresis was taken and then the simplified model $y = f(x,\beta) + \varepsilon$ was considered, where the term $\varepsilon$ contains all random errors due to dilution series and LD-PCR. Based on the analysis, the error resulting from dilution series could be regarded as negligible compared to the error derived from the LD-PCR. The calibration task of specifying x based on measurements y was referred to as inverse regression. The computation of confidence intervals of x was performed in Matlab using polynomial regression as described [97].

#### 3.1.4.2 Establishment of calibration curves

Calibration curves were established for the detection and quantification of 21 point mutations, M244V, L248V, V299L-C/T, G250E, Q252H-C/T, Y253F, Y253H, E255K, T315A, T315I, F317C, F317I, F317L-A/G, F317V, M351T, F359V, H396P and H396R located in the *BCR-ABL1* TK domain. For this task, dilution series were generated by mixing MUT- in WT-plasmid DNA as described above.

To evaluate the number of experiments needed for the generation of calibration curves of high quality and to determine the parameters of sensitivity, divergence, specificity and reproducibility, a training-set including three mutations (G230E, Y253F and T315I) was analyzed. For this purpose each, three independent dilutions series were prepared for each mutation, which were tested by three independent semi-nested PCR amplification reactions. Each target was investigated three times using the appropriate LD-PCR assay and analyzed twice by capillary electrophoresis. Within this set of experiments, 702 data points were generated and evaluated by statistical methods as described. Results indicated that the LD-PCR itself was the only factor significantly influencing the outcome of the analyses.

Based on the observations in the training set, it was decided to limit the number of experiments for the establishment of calibration curves for the remaining point mutations (test set). Thus, one dilution series was used to perform one semi-nested PCR, which was analyzed by LD-PCR in triplicates and separated by a single run on the capillary electrophoresis instrument. An example of peaks obtained after capillary electrophoresis is shown in Figure 12.

The results were used to prepare calibration curves, a selection of which is shown in Figures 13a -13f.

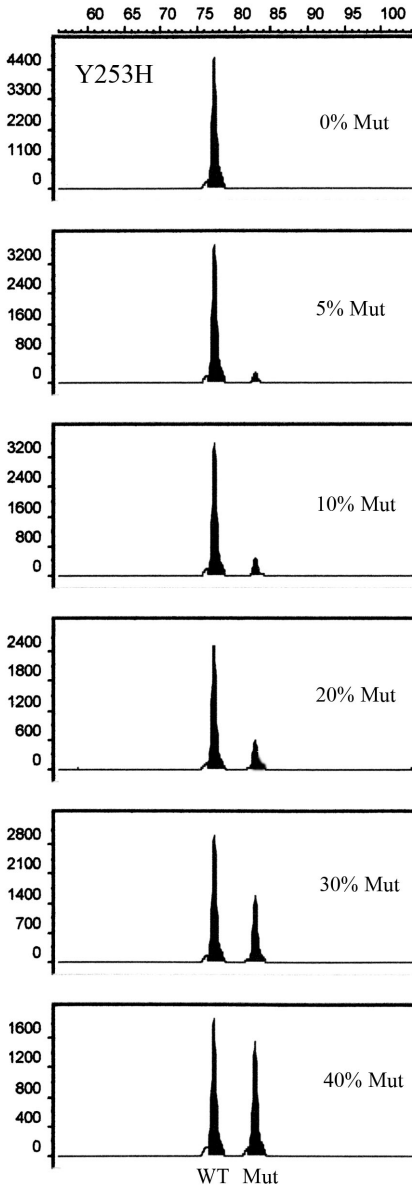


**Figure 12.** Displayed are results for parts of the Y253F plasmid dilution series (0% Mut to 40% Mut). LD-PCR products were separated by capillary electrophoresis. The x-axis shows the peak heights in rfu (relative fluorescence units), the y-axis shows the PCR products lengths in bp. The left peak indicates the WT PCR product, the right peak the MUT PCR product. Due to the stuffer sequence within the Lig-MUT oligo, the MUT PCR product is six bp longer.

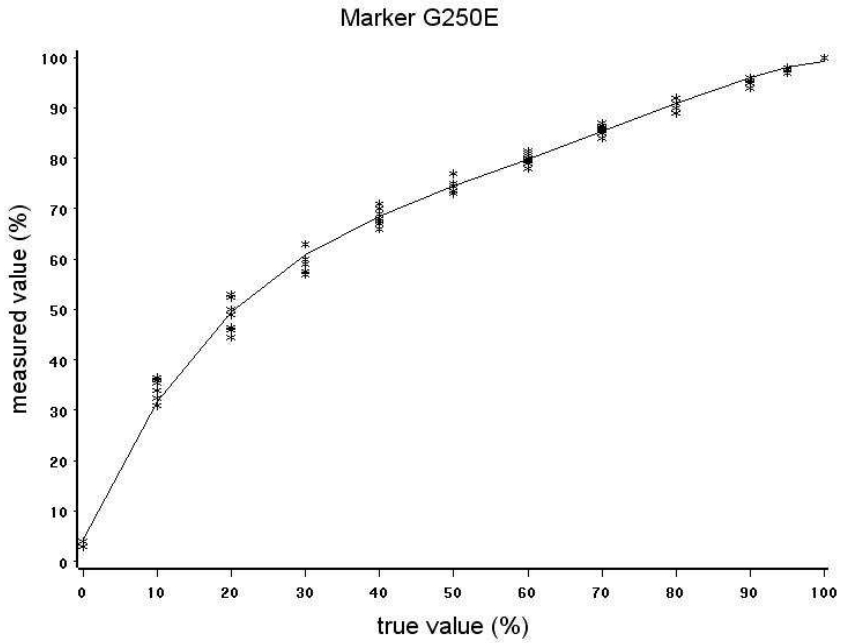


**Figure 13a.** Calibration curve for G250E.

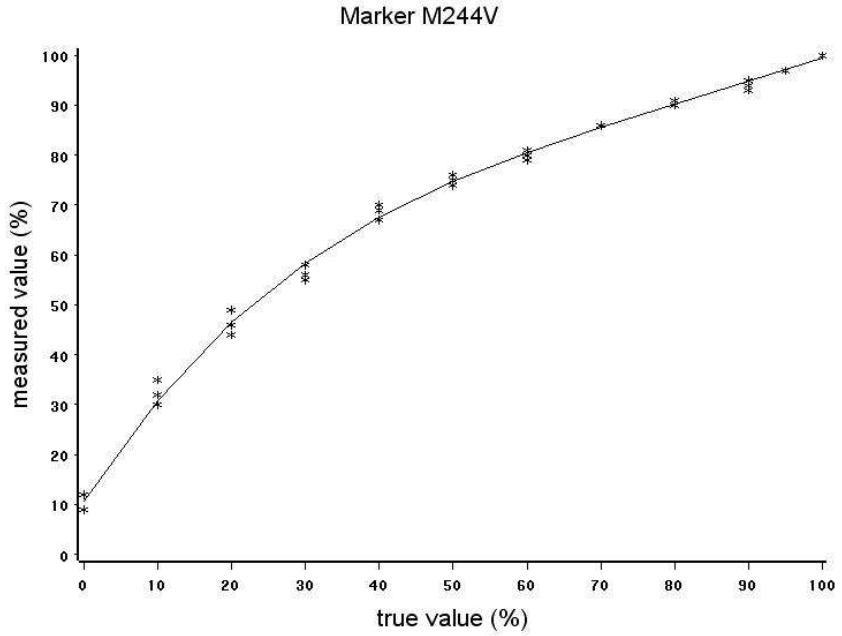


**Figure 13b.** Calibration curve for M244V.

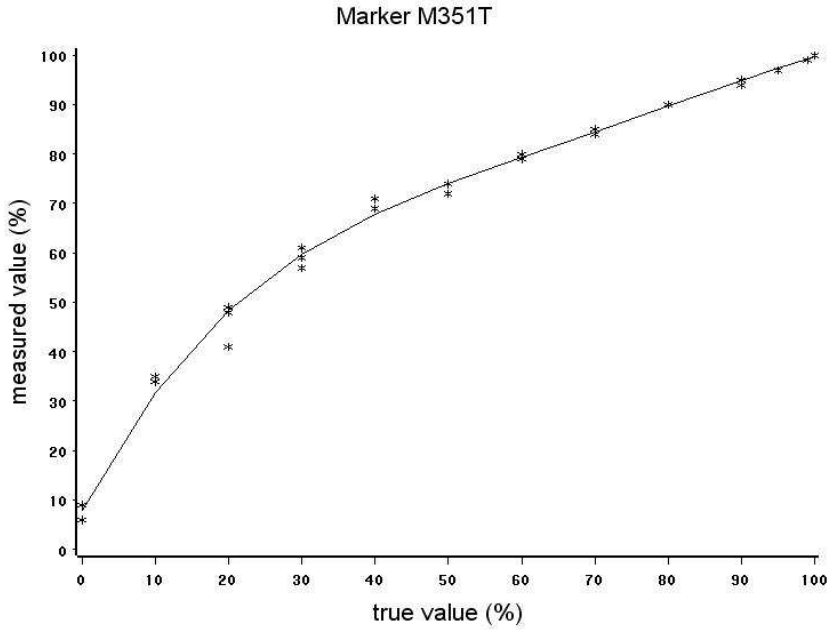


**Figure 13c.** Calibration curve for M351T.

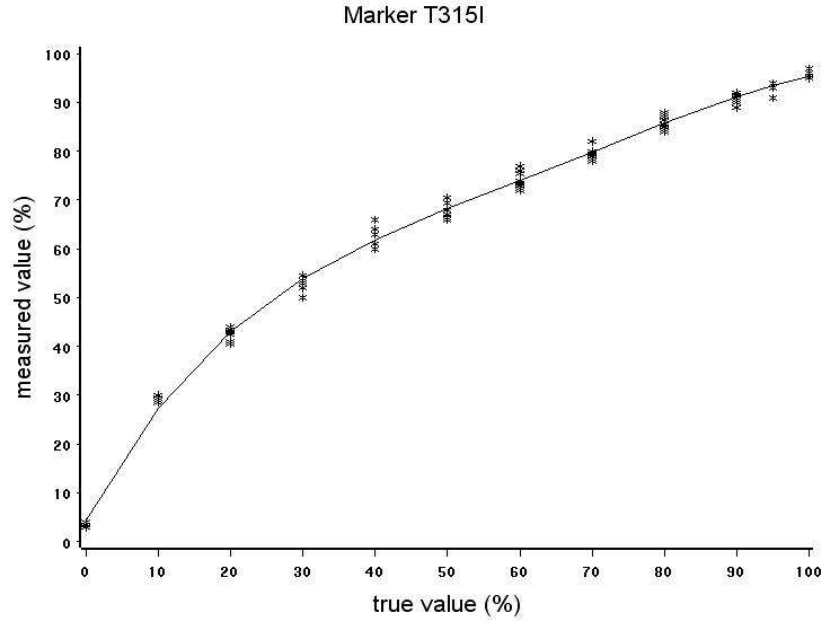


**Figure 13d.** Calibration curve for T315I.

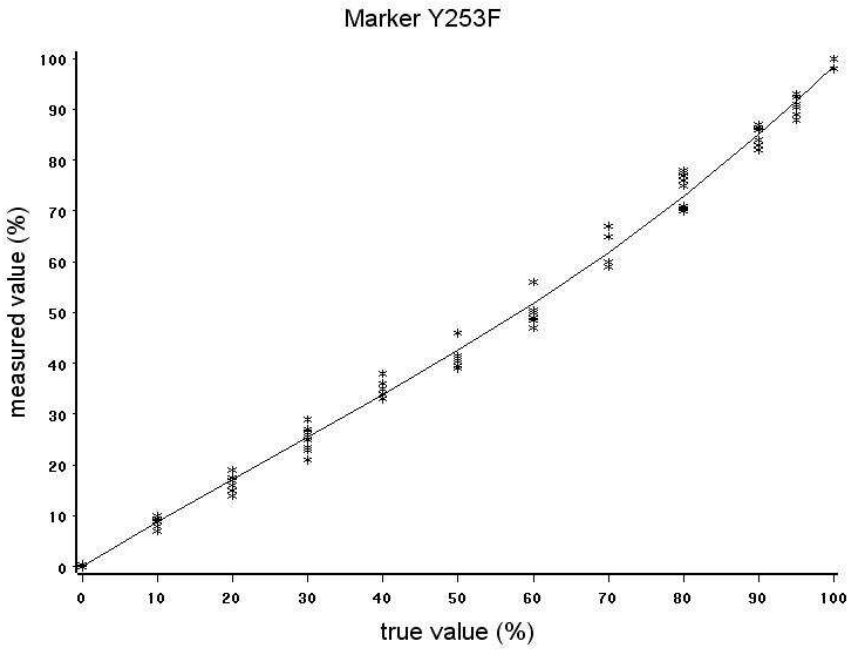


**Figure 13e.** Calibration curve for Y253F.

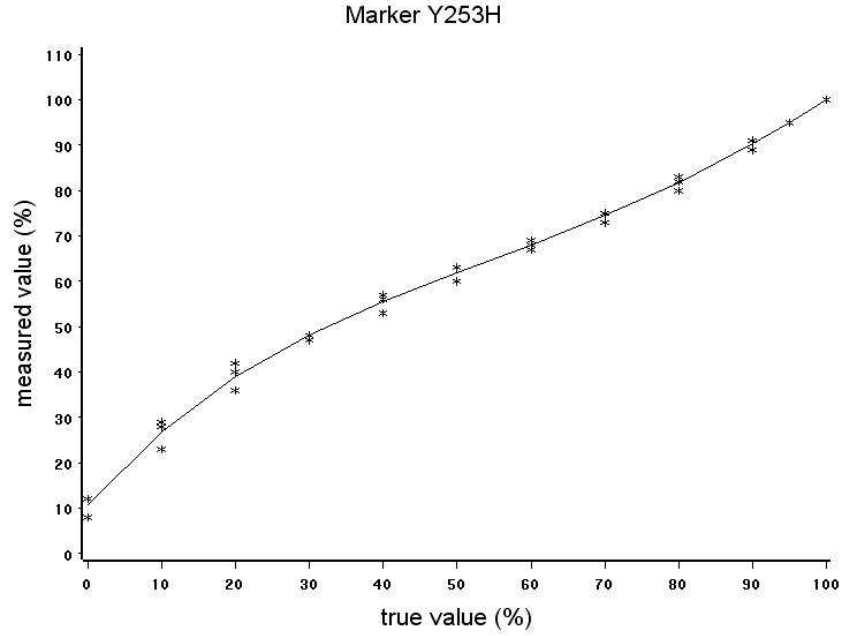


**Figure 13f.** Calibration curve for Y253H.

#### 3.1.4.3 Sensitivity, specificity and reproducibility of the LD-PCR assays

Based on the analyses of dilution series, sensitivity, specificity and reproducibility were tested for all 21 LD-PCR systems. The lowest reproducibly detected dilution step lacking cross-reactivity was defined as the detection limit (sensitivity) of the assays. Depending on the level of cross-reactivity with the WT sequence, detection limits of 1% (for LD-PCR systems M244V, M351T, F317L-A, Q252H-T, F317C, F317V, L248V, T315A, V299L-C, V299L-T, F359V, H396P and H396R), and 1-5% (for Y253H, F317L-G, E255K, Q252H-C, F317I, T315I, G250E and Y253F) were identified.

Cross-reactions with the WT sequence, differing by a single base, influenced the specificity of the assays. Thus, the expected (i.e. true) and the measured values were not concordant. Calibration curves were established, facilitating correction of the measured value to determine the true value. The implementation of calibration curves as a correction tool was feasible because the reproducibility of the assays was high, revealing an inter-assay variability of ± 2%. Results obtained from calibration curves analyses were the basis for a dedicated computer program established by the statistician, which facilitated automatic conversion of LD-PCR results to the size of mutant clones. Moreover, 95% confidence intervals (CI) were calculated and determined to be in a range of ± 5%. This implies that consecutive measurements of mutant clones in a patient can be regarded as true changes if the 95% CIs do not overlap. Hence, the elevation or decrease by 10% can be regarded as a true change in the size of mutant clones.

### 3.1.5 Analysis of patient samples

#### 3.1.5.1 Proof of principle experiment

To assess the clinical applicability of the LD-PCR systems, a cohort of 30 chronic phase CML patients with suboptimal response to imatinib and 7 control patients with optimal response to treatment were included in a pilot study. RNA extraction and cDNA synthesis were performed as indicated above. Detection of *BCR-ABL1* point mutation was done by bidirectional sequencing. Seven patients revealed four different point mutations including M244V, Y253H, G250E and M351T (Table 5). In contrast, none of the control patients showed *BCR-ABL1* TK point mutations.

| Patient | Result Direct Sequencing | Result LD-PCR (% MUT) |
|---|---|---|
| 1 | G250E | 100 |
| 2 | Y253H | 100 |
| 3 | G250E | 100 |
| 4 | M351T | 14 |
| 5 | M244V | 97 |
| 6 | G250E | 51 |
| 7 | M351T | 100 |

**Table 5. Results of "Proof of principle experiment" for the applicability of LD-PCR.** Type of mutation detected by sequence analysis in seven CML patients with suboptimal response to treatment with imatinib and proportion of mutant clones determined at individual time points by LD-PCR and fluorescent capillary electrophoresis are displayed.

Moreover, this proof of principle experiment was used to determine the applicability of LD-PCR to the monitoring of subclone-specific proliferation kinetics. Serial blood specimens obtained from a CML patient under imatinib treatment, with a M351T point mutation were analyzed by LD-PCR. LD-PCR results were correlated with the *BCR-ABL1/ABL1* ratio measured by real-time

PCR analysis. As shown in Figure 14, the mutant subclone (solid line) was not detectable within the first weeks of imatinib treatment, with the exception of day 48, when the clone was transiently detected at a level of 6%. After approximately one year of treatment, the size of the M351T subclone increased to 82%, and within the next two months, to 92% of the *BCR-ABL1* expressing cells. During the entire observation period, fluctuating *BCR-ABL1/ABL1* expression (dashed line) was detected, with an increase to 100% concomitantly with the expansion of the mutated subclone.

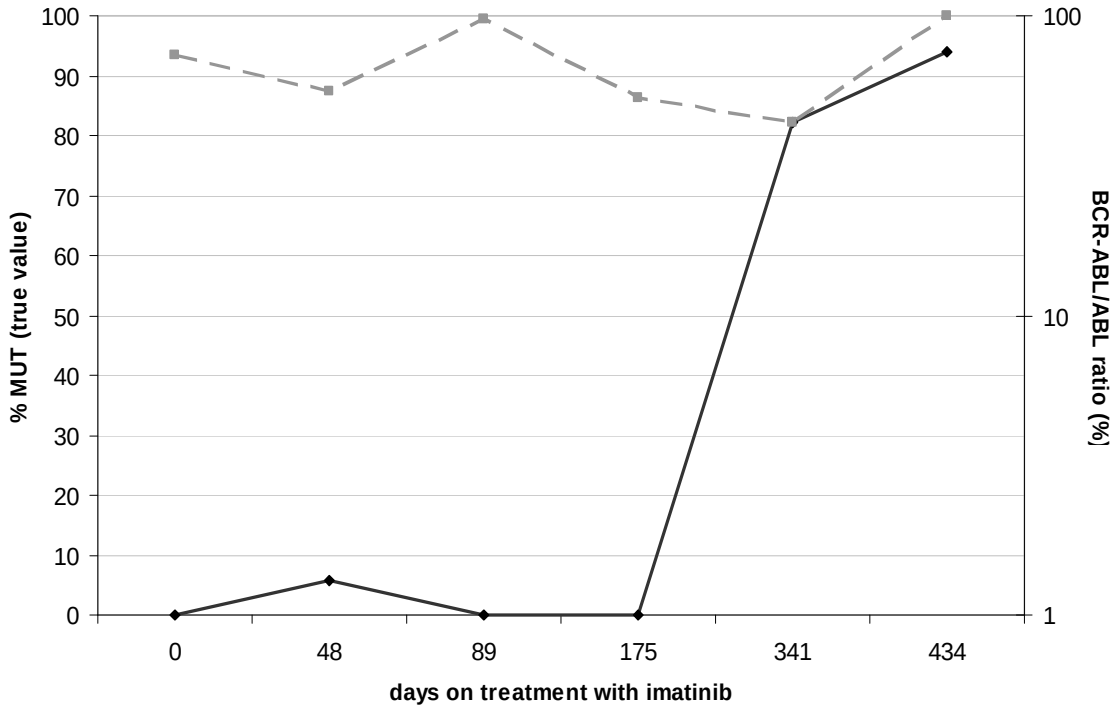


**Figure 14.** Proliferation kinetics of a M315I point mutated subclone in a CML patient under imatinib treatment.

### 3.1.6 LD-PCR application to the detection/quantification of the V617F mutation within the JAK2 gene

The point mutation leading to replacement of the amino acid valine by phenylalanine at position 617 in the JAK2 protein is a critical activating genetic event in patients with myeloproliferative disorders (MPD). The detection of this mutation and quantitative monitoring of cells carrying the underlying nucleotide exchange are essential diagnostic tests in the surveillance of patients with MPD. In view of the clinical importance, it was of great interest to assess the applicability of the LD-PCR technique at this task.

### 3.1.7 Design of the LD-PCR system for analysis of the V617F mutation

Based on the experience gained from the related work in CML, LD-PCR oligonucleotides required for the detection/quantification of the point mutation in the *JAK2* gene leading to the V617F variant were designed as described above. Oligonucleotides were designed in a reverse complementary fashion to display a hybridization temperature of 70℃ (Table 6)

| **LD-System** | Primer *Stuffer* **Oligo** | **Hybridization-temperature (C°)** | **Lig/Hyb oligo properties** | | |
|---|---|---|---|---|---|
| **JAK2** | | | lengths (bp) | G/C content (%) | TM (°C) |
| Lig Oligo WT | gggttccctaagggttgga**ctcacaagcatttggttttaaattatggagtatgtg** | 70 | 36 | 33 | 71 |
| Lig Oligo Mut | gggttccctaagggttgga*caaccc***ctcacaagcatttggttttaaattatggagtatgtt** | | 36 | 31 | 70 |
| Hyb Oligo | 5´Phos **tctgtggagacgagaatattctggttcag**tctagattggatcttgctggcac | | 29 | 45 | 71 |

**Table 6.** Characteristics of the LD-PCR detection system for JAK2 V617F.

### 3.1.8 Experimental set-up

To pre-amplify the LD-PCR target sequence of interest, a specific PCR reaction was established. PCR fw and rev primers were designed using the following gene-bank sequence: [>gi|13325062|ref|NM_004972.2| Homo sapiens Janus kinase 2 (a protein tyrosine kinase) (JAK2), mRNA] and the PrimerExpress software 2.0 (AB). From a list of potential fw and rev primers provided by the program, three fw primers (JAK2 fw1 5´ GCAGCAAGTATGATGAGCAAGCT 3`; JAK2 fw2 5´ TGAAGCAGCAAGTATGATGAGCA 3´; JAK2 fw3 5´ TCAGAGTCTTTCTTTGAAGCAGCA 3´) and one rev primer (JAK2 rev 5´ TGCCAACTGTTTAGCAACTTCAAG 3`) were selected and tested for the best PCR performance. The PCR reaction included the following reagents: each 400 nM of each fw and rev primer, 2 mM dNTPs, 0,5 U HotStar® Polymerase (Promega), 10 x buffer (Promega) and 50 ng template DNA (100% WT plasmid DNA) in a total volume of 25 µl. The PCR reaction was performed according to the following cycling protocol: 94℃ for 5 min, fol lowed by 30 cycles of 94℃ for 1 min, 60℃ for 30 sec. and 72℃ for 1 min, and coo ling to 4℃. PCR products were analyzed on a 1.5% agarose gel. Based on its superior performance, the JAK2 fw1 primer was selected for further experiments.

Appropriate dilution series of WT and mutant plasmids were generated, and the LD-PCR approach was carried out as described. Statistical analysis of the sensitivity, specificity and reproducibility were performed. The detection limit of the assay was determined to be 1% and the data generated were analyzed by a dedicated computer program to convert the measured into true values.

### 3.1.9 Analysis of patient samples

Fifteen patient specimens, either methanol/acetic acid-fixed cells or fresh white blood cells from patients suffering from different myeloproliferative disorders (including essential thrombocytopenia and myelofibrosis) were analyzed for the presence and amount of V617F positive cells according to the protocols established. In 12 patients, the V617F mutation could be detected in different proportions of the cells analyzed. The results are displayed in Table 7.

| Patient | Result of LD-PCR (% Mut) |
|---|---|
| Pat 1 | 15 |
| Pat 2 | 95 |
| Pat 3 | 93 |
| Pat 4 | 45 |
| Pat 5 | 0 |
| Pat 6 | 6 |
| Pat 7 | 41 |
| Pat 8 | 0 |
| Pat 9 | 0 |
| Pat 10 | 46 |
| Pat 11 | 13 |
| Pat 12 | 57 |
| Pat 13 | 60 |
| Pat 14 | 31 |
| Pat 15 | 23 |

**Table 7.** LD-PCR results obtained in 15 patients with suspicion of V617F within the JAK2 gene.

## 3.2 PNA/hybprobe assay

In view of the well established applicability of PNA-based assays to specific detection of point mutations, it was of interest to test this approach in comparison to the LD-PCR technique in order to assess whether one of these methods would provide advantages for diagnostic applications in the clinical setting.

### 3.2.1 Design of Hybprobes and PNA oligonucleotides

The LightCycler Probe Design Software 2.0 was used to design hybprobes specifically detecting the T315I point mutation. The proportion of the *ABL1* TK sequence part containing the AA position 315 was used as a basis for the design and the following setting were chosen: *LC DNA HP Master; Experiment type: mutations; Hybprobes; assign the base to be targeted; select specificity of the hybprobes for the WT or the mutated base*. Under “primer and probe sets”, a list of potential fw and rev primers, anchor- and sensor probes was displayed. The final primer and probe set was selected based on the ranking established by the software.

PNA oligonucleotide design was done according to several criteria: i) the PNA oligonucleotide was designed to be complementary to the WT sequence; ii) it had to be located within the sequence flanked by fw and rev primers; iii) the location of the point mutation had to be in the middle part of the PNA sequence, resulting in the competitive hybridization of anchor or sensor probes with the PNA oligonucleotide; iv) the maximum lengths of the PNA oligonucleotide was 19 bp to provide adequate solubility; v) the melting temperature of the PNA oligonucleotide had to be higher than the extension temperature of the polymerase to prevent premature displacement vi) the ABI PNA Probe designer (http://www.appliedbiosystems.com/support/pnadesigner.cfm) was employed to prevent secondary structure formation.

### 3.2.2 Establishment of the PNA/hybprobe assay

#### 3.2.2.1 Optimization of reaction conditions

To find optimal reaction conditions, a variety of experiments using different concentrations of hybprobes, PNA oligonucleotides and control plasmid/patient DNA were performed (overview in Table 8).

| PNA conc. (µM) | Anchor/Sensor probe conc. (µM) | Plasmid conc.(ng) | Patient DNA conc. (ng) |
|---|---|---|---|
| 0,25 | 0,2 | 100 | 50 |
| 0,35 | 0,32 | 50 | 100 |
| 0,45 | | 0,5 | |
| 0,55 | | 0,005 | |
| 0,65 | | 0,00005 | |
| 0,75 | | | |
| 1,25 | | | |

**Table 8.** Reaction conditions tested for the establishment of the PNA/hybprobe assay.

Within this first set of experiments, a rough titration of the PNA oligonucleotide (0,25 µm; 0,75 µM and 1,25 µM) was performed, while the amounts of fw (5´CTGCAGTCATGAAAGAGATCAA 3´) and rev primers (5´ CATGTACAGCAGCACCAC 3´), anchor (5´ LC Red 640-CTCAATGATGATATAGAACGGGGGCTC-Phosphate) and sensor (5´ TCCAGGAGGTTCCCGTAGGTCATG-Fluorescein 3`) probes remained constant using standard concentrations of 500 nM and 0,2 µM, respectively, in the presence of 5 x Genoptyping Mastermix for LightCycler®480. The hybrobe/PNA assay was carried out using a modified hybprobe amplification program, adding a PNA annealing step at the corresponding PNA melting temperature (70℃): pre-incubation for 10 sec at 95℃, followed by 30 amplification cycles with 10 sec at 95℃, 10 sec at 70℃, 10 sec at 60℃ and 10 sec at 72℃. The melting curve was established under the following conditions: 1 min at 95℃ followed by 2 min of gradual increase in temperature from 40℃ to 95℃, and subsequent cooling to 4℃.

The concentration of the template plasmid DNA was 50 ng for analysis of 100% WT, T315I, T315A. Results showed that the amplification of the WT plasmid DNA could be strongly inhibited by all 3 PNA concentrations tested, in contrast to the control experiment lacking any PNA oligonucleotide (Figure 16).

The PNA concentration of 1,25 µM, provided only slightly stronger inhibition of WT amplification than that observed at 0,75 µM. The latter concentration was therefore favoured in order to save costs. The inhibition by 0,25 µM PNA oligonucleotide concentration was weaker in comparison to 0,75 µM. To further optimize the PNA oligonucleotide concentration, a fine titration experiment was performed covering the range of 0,25 µM and 0,75 µM (0,35 µM, 0,45 µM, 0,55 µM and 0,65 µM; data not shown). No further improvement could be achieved and the optimal concentration for the PNA oligonucleotide was therefore defined at 0,75 µM.

To optimize the input of plasmid DNA, different amounts (50 ng, 500 pg, 5 pg, 50 fg) were tested using 100% WT, T315I and T315A and T315I dilution steps (0,01%, 0,1%, 1%, 5% and 10%). Template amounts of 50 ng and 500 pg permitted the detection of the 1% dilution step, while this level of sensitivity was not achievable with 5 pg and 50 fg template. The dilution steps of 0,01% and 0,1% could not be detected at any of the template concentrations tested indicating that the limit of detection for mutant subclones by the PNA/hybprobe assay might be around 1%. Fifty ng of plasmid DNA was the finally selected amount of template because it provided slightly higher fluorescence intensity than 500 pg template

In attempts to improve the fluorescence intensity and thus the limit of detection of the assay, the concentrations of anchor and sensor probes were increased to 0,32 µM. The results showed, however, that the sensitivity could not be significantly improved.

Hence the initial experiments indicated that the following reaction conditions are optimal: 500 nM each fw and rev primer; 0.2 µM each anchor and sensor probe; 0.75 µM PNA oligonucleotide and 50 ng plasmid DNA template .

### 3.2.2.2 Testing of sensitivity and specificity

To determine the occurrence of cross-reactions and thus define the specificity of the assay, 100% WT, T315I and T315A plasmids were analyzed. Melting curve analyses permitted the differentiation between WT, T315I and T315A. The strongly inhibited WT clone showed a melting temperature of 55℃, T315A of 61℃ and T315I of 67℃. The results revealed tha t overlapping melting temperatures did not occur and WT and both mutated clones could be unambiguously discriminated.

To define the sensitivity of the hybprobe/PNA assay, 50 ng of the dilution steps 0%, 0,1% 1%, 5%, and 100% MUT (mutant clone), generated for LD-PCR analyses were amplified using the optimized reaction conditions: 0,2 µM of each anchor and sensor hybprobes and 0.75 µM PNA oligonucleotide.

The assay was shown to display a detection limit of 1% mutated cell clones (Figure 15).

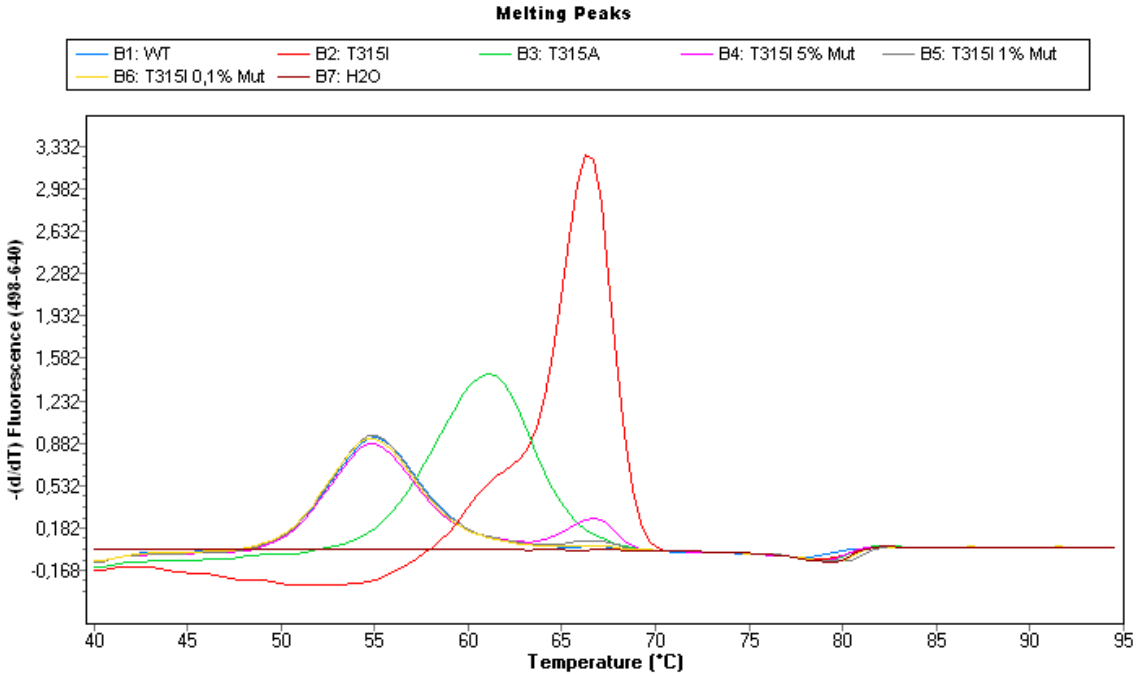


**Figure 15.** Experimental results of the assessment of sensitivity. The Y-axis shows the relative fluorescence intensity (displayed as first derivation) of the melting peaks, and the X-axis the melting temperature of the PCR amplicons in ℃. The last dilution step detected was 1%,

whereas the 0,1% step showed no amplification distinguishable from the negative control (A. bidestillata).

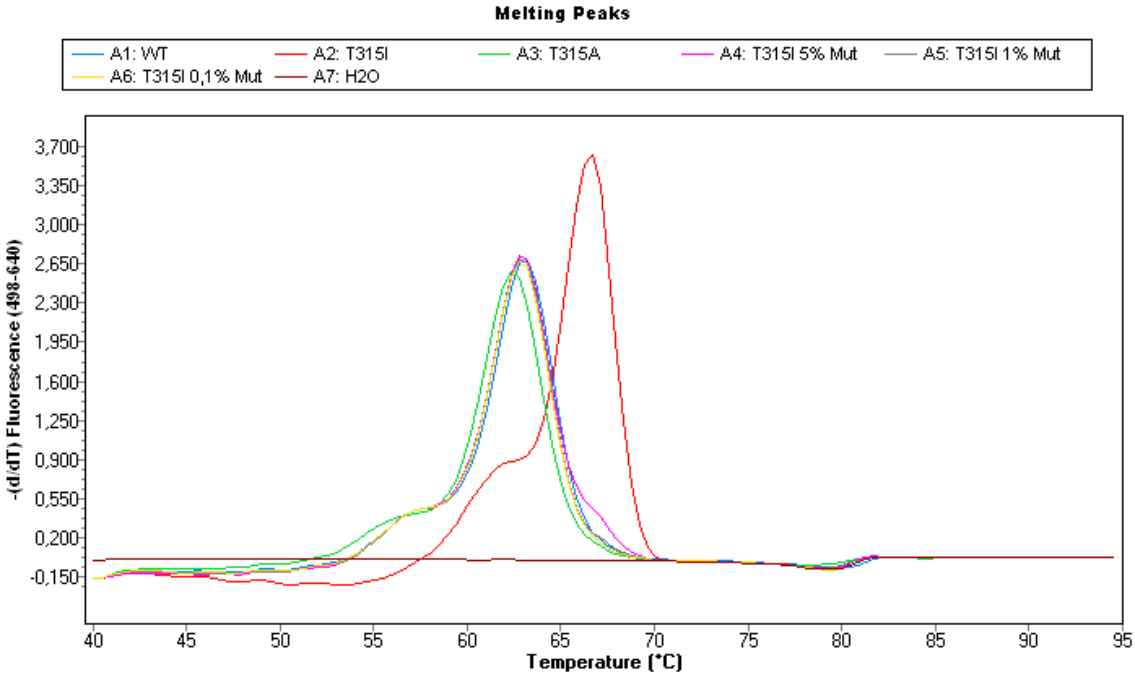


**Figure 16**. PNA/Hybprobe approach without PNA oligonucleotide addition. The Y-axis shows the relative fluorescence intensity (displayed as first derivation) of the melting peaks, the X-axis the melting temperature of the PCR amplicons in ℃. Amplification of WT, T315A ,and T315I plasmid DNA is shown.

### 3.2.2.3 PNA oligonucleotide re-design

The PNA oligonucleotide was designed to overlap and thus interfere both the anchor and the sensor hybprobe. Since from the theoretical point of view, this design could result in a weaker inhibition of the WT signal, the PNA oligonucleotide was re-designed to only overlap with the sensor hybprobe. Additionally the PNA oligonucleotide was extended in length to achieve a higher hybridization temperature, clearly different from the Hybprobe annealing temperature. The newly designed PNA oligonucleotide was tested by applying the optimized parameters indicated above. Indeed, a considerably stronger inhibition of the WT signal, compared to the original PNA could be achieved

(Figure 17). However, the sensitivity of the assay for the detection of T315I mutant cells remained at 1%.

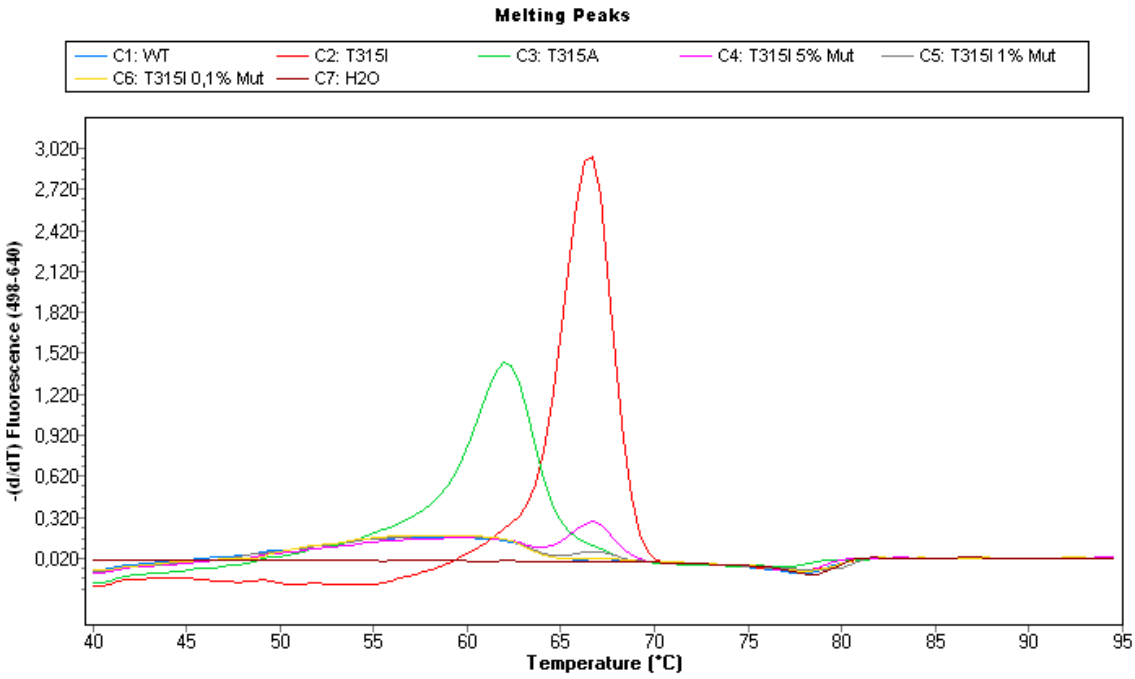


**Figure 17.** Test results of the newly designed PNA oligonucleotide. The Y-axis shows the relative fluorescence intensity (displayed as first derivation) of the melting peaks, the X-axis the melting temperature of the PCR amplicons in ℃. The signal for the WT sequence is strongly inhibited. The last dilution step detected was 1% T315I point mutated subclone.

## 3.2.2. Analyses of patient samples

To demonstrate the clinical applicability of the T315I PNA/hybprobe approach, CML patient samples with known T315I mutation were analyzed. However, using the optimal reaction conditions established for plasmid DNA, no results could be obtained in the majority of instances. Therefore, further optimization steps had to be implemented. This mainly concerned the number of amplification cycles, which were increased from 30 to 50, and the input of patient DNA, which was increased to 100 ng. Under these conditions, the T315I could be detected in all patients analyzed (Figure 18).

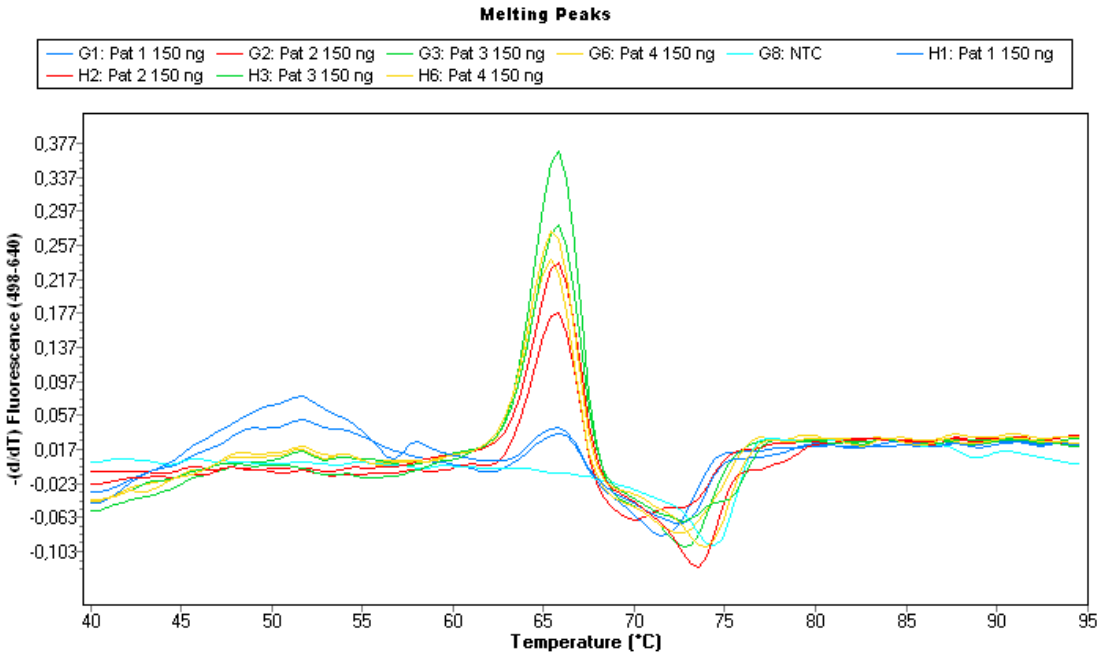


**Figure 18.** Analysis of CML patients with known T315I mutation. The Y-axis shows the relative fluorescence intensity (displayed as first derivation) of the melting peaks, the X-axis the melting temperature of the PCR amplicons in ℃. Patient sam ples were analyzed in duplicates clearly indicating a T315I mutation by revealing a melting temperature of 67℃.

# 4 Discussion

Point mutations within the *ABL1* TK domain are the most frequent cause of imatinib failure in CML [44], and can result in disease progression. This finding may necessitate the change of treatment to another TKI, such as nilotinib or dasatinib or, in some instances, the implementation of allogeneic stem cell transplantation.

Accordingly, the ELN organization recommends to search for point mutations upon diagnosis of suboptimal response or treatment failure [35]. Bidirectional sequencing of the entire *BCR-ABL1* TK domain currently represents the method of choice offering a sensitivity of about 20%. This detection limit could be inadequate in the clinical setting because it may result in delayed detection of point mutations and consequently late diagnosis of impending relapse.

More sensitive methods are available, e.g. HPLC (high pressure liquid chromatography), described to provide a sensitivity of 0,1-15% [79-81]. However, HPLC is a rather laborious procedure requiring appropriate, expensive equipment. Another technique, ASO-PCR, displays extraordinarily high levels of sensitivity, but the applicability of this technique in the clinical setting is questionable because the clinical relevance of very small mutant cells clones appears to be very low [83].

However, even the presence of point mutated subclones at higher levels is not necessarily predictive for the onset of clinical resistance. Results obtained from analyses of several patient samples indicated that mutant clones can either disappear spontaneously, possibly attributable to the restricted self-renewal capacity of such clones, or they can persist on low levels without further clonal evolution, or clones can increase in size and ultimately confer resistance to treatment [95].

The aim of this study was therefore the development of methodological approaches to the detection of point mutated subclones in a clinically relevant range of sensitivity, based on the use of standard equipment available in most molecular laboratories. Moreover, the possibility to determine the size of

mutated subclones permitting the monitoring of proliferation kinetics was envisaged.

In their paper, Schouten et al [87] presented the power of the MLPA technology for the detection of multiple point mutations and SNPs. This provided the basis for the idea to develop a new methodology, based on the principle of this technique.

The newly established ligation-dependent PCR technique (LD-PCR) was designed to target only one point mutation per reaction, and therefore contains only few oligonucleotides including one specific for the WT sequence, and one specific for the point-mutated sequence (6 bp longer) which bind to their target sequences in a competitive manner (ligation oligonucleotides). A third, the so-called hybridization oligonucleotide, which binds immediately 3´ to the point mutation, is subsequently ligated to its adjacent counterpart. The inclusion of a ligation step at the site of mutation is an important feature providing increased specificity in comparison to techniques such as ASO-PCR, which rely only on sequence-specific hybridization of primers. Moreover, the possibility of using universal primers for PCR amplification of the ligated template molecules provides the ability to analyze different point mutations within one workflow, which is both time-saving and convenient.

An important modification compared to the MLPA approach was the reduction of the hybridization time from 16 hours to one minute only. This modification was introduced to due several reasons: i) the LD-PCR assay includes only three oligonucleotides instead of up to 80, and long hybridization times are therefore not required ii) extension of the hybridization time affects the ratio of WT- and MUT- specific signals (data not shown). This might be mainly attributable to the increased occurrence of non-specific hybridization of the ligation oligonucleotides, as described (www.mlpa.com). Hence, regardless of the high specificity provided by the ligase enzyme, cross-reactivity of the ligation oligonucleotides with the WT- and MUT- sequence occurs, and this seems to be intensified by long hybridization times.

With regard to the design of LD-PCR oligonucleotides, the rules published for MLPA were followed whenever possible, but this aim was not achievable in all

instances. The major challenge was the fixed position of the point mutation within the *BCR-ABL1* TK sequence. This is an important difference to MLPA approaches, which target specific genes, but not specific bases. Difficulties were observed in the design of tests for mutations within the p-loop of the *BCR-ABL1* TK domain. This was mainly attributable to the very high C/G content within this region, which required the design of short oligonucleotides, far below the lengths of 21 nt recommended by the MLPA guidelines. Shorter oligonucleotides, however, show a higher frequency to hybridize to similar but incompletely homologous nucleotide sequences. To overcome this difficulty, LD-PCR systems were designed to bind at a higher hybridization temperature of 75℃.

To set up the new technique and to test the designed LD-PCR oligonucleotides, calibration and positive control samples had to be implemented. Synthetically produced oligonucleotide template sequences were first used to determine the functionality of several LD-PCR oligonucleotides. These synthetic templates contained the oligonucleotide sequences targeted within the patient cDNA, and dilution series of MUT and WT sequence were generated across a range from 0%-100% mutated sequence mixed in WT sequence (0%, 5%, 10% 20%, 30%, 40%, 50%, 60%, 70%, 80% 90%, 100%). This approach was subsequently abandoned, because it does not adequately reflect the physiological situation owing to the lack of background cDNA present in the patient samples. A test system, more closely mimicking patient cDNA might be a cell line. A BaF3 murine cell line carrying the *BCR-ABL1* rearrangement was generated by a group in Oregon [98], and this cell line is also available with a variety of *BCR-ABL1* TK domain point mutations. However, the BaF3 cell line did not appear to be adequate as a reference system based on the following considerations:

a) only a limited number of point mutated Baf3 cell lines were available either commercially, or to a small extent, within scientific collaborations, and the costs of the commercial products were prohibitive. b) the generation of different point mutated BaF3 cell lines, for all mutations (≥ 21) required would have been too laborious and time-consuming. Based on these considerations, it was decided to generate plasmids carrying the *BCR-ABL1* sequence of interest and to

introduce the required point mutations via mutagenesis assays. This procedure seemed to be a straight-forward concept. Plasmid-based positive control samples were generated for 21 point mutations frequently occurring within the *BCR-ABL1* TK domain, and for the V617F mutation within the JAK2 gene. For each LD-PCR system, plasmid dilution series were generated as indicated above and used to validate the assays with regard to sensitivity, specificity and reproducibility.

The sensitivity of the LD-PCR assays was demonstrated to be in a range of 1-5%. This was mainly attributable to some degree of cross-reactivity of the MUT Lig oligonucleotide with the WT sequence and vice versa, as already described. It needs to be considered, however, that capillary electrophoresis which had been selected as the detection method, cannot provide a much better sensitivity than 1%. This results from the fact that the peak heights of PCR amplicons can be detected only up to a maximum of about 6 000 rfu (relative fluorescence units) and a minimum of 50 rfu. Since LD-PCR is a comparative assay between WT and MUT sequences, the detectable signal intensities indicated maximally permit the analysis of peak ratios of 6 000 : 50, which corresponds to 0.8%. The assay reproducibility of the assay was demonstrated to be in a range of ± 2%. However, this does not reflect the intrinsic variability in the clinical setting but only describes the robustness of the assays. Thus, the most important issue was to determine which results reflect true changes in the size of mutant clones when measuring consecutive patient samples. Based on the statistical calculations, a true change was determined to be in a range of ± 5%, based on the lack of overlap between 95% confidence intervals. The size of the mutant clones and the corresponding 95% confidence intervals can be easily calculated by implementing the computer program, generated specifically for this technique.

Based on the accurate evaluation of the LD-PCR method, the technique was tested on patient samples obtained from CML patients with suboptimal response to imatinib treatment in a proof-of-principle study. Analyses in 30 patients demonstrated that the LD-PCR system can reliably detect the mutant subclones and their size can be calculated using a dedicated computer

program. Moreover, it could be demonstrated that the proliferation kinetics of a mutant subclone can be documented by the LD-PCR approach. Since these observations were based on a preliminary set of experiments, the benefit of the LD-PCR approach in the clinical setting had to be confirmed in a lager cohort of patients. The first results of the study indicate that the percentage of *BCR-ABL1* positive cells in the samples tested might be an additional parameter influencing the accuracy of the LD-PCR approach. Further testing within extensive clinical studies is ongoing.

A further aim of this diploma thesis was to proof whether the LD-PCR technique developed could be adapted to sensitive detection/quantification of point mutations in genes other than *BCR-ABL1.* This was demonstrated by using the clinically important point mutation V617F in the *JAK2* gene in patients suffering from different myeloproliferative disorders. The detection of this point mutation was shown to be of clinical relevance because it is associated with a constitutive tyrosine kinase activity contributing to malignant transformation [99]. The LD-PCR assay detecting/quantifying the JAK2 V617F mutation was established according to the procedure described for the *BCR-ABL1* point mutations. To demonstrate that this method provides reliable results, patients who tested positive for this mutation at the University of Innsbruck by a different qualitative method were re-evaluated using the LD-PCR technique. Identical results were obtained by both methods, thus confirming the clinical applicability of the LD-PCR method for the detection of the *JAK2* V617F mutation. Moreover, the available results indicated, that the LD-PCR technique can be adapted to detection/quantification of virtually any other point mutation of interest, provided that the target region contains a DNA/cDNA sequence permitting the design of LD-PCR oligonucleotides.

As potential alternative to the LD-PCR method, a technique based on specific amplification of the mutant subclone and simultaneous repression of WT amplification was established. This method combined the use hybprobes, specifically amplifying the point mutated sequence with PNA clamping of the WT sequence. This assay was expected to permit more sensitive qualitative detection of the clinically important T315I point mutation. However, despite the

efforts to optimize the PNA/hybprobe assay for maximum sensitivity, the lowest achievable limit of detection for the T315I point mutated subclones was 1%, which is not superior to the LD-PCR approach. Since the LD-PCR technique also permits quantitative assessment of the mutant subclones, it remains the method of choice in our hands. If in specific instances a higher level of sensitivity is desired, ASO-PCR can be employed. It is currently not clear, however, whether the detection if mutant subclones at a higher level of sensitivity is of potential clinical relevance. It can be expected that clinical implementation of the LD-PCR technique in CML and other disease entities will permit early assessment of impending resistance to treatment as a basis for timely and appropriate modification of therapy.

## Concluding remarks

The description of the LD-PCR technique and its application to the detection and quantification of point mutations within the *BCR-ABL1* TK domain was recently published in *Leukemia* [100].

# 5 References


1. Hehlmann R, Hochhaus A, Baccarani M. Chronic myeloid leukaemia. *Lancet*, 370(9584), 342-350 (2007).
2. Kantarjian HM, Deisseroth A, Kurzrock R, Estrov Z, Talpaz M. Chronic myelogenous leukemia: a concise update. *Blood*, 82(3), 691-703 (1993).
3. Faderl S, Talpaz M, Estrov Z, Kantarjian HM. Chronic myelogenous leukemia: biology and therapy. *Annals of internal medicine*, 131(3), 207-219 (1999).
4. http://www.cancer.gov/cancertopics/pdq/treatment/CML/Patient/. General information about chronic myelogenous leukemia. (2010)
5. Kantarjian HM, Dixon D, Keating MJ *et al.* Characteristics of accelerated disease in chronic myelogenous leukemia. *Cancer*, 61(7), 1441-1446 (1988).
6. Sokal JE, Baccarani M, Russo D, Tura S. Staging and prognosis in chronic myelogenous leukemia. *Seminars in hematology*, 25(1), 49-61 (1988).
7. Rowley JD. Letter: A new consistent chromosomal abnormality in chronic myelogenous leukaemia identified by quinacrine fluorescence and Giemsa staining. *Nature*, 243(5405), 290-293 (1973).
8. Hazlehurst LA, Bewry NN, Nair RR, Pinilla-Ibarz J. Signaling networks associated with BCR-ABL-dependent transformation. *Cancer Control*, 16(2), 100-107 (2009).
9. Novel P, Hungerford D. A minute chromosome in human chronic granulocytic leukemia. *Science*, 32, 1497-1501 (1960).
10. Winslow T. Philadelphia Chromosome. (National Cancer Institute, 2008)
11. Robinson DR, Wu YM, Lin SF. The protein tyrosine kinase family of the human genome. *Oncogene*, 19(49), 5548-5557 (2000).
12. Gu J, Gu X. Natural history and functional divergence of protein tyrosine kinases. *Gene*, 317(1-2), 49-57 (2003).

13. Colloni D, Saglio P. Bcr-Abl and Signal Transduction. In: *Myeloproliferative Disorders.* Melo, JV, Goldman, JM (Springer Berlin Heidelberg, Berlin, 2007)
14. Ma G, Lu D, Wu Y, Liu J, Arlinghaus RB. Bcr phosphorylated on tyrosine 177 binds Grb2. *Oncogene*, 14(19), 2367-2372 (1997).
15. Deininger MW, Bose S, Gora-Tybor J *et al.* Selective induction of leukemia-associated fusion genes by high-dose ionizing radiation. *Cancer research*, 58(3), 421-425 (1998).
16. Druker BJ, Tamura S, Buchdunger E *et al.* Effects of a selective inhibitor of the Abl tyrosine kinase on the growth of Bcr-Abl positive cells. *Nature medicine*, 2(5), 561-566 (1996).
17. Faderl S, Talpaz M, Estrov Z *et al.* The biology of chronic myeloid leukemia. *The New England journal of medicine*, 341(3), 164-172 (1999).
18. Mauro MJ, Druker BJ. Chronic myelogenous leukemia. *Current opinion in oncology*, 13(1), 3-7 (2001).
19. McWhirter JR, Galasso DL, Wang JY. A coiled-coil oligomerization domain of Bcr is essential for the transforming function of Bcr-Abl oncoproteins. *Molecular and cellular biology*, 13(12), 7587-7595 (1993).
20. Quintas-Cardama A, Cortes J. Molecular biology of bcr-abl1-positive chronic myeloid leukemia. *Blood*, 113(8), 1619-1630 (2009).
21. Zhao X, Ghaffari S, Lodish H, Malashkevich VN, Kim PS. Structure of the Bcr-Abl oncoprotein oligomerization domain. *Nature structural biology*, 9(2), 117-120 (2002).
22. Kantarjian HM, Talpaz M, Giles F, O'Brien S, Cortes J. New insights into the pathophysiology of chronic myeloid leukemia and imatinib resistance. *Annals of internal medicine*, 145(12), 913-923 (2006).
23. Skorski T, Kanakaraj P, Nieborowska-Skorska M *et al.* Phosphatidylinositol-3 kinase activity is regulated by BCR/ABL and is required for the growth of Philadelphia chromosome-positive cells. *Blood*, 86(2), 726-736 (1995).
24. Valent P. Emerging stem cell concepts for imatinib-resistant chronic myeloid leukaemia: implications for the biology, management, and

therapy of the disease. *British journal of haematology*, 142(3), 361-378 (2008).

25. Medina J, Kantarjian H, Talpaz M *et al.* Chromosomal abnormalities in Philadelphia chromosome-negative metaphases appearing during imatinib mesylate therapy in patients with Philadelphia chromosome-positive chronic myelogenous leukemia in chronic phase. *Cancer*, 98(9), 1905-1911 (2003).
26. Jabbour E, Kantarjian HM, Abruzzo LV *et al.* Chromosomal abnormalities in Philadelphia chromosome negative metaphases appearing during imatinib mesylate therapy in patients with newly diagnosed chronic myeloid leukemia in chronic phase. *Blood*, 110(8), 2991-2995 (2007).
27. Hehlmann R, Berger U, Pfirrmann M *et al.* Randomized comparison of interferon alpha and hydroxyurea with hydroxyurea monotherapy in chronic myeloid leukemia (CML-study II): prolongation of survival by the combination of interferon alpha and hydroxyurea. *Leukemia*, 17(8), 1529-1537 (2003).
28. Holland J, Frei E, Kufe D. Mode of action of STI571. In: *Cancer Medicine* (BC Decker, Inc., Hamilton, Ontario, 2003)
29. Gambacorti-Passerini CB, Gunby RH, Piazza R *et al.* Molecular mechanisms of resistance to imatinib in Philadelphia-chromosome-positive leukaemias. *The lancet oncology*, 4(2), 75-85 (2003).
30. O'Hare T, Eide CA, Deininger MW. Bcr-Abl kinase domain mutations and the unsettled problem of Bcr-AblT315I: looking into the future of controlling drug resistance in chronic myeloid leukemia. *Clin Lymphoma Myeloma*, 7 Suppl 3, S120-130 (2007).
31. Jabbour E, Cortes JE, Giles FJ, O'Brien S, Kantarjian HM. Current and emerging treatment options in chronic myeloid leukemia. *Cancer*, 109(11), 2171-2181 (2007).
32. O'Brien SG, Guilhot F, Larson RA *et al.* Imatinib compared with interferon and low-dose cytarabine for newly diagnosed chronic-phase chronic myeloid leukemia. *The New England journal of medicine*, 348(11), 994-1004 (2003).

33. Valent P, Lion T, Wolf D *et al.* Diagnostic algorithms, monitoring, prognostication, and therapy in chronic myeloid leukemia (CML): a proposal of the Austrian CML platform. *Wiener klinische Wochenschrift*, 120(21-22), 697-709 (2008).
34. Litzow MR. Imatinib resistance: obstacles and opportunities. *Archives of pathology & laboratory medicine*, 130(5), 669-679 (2006).
35. Baccarani M, Cortes J, Pane F *et al.* Chronic myeloid leukemia: an update of concepts and management recommendations of European LeukemiaNet. *J Clin Oncol*, 27(35), 6041-6051 (2009).
36. Gorre ME, Mohammed M, Ellwood K *et al.* Clinical resistance to STI-571 cancer therapy caused by BCR-ABL gene mutation or amplification. *Science*, 293(5531), 876-880 (2001).
37. Melo JV, Chuah C. Resistance to imatinib mesylate in chronic myeloid leukaemia. *Cancer letters*, 249(2), 121-132 (2007).
38. Mahon FX, Belloc F, Lagarde V *et al.* MDR1 gene overexpression confers resistance to imatinib mesylate in leukemia cell line models. *Blood*, 101(6), 2368-2373 (2003).
39. White DL, Saunders VA, Dang P *et al.* Most CML patients who have a suboptimal response to imatinib have low OCT-1 activity: higher doses of imatinib may overcome the negative impact of low OCT-1 activity. *Blood*, 110(12), 4064-4072 (2007).
40. Volpe G, Panuzzo C, Ulisciani S, Cilloni D. Imatinib resistance in CML. *Cancer letters*, 274(1), 1-9 (2009).
41. Takayama N, Sato N, O'Brien SG, Ikeda Y, Okamoto S. Imatinib mesylate has limited activity against the central nervous system involvement of Philadelphia chromosome-positive acute lymphoblastic leukaemia due to poor penetration into cerebrospinal fluid. *British journal of haematology*, 119(1), 106-108 (2002).
42. Senior K. Gleevec does not cross blood-brain barrier. *The lancet oncology*, 4(4), 198 (2003).
43. Dai H, Marbach P, Lemaire M, Hayes M, Elmquist WF. Distribution of STI-571 to the brain is limited by P-glycoprotein-mediated efflux. *The*

*Journal of pharmacology and experimental therapeutics*, 304(3), 1085-1092 (2003).

44. Quintas-Cardama A, Kantarjian H, Cortes J. Flying under the radar: the new wave of BCR-ABL inhibitors. *Nat Rev Drug Discov*, 6(10), 834-848 (2007).
45. Weisberg E, Manley PW, Cowan-Jacob SW, Hochhaus A, Griffin JD. Second generation inhibitors of BCR-ABL for the treatment of imatinib-resistant chronic myeloid leukaemia. *Nature reviews*, 7(5), 345-356 (2007).
46. Nagar B, Bornmann WG, Pellicena P *et al.* Crystal structures of the kinase domain of c-Abl in complex with the small molecule inhibitors PD173955 and imatinib (STI-571). *Cancer research*, 62(15), 4236-4243 (2002).
47. Cortes J, Jabbour E, Kantarjian H *et al.* Dynamics of BCR-ABL kinase domain mutations in chronic myeloid leukemia after sequential treatment with multiple tyrosine kinase inhibitors. *Blood*, 110(12), 4005-4011 (2007).
48. Tokarski JS, Newitt JA, Chang CY *et al.* The structure of Dasatinib (BMS-354825) bound to activated ABL kinase domain elucidates its inhibitory activity against imatinib-resistant ABL mutants. *Cancer research*, 66(11), 5790-5797 (2006).
49. O'Hare T, Eide CA, Deininger MW. Bcr-Abl kinase domain mutations, drug resistance, and the road to a cure for chronic myeloid leukemia. *Blood*, 110(7), 2242-2249 (2007).
50. Branford S, Rudzki Z, Walsh S *et al.* Detection of BCR-ABL mutations in patients with CML treated with imatinib is virtually always accompanied by clinical resistance, and mutations in the ATP phosphate-binding loop (P-loop) are associated with a poor prognosis. *Blood*, 102(1), 276-283 (2003).
51. Nicolini FE, Corm S, Le QH, Roche-Lestienne C, Preudhomme C. The prognosis impact of BCR-ABL P-loop mutations: worse or not worse? *Leukemia*, 21(2), 193-194 (2007).

52. Stuart SA, Minami Y, Wang JY. The CML stem cell: evolution of the progenitor. *Cell cycle (Georgetown, Tex*, 8(9), 1338-1343 (2009).
53. Bhatia R, Holtz M, Niu N *et al.* Persistence of malignant hematopoietic progenitors in chronic myelogenous leukemia patients in complete cytogenetic remission following imatinib mesylate treatment. *Blood*, 101(12), 4701-4707 (2003).
54. Copland M, Hamilton A, Elrick LJ *et al.* Dasatinib (BMS-354825) targets an earlier progenitor population than imatinib in primary CML but does not eliminate the quiescent fraction. *Blood*, 107(11), 4532-4539 (2006).
55. Jorgensen HG, Allan EK, Jordanides NE, Mountford JC, Holyoake TL. Nilotinib exerts equipotent antiproliferative effects to imatinib and does not induce apoptosis in CD34+ CML cells. *Blood*, 109(9), 4016-4019 (2007).
56. Rousselot P, Huguet F, Rea D *et al.* Imatinib mesylate discontinuation in patients with chronic myelogenous leukemia in complete molecular remission for more than 2 years. *Blood*, 109(1), 58-60 (2007).
57. Valent P, Deininger M. Clinical perspectives of concepts on neoplastic stem cells and stem cell-resistance in chronic myeloid leukemia. *Leukemia & lymphoma*, 49(4), 604-609 (2008).
58. Chu S, Xu H, Shah NP *et al.* Detection of BCR-ABL kinase mutations in CD34+ cells from chronic myelogenous leukemia patients in complete cytogenetic remission on imatinib mesylate treatment. *Blood*, 105(5), 2093-2098 (2005).
59. Luzzatto L, Melo JV. Acquired resistance to imatinib mesylate: selection for pre-existing mutant cells. *Blood*, 100(3), 1105 (2002).
60. Martinelli G, Soverini S, Rosti G, Cilloni D, Baccarani M. New tyrosine kinase inhibitors in chronic myeloid leukemia. *Haematologica*, 90(4), 534-541 (2005).
61. Pavlovsky C, Kantarjian H, Cortes JE. First-line therapy for chronic myeloid leukemia: Past, present, and future. *American journal of hematology*, 84(5), 287-293 (2009).

62. Weisberg E, Manley PW, Breitenstein W *et al.* Characterization of AMN107, a selective inhibitor of native and mutant Bcr-Abl. *Cancer cell*, 7(2), 129-141 (2005).
63. O'Hare T, Walters DK, Stoffregen EP *et al.* In vitro activity of Bcr-Abl inhibitors AMN107 and BMS-354825 against clinically relevant imatinib-resistant Abl kinase domain mutants. *Cancer research*, 65(11), 4500-4505 (2005).
64. Kantarjian HM, Giles F, Gattermann N *et al.* Nilotinib (formerly AMN107), a highly selective BCR-ABL tyrosine kinase inhibitor, is effective in patients with Philadelphia chromosome-positive chronic myelogenous leukemia in chronic phase following imatinib resistance and intolerance. *Blood*, 110(10), 3540-3546 (2007).
65. le Coutre P, Ottmann OG, Giles F *et al.* Nilotinib (formerly AMN107), a highly selective BCR-ABL tyrosine kinase inhibitor, is active in patients with imatinib-resistant or -intolerant accelerated-phase chronic myelogenous leukemia. *Blood*, 111(4), 1834-1839 (2008).
66. Jabbour E, Hochhaus A, Cortes J, La Rosee P, Kantarjian HM. Choosing the best treatment strategy for chronic myeloid leukemia patients resistant to imatinib: weighing the efficacy and safety of individual drugs with BCR-ABL mutations and patient history. *Leukemia*, 24(1), 6-12 (2010).
67. Cortes JE, Jones D, O'Brien S *et al.* Nilotinib as front-line treatment for patients with chronic myeloid leukemia in early chronic phase. *J Clin Oncol*, 28(3), 392-397).
68. Rosti G, Palandri F, Castagnetti F *et al.* Nilotinib for the frontline treatment of Ph(+) chronic myeloid leukemia. *Blood*, 114(24), 4933-4938 (2009).
69. Hochhaus A, Kantarjian HM, Baccarani M *et al.* Dasatinib induces notable hematologic and cytogenetic responses in chronic-phase chronic myeloid leukemia after failure of imatinib therapy. *Blood*, 109(6), 2303-2309 (2007).

70. Schorck N, Taylor S. Computional cancer biology of protein kinases: evolution, structure, dynamics and binding. verklab.bioinformatics.ku.edu/ccbkinase.php (2009)
71. Quintas-Cardama A, Cortes J. Therapeutic options against BCR-ABL1 T315I-positive chronic myelogenous leukemia. *Clin Cancer Res*, 14(14), 4392-4399 (2008).
72. Van Etten R, Chan W, Zaleskas V, et al. DCC-2036: a novel switch pocket inhibitor of ABL tyrosine kinase with therapeutic efficacy against BCR-ABL T315I in vitro and in a CML mouse model (abstract 463). *Blood*, 110 (2007).
73. Cortes J, Quintas-Cardama A, Garcia-Manero G *et al.* Phase 1 study of tipifarnib in combination with imatinib for patients with chronic myelogenous leukemia in chronic phase after imatinib failure. *Cancer*, 110(9), 2000-2006 (2007).
74. Neviani P, Santhanam R, Trotta R *et al.* The tumor suppressor PP2A is functionally inactivated in blast crisis CML through the inhibitory activity of the BCR/ABL-regulated SET protein. *Cancer cell*, 8(5), 355-368 (2005).
75. Thomas ED, Clift RA, Fefer A *et al.* Marrow transplantation for the treatment of chronic myelogenous leukemia. *Annals of internal medicine*, 104(2), 155-163 (1986).
76. Branford S, Hughes T. Detection of BCR-ABL mutations and resistance to imatinib mesylate. *Methods Mol Med*, 125, 93-106 (2006).
77. Khorashad JS, Anand M, Marin D *et al.* The presence of a BCR-ABL mutant allele in CML does not always explain clinical resistance to imatinib. *Leukemia*, 20(4), 658-663 (2006).
78. Jabbour E, Kantarjian H, Jones D *et al.* Frequency and clinical significance of BCR-ABL mutations in patients with chronic myeloid leukemia treated with imatinib mesylate. *Leukemia*, 20(10), 1767-1773 (2006).

79. Deininger MW, McGreevey L, Willis S *et al.* Detection of ABL kinase domain mutations with denaturing high-performance liquid chromatography. *Leukemia*, 18(4), 864-871 (2004).
80. Soverini S, Martinelli G, Amabile M *et al.* Denaturing-HPLC-based assay for detection of ABL mutations in chronic myeloid leukemia patients resistant to Imatinib. *Clin Chem*, 50(7), 1205-1213 (2004).
81. Ernst T, Erben P, Muller MC *et al.* Dynamics of BCR-ABL mutated clones prior to hematologic or cytogenetic resistance to imatinib. *Haematologica*, 93(2), 186-192 (2008).
82. Vivante A, Amariglio N, Koren-Michowitz M *et al.* High-throughput, sensitive and quantitative assay for the detection of BCR-ABL kinase domain mutations. *Leukemia*, 21(6), 1318-1321 (2007).
83. Willis SG, Lange T, Demehri S *et al.* High-sensitivity detection of BCR-ABL kinase domain mutations in imatinib-naive patients: correlation with clonal cytogenetic evolution but not response to therapy. *Blood*, 106(6), 2128-2137 (2005).
84. Kang HY, Hwang JY, Kim SH *et al.* Comparison of allele specific oligonucleotide-polymerase chain reaction and direct sequencing for high throughput screening of ABL kinase domain mutations in chronic myeloid leukemia resistant to imatinib. *Haematologica*, 91(5), 659-662 (2006).
85. Roche-Lestienne C, Soenen-Cornu V, Grardel-Duflos N *et al.* Several types of mutations of the Abl gene can be found in chronic myeloid leukemia patients resistant to STI571, and they can pre-exist to the onset of treatment. *Blood*, 100(3), 1014-1018 (2002).
86. Nardi V, Raz T, Cao X *et al.* Quantitative monitoring by polymerase colony assay of known mutations resistant to ABL kinase inhibitors. *Oncogene*, 27(6), 775-782 (2008).
87. Schouten JP, McElgunn CJ, Waaijer R *et al.* Relative quantification of 40 nucleic acid sequences by multiplex ligation-dependent probe amplification. *Nucleic acids research*, 30(12), e57 (2002).

88. Nielsen PE, Egholm M, Berg RH, Buchardt O. Sequence-selective recognition of DNA by strand displacement with a thymine-substituted polyamide. *Science*, 254(5037), 1497-1500 (1991).
89. Egholm M, Buchardt O, Christensen L *et al.* PNA hybridizes to complementary oligonucleotides obeying the Watson-Crick hydrogen-bonding rules. *Nature*, 365(6446), 566-568 (1993).
90. Pellestor F, Paulasova P. The peptide nucleic acids (PNAs), powerful tools for molecular genetics and cytogenetics. *Eur J Hum Genet*, 12(9), 694-700 (2004).
91. Orum H, Nielsen PE, Egholm M *et al.* Single base pair mutation analysis by PNA directed PCR clamping. *Nucleic acids research*, 21(23), 5332-5336 (1993).
92. Orum H. PCR clamping. *Current issues in molecular biology*, 2(1), 27-30 (2000).
93. Dabritz J, Hanfler J, Preston R, Stieler J, Oettle H. Detection of Ki-ras mutations in tissue and plasma samples of patients with pancreatic cancer using PNA-mediated PCR clamping and hybridisation probes. *British journal of cancer*, 92(2), 405-412 (2005).
94. Beau-Faller M, Legrain M, Voegeli AC *et al.* Detection of K-Ras mutations in tumour samples of patients with non-small cell lung cancer using PNA-mediated PCR clamping. *British journal of cancer*, 100(6), 985-992 (2009).
95. Khorashad JS, Milojkovic D, Mehta P *et al.* In vivo kinetics of kinase domain mutations in CML patients treated with dasatinib after failing imatinib. *Blood*, 111(4), 2378-2381 (2008).
96. Beillard E, Pallisgaard N, van der Velden VH *et al.* Evaluation of candidate control genes for diagnosis and residual disease detection in leukemic patients using 'real-time' quantitative reverse-transcriptase polymerase chain reaction (RQ-PCR) - a Europe against cancer program. *Leukemia*, 17(12), 2474-2486 (2003).
97. Lundberg E, De Mare J. Interval estimates in the spectroscopy calibration problem. *Scand J Statistics*, 7, 40-42 (1980).

98. La Rosee P, Corbin AS, Stoffregen EP, Deininger MW, Druker BJ. Activity of the Bcr-Abl kinase inhibitor PD180970 against clinically relevant Bcr-Abl isoforms that cause resistance to imatinib mesylate (Gleevec, STI571). *Cancer research*, 62(24), 7149-7153 (2002).

99. Levine RL, Wadleigh M, Cools J *et al.* Activating mutation in the tyrosine kinase JAK2 in polycythemia vera, essential thrombocythemia, and myeloid metaplasia with myelofibrosis. *Cancer cell*, 7(4), 387-397 (2005).

100. Preuner S, Denk D, Frommlet F, Nesslboeck M, Lion T. Quantitative monitoring of cell clones carrying point mutations in the BCR-ABL tyrosine kinase domain by ligation-dependent polymerase chain reaction (LD-PCR). *Leukemia*, 22(10), 1956-1961 (2008)

# Danksagung

Mein erster Dank gilt meinem Gruppenleiter und dem Betreuer meiner Diplomarbeit Prof. DDr. Thomas Lion vom Children´s Cancer Research Institute. Thomas, danke für die Betreuung meiner Diplomarbeit! Du hast mir die Möglichkeit gegeben, mich weiterzuentwickeln, und das hat wiederum die Grundlage für mein Studium und für meine Diplomarbeit geschaffen.
Weiters möchte ich mich bei Prof. Dr. Angela Witte bedanken, die sich dazu bereit erklärt hat, die Betreuung meiner Diplomarbeit von Seiten der Universität Wien zu übernehmen.

Die letzten Jahre waren sehr entbehrungsreich was jegliche Freizeit und freie Zeit betrifft. Das war vor allem auch für meinen Freund Helmut keine leichte Zeit. Du hast auf viele Stunden unserer gemeinsame Zeit verzichtet! Ich danke Dir, dass Du trotzdem mit mir durchgehalten hast, dass Du mich in schweren Stunden getröstet hast und dass Du an mich geglaubt hast!
Michi, Margit und Susanne, Ihr habt mir während der gesamten Zeit des Studiums beigestanden. Ihr habt mir zugehört, habt mich aufgebaut und mich immer wieder motiviert weiterzumachen. Ich danke Euch für Eure Freundschaft und Unterstützung!
Ein großer Dank gebührt auch meinen Eltern, die mir meine erste Ausbildung ermöglicht haben und somit den Grundstein zu meinem Werdegang gelegt haben. Ich danke Euch auch, dass Ihr an mich glaubt, mich immer unterstützt und dass ihr in den letzten Jahren Verständnis dafür aufgebracht habt, dass ich wenig Zeit für die Familie hatte.
Oma und Opa, ich danke Euch dafür, dass Ihr mich immer unterstützt habt und davon überzeugt wart, dass ich das schaffe!
Ich bin froh, dass ich mich dazu entschieden habe mein Studium, das ich nach der Matura begonnen habe, auf zweitem Bildungsweg abzuschließen. Es war hart, neben einem Vollzeitjob zu studieren. Ich bin froh und auch ein bisschen stolz, dass ich das gewagt habe.

# Curriculum vitae


Born: 30th May 1977, Vöcklabruck, Upper Austria

Nationality: Austria

Adress: Märzstrasse 30/17A, 1150 Vienna

Email: sandra_preuner@yahoo.de


## Education

| | |
|---|---|
| 1983 -1987 | Volksschule Vöcklamarkt |
| 1987 -1991 | Hauptschule Vöcklamarkt, music class |
| 1991 -1995 | Oberstufenrealgymnasium der Schulschwestern, musical branch, Vöcklabruck |

## Studies

| | |
|---|---|
| 1995-1997 | University of Salzburg, Faculty of Natural Science, Studies of Biology |
| 1997-2000 | Studies at the Academy for Advanced Laboratory Science, Diploma for Advanced Laboratory Service, October 2000 |
| 2006-2010 | University of Vienna, Faculty of Natural Science Studies of Biology / Microbiology and Genetics |

## Employment

| | |
|---|---|
| 2000-2002 | Research technician at the Department of Hygiene and Microbiology, Medical University of Vienna |
| since 2002 | Research technician at the Department of Molecular Microbiology and Development of Genetic Diagnostics, Children´s Cancer Research Institute (CCRI), Vienna |

## Publications

***Molecular monitoring of adenovirus in peripheral blood after allogeneic bone marrow transplantation permits early diagnosis of disseminated disease.***

Lion T, Baumgartinger R, Watzinger F, Matthes-Martin S, Suda M, **Preuner S**, Futterknecht B, Lawitschka A, Peters C, Potschger U, Gadner H. Blood. 2003 Aug 1;102(3):1114-1120.

***Real-time quantitative PCR assays for detection and monitoring of pathogenic human viruses in immunosuppressed pediatric patients.***

Watzinger F, Suda M, **Preuner S**, Baumgartinger R, Ebner K, Baskova L, Niesters HG, Lawitschka A, Lion T. Journal of clinical microbiology. 2004 Nov;42(11):5189-5198.

***Typing of human adenoviruses in specimens from immunosuppressed patients by PCR-fragment length analysis and real-time quantitative PCR.***

Ebner K, Rauch M, **Preuner S**, Lion T. Journal of clinical microbiology. 2006 Aug;44(8):2808-2815.

***Large granular lymphocyte proliferation and revertant mosaicism: two rare events in a Wiskott-Aldrich syndrome patient.***

Boztug K, Baumann U, Ballmaier M, Webster D, Sandrock I, Jacobs R, Lion T, **Preuner S**, Germeshausen M, Hansen G, Welte K, Klein C. Haematologica. 2007 Mar;92(3):e43-45.

***The Pan-AC assay: a single-reaction real-time PCR test for quantitative detection of a broad range of Aspergillus and Candida species.***

Baskova L, Landlinger C, **Preuner S**, Lion T. Journal of medical microbiology. 2007 Sep;56(Pt 9):1167-1173.

***Quantitative monitoring of cell clones carrying point mutations in the BCR-ABL tyrosine kinase domain by ligation-dependent polymerase chain reaction (LD-PCR).***

**Preuner S**, Denk D, Frommlet F, Nesslboeck M, Lion T. Leukemia. 2008 Oct;22(10):1956-1961.

***Identification of fungal species by fragment length analysis of the internally transcribed spacer 2 region.***

Landlinger C, Baskova L, **Preuner S**, Willinger B, Buchta V, Lion T. Eur J Clin Microbiol Infect Dis. 2009 Jun;28(6):613-622.

**Species-specific identification of a wide range of clinically relevant fungal pathogens by use of Luminex xMAP technology.**

Landlinger C, **Preuner S**, Willinger B, Haberpursch B, Racil Z, Mayer J, Lion T. Journal of clinical microbiology,.2009 Apr;47(4):1063-1073.

***Towards molecular diagnostics of invasive fungal infections.***

**Preuner S**, Lion T. Expert review of molecular diagnostics, 2009 Jul;9(5):397-401.

***Monitoring of adenovirus load in stool by real-time PCR permits early detection of impending invasive infection in patients after allogeneic stem cell transplantation.***

Lion T, Kosulin K, Landlinger C, Rauch M, **Preuner S**, Jugovic D, Potschger U, Lawitschka A, Peters C, Fritsch G, Matthes-Martin S. Monitoring of adenovirus load in stool by real-time PCR permits early detection of impending invasive infection in patients after allogeneic stem cell transplantation. Leukemia. 2010 Feb 11.

## Book Chapter

***Nucleic acid-based pan-fungal detection.***

**Preuner S**, Lion T.

Taylor&Francis CRC Press 2010 (in press).

## Varia

### Talks

***„Eurochimerism microsatellite panel for the monitoring of chimerism in haematopoetic stem cell transplant recipients“***

XIX. Jahrestagung der Kind-Philipp-Stiftung für Leukämieforschung, Wilsede, Juni 2006

***„Rapid and sensitive detection of invasive fungal infections- a two step panfungal assay by realtime PCR”***

QPCR Meeting, München, März 2007

***"Quantitative monitoring of cell clones carrying point mutations in the BCR-ABL tyrosine kinase domain by ligation-dependent polymerase chain reaction (LD-PCR)"***

GPOH, Vienna, September 2008

***„Species specific identification of clinically relevant fungal pathogens by use of Luminex xMAP technology"***

Luminex Meeting, Amsterdam, October 2009

Scientific presentations at the Children´s Cancer Research Institute

**Posters**

***„Detection of impending graft rejection by monitoring of chimerism within specific leucocyte subsets in children after allogeneic stem cell transplantation"***

GPOH, Vienna, November 2003

***"Quantitative monitoring of cell clones carrying point mutations in the BCR-ABL tyrosine kinase domain by ligation-dependent polymerase chain reaction (LD-PCR)"***

"Bridge 08", Vienna, November 2008

**Review of scietific articles**

***Real-time PCR quantification of haematopoietic chimerism after transplantation: a comparison between TaqMan and hybridization probes technologies.***

Joaquin Martinez-Lopez et al, JMD, September 2007

***High sensitive multiplex STR kit for the early detection of mixed chimerism after allogenic HSCT.***
Müller et al, Bone Marrow Transplant, May 2008

Member of the steering group at the coordinating center of the EuroChimerism EU-Project within the 5th. Framework program (Nr.:QLRT2001-01485) with the participation of 12 European centers

## Skills and Qualifications

| | |
|---|---|
| Computer: | Microsoft Office, various scientific computer programs |
| Languages: | German (native), English (fluently), French (basics) |
| Interests: | Literature, Yoga, Music and Friends |

Leukemia (2008), 1–6

www.nature.com/leu

## LETTER TO THE EDITOR

# Quantitative monitoring of cell clones carrying point mutations in the BCR–ABL tyrosine kinase domain by ligation-dependent polymerase chain reaction (LD–PCR)

*Leukemia* advance online publication, 24 April 2008;
doi:10.1038/leu.2008.97

Tyrosine kinase (TK) inhibitors directed against the *BCR–ABL* TK domain have become the standard of treatment in patients with chronic myeloid leukemia (CML). In a proportion of patients, however, resistance to TK inhibitors may occur, which, in the case of imatinib, has been associated with point mutations within the *ABL* TK domain in 40–90% of instances, depending on the CML phase, the methodology of detection and the definition of resistance.[1] Mutations conferring resistance frequently occur at the ATP-binding site (P-loop) or at other sites directly affecting drug binding or conformation of the kinase (activation loop, catalytic domain). The level of resistance to individual TK inhibitors may vary from slightly reduced sensitivity to total insensitivity. In patients receiving treatment with imatinib, mutations conferring only moderately impaired sensitivity may be approached by increasing the dose, while the presence of mutations associated with a high level of resistance provides an indication for switching treatment to second generation compounds, such as dasatinib or nilotinib.[2] Point mutations reported to confer high levels of resistance to imatinib include for example, Y253F/H, E255K/V, T315I, or H396P/R.[2] Dasatinib and nilotinib were shown to be instrumental against most of these mutations,[3] but the AA position 315 (→T315I) remains problematic because none of the currently approved TK inhibitors are effective in this instance.[4] Moreover, recent data indicate that a range of specific mutations other than the T315I may occur before and during treatment with dasatinib (V299L, T315A, F317I/S/V, F317L) or nilotinib (Y253H, E255V, F359C).[5] These observations underscore the importance of monitoring patients on treatment with TK inhibitors for the presence of mutations. A number of studies in CML patients report on the occurrence of mutations in the entire *BCR–ABL* TK domain. Recent studies in patients treated with imatinib indicate that E250K, Y253F, E255K, T315I, M351T and F359V account for 60–70% of all mutations. Mutations located within the P-loop appear to be most frequent and are suggested to correlate with poor outcome.[6] A number of methods have been employed to detect mutant clones including, for example, PCR amplification coupled with direct sequencing of the *BCR–ABL* TK domain, high-performance liquid chromatography, the SEQUENOM MassARRAY system, or allele-specific oligonucleotide-PCR amplification. These techniques display different detection limits for the identification of mutant clones ranging from 0.01–30%. Detection of a mutation within the *ABL* TK domain does not necessarily imply impending onset of clinically resistant disease, particularly if the size of a mutant clone is small.[7] Mutant clones have been reported to disappear spontaneously which may, at least in part, be attributable to the occurrence of mutations in cells with restricted proliferative capacity.[8,9] Qualitative methods for mutational analysis may therefore have limited potential to reliably assess the risk of clinically resistant disease, especially if mutant clones present at very low levels are detected.[8] It is currently a matter of discussion whether the detection of small mutant *BCR–ABL* clones, for example, below the level of 1%, is clinically useful. The clinical benefit of sensitive techniques for mutational analysis could be increased if the size of mutant clones could be monitored, to facilitate timely detection of clonally expanding mutant cells during treatment.[8] Current approaches to assessing the size of mutant clones include for example, pyrosequencing,[9] SEQUENOM MassARRAY analysis,[10] or the polymerase colony assay.[11] These techniques, however, have limitations with regard to broad application in clinical diagnosis, such as the requirement of very expensive equipment,[10] rather complex and laborious design,[11] or the apparent inability to quantify mutant clones in the range below 20%.[9] We have therefore established a relatively simple method facilitating quantitative analysis of single nucleotide polymorphisms. The technique is based on ligation-dependent competitive PCR (LD–PCR) and represents a modification of the MLPA technology.[12] The LD–PCR technique presented displays a detection limit for *BCR–ABL* TK mutations in a range of apparent clinical relevance, and permits accurate quantitative analysis of mutant clones. In a pilot study, we demonstrate that the technique can be readily applied to the detection and monitoring of clones exhibiting specific mutations within the *BCR–ABL* TK domain in patients with CML.

The panel of quantification assays presented covers 18 different mutations including all important base substitutions located in the P-loop of the tyrosine kinase domain, and other mutations known to confer a high level of resistance to imatinib, dasatinib and nilotinib (Table 1). The current panel of LD–PCR assays permits detection and quantitative monitoring of the following mutations: M244V, L248V, V299L-C, V299L-T, G250E, Q252H-C, Q252H-T, Y253F, Y253H, E255K, T315A, T315I, F317C, F317I, F317L-A, F317L-G, F317V and M351T (Table 1).

The probes for individual LD–PCR assays including the ligation (Lig) and hybridization (Hyb) oligonucleotides were designed according to the criteria established for MLPA analysis, as specified by MRC Holland (www.mpla.com). Lig specifies the probes whose 3′ terminal bases hybridize to the nucleotide of interest, and Hyb indicates the adjacent probe (Figure 1). The Hyb probe is phosphorylated at the 5′end as a prerequisite for the ligation step. The Lig probes for the wild-type (WT) and the mutant (MUT) sequences display different nucleotides at their 3′ terminal positions. Moreover, the Lig-MUT probes contain an additional 'stuffer-sequence' located between the hybridization sequence and the primer-binding site. The stuffer-sequence is a stretch of six non-homologous nucleotides which render the mutation-specific PCR product longer, and thus, readily distinguishable from the wild-type PCR product by capillary electrophoresis (Figure 1). The sequences of the Lig and the Hyb oligonucleotide probes were controlled for the possible formation of secondary structures under conditions close to the hybridization temperature, using a program freely available online: http://frontend.bioinfo.rpi.edu/applications/mfold/cgi-bin/dna-form1.cgi.

**Table 1** LD–PCR detection systems for 18 mutations in the *BCR–ABL* TK domain

| *LD-system* | Primer tag sequence *Stuffer sequence* **Target hybridization sequence** | *Hybridization temperature (C°)* |
|---|---|---|
| *M244V* | | |
| Lig Oligo WT | gggttccctaagggttgga**gaacgcacggacatcacca** | 70 |
| Lig Oligo Mut | gggttccctaagggttgga*atgacct***gaacgcacggacatcaccg** | |
| Hyb Oligo | 5′Phos **tgaagcacaagctgggcgg**tctagattggatcttgctggcac | |
| *L248V* | | |
| Lig Oligo WT | gggttccctaagggttgga**ggacatcaccatgaagcacaagc** | 70 |
| Lig Oligo Mut | gggttccctaagggttgga*taatct***ggacatcaccatgaagcacaagg** | |
| Hyb Oligo | 5′Phos **tgggcgggggccagt**tctagattggatcttgctggcac | |
| *V299L-C* | | |
| Lig Oligo WT | gggttccctaagggttgga**catgaaagagatcaaacaccctaacctgg** | 70 |
| Lig Oligo Mut | gggttccctaagggttgga*gttgtg***catgaaagagatcaaacaccctaacctgc** | |
| Hyb Oligo | 5′Phos **tgcagctccttgggtctg**tctagattggatcttgctggcac | |
| *V299L-T* | | |
| Lig Oligo WT | gggttccctaagggttgga**catgaaagagatcaaacaccctaacctgg** | 70 |
| Lig Oligo Mut | gggttccctaagggttgga*gttgtg***catgaaagagatcaaacaccctaacctgt** | |
| Hyb Oligo | 5′Phos **tgcagctccttgggtctg**tctagattggatcttgctggcac | |
| *G250E* | | |
| Lig Oligo WT | gggttccctaagggttgga**tgaagcacaagctgggcgg** | 70 |
| Lig Oligo Mut | gggttccctaagggttgga*gtgttg***tgaagcacaagctgggcga** | |
| Hyb Oligo | 5′Phos **gggccagtacggggagg**tctagattggatcttgctggcac | |
| *Q252H-C*[a] | | |
| Lig Oligo WT | gggttccctaagggttgga**gccctcgtacacctccccgtac** | 75 |
| Lig Oligo Mut | gggttccctaagggttgga*tacaga***gccctcgtacacctccccgtag** | |
| Hyb Oligo | 5′Phos **tggccccccgcccagctt**tctagattggatcttgctggcac | |
| *Q252H-T*[a] | | |
| Lig Oligo WT | gggttccctaagggttgga**gccctcgtacacctccccgtac** | 75 |
| Lig Oligo Mut | gggttccctaagggttgga*tacaga***gccctcgtacacctccccgtaa** | |
| Hyb Oligo | 5′Phos **tggccccccgcccagctt**tctagattggatcttgctggcac | |
| *Y253F* | | |
| Lig Oligo WT | gggttccctaagggttgga**gctgggcgggggccagta** | 75 |
| Lig Oligo Mut | gggttcccgaagggttgga*tagtcc***gctgggcgggggccagtt** | |
| Hyb Oligo | 5′Phos **cggggaggtgtacgagggcg**tctagattggatcttgctggcac | |
| *Y253H* | | |
| Lig Oligo WT | gggttccctaagggttgga**ctgggcgggggccagt** | 75 |
| Lig Oligo Mut | gggttccctaagggttgga*tgtggt***ctgggcgggggccagc** | |
| Hyb Oligo | 5′Phos **acggggaggtgtacgagggcg**tctagattggatcttgctggcac | |
| *E255K* | | |
| Lig Oligo WT | gggttccctaagggttgga**cgggggccagtacgggg** | 75 |
| Lig Oligo Mut | gggttccctaagggttgga*ttcaat***cgggggccagtacggga** | |
| Hyb Oligo | 5Phos **aggtgtacgagggcgtgtggaag**tctagattggatcttgctggcac | |
| *T315A* | | |
| Lig Oligo WT | gggttccctaagggttgga**ggagcccccgttctatatcatca** | 70 |
| Lig Oligo Mut | gggttccctaagggttgga*tcttat***ggagcccccgttctatatcatcg** | |
| Hyb Oligo | 5′Phos **ctgagttcatgacctacgggaacctc**tctagattggatcttgctggcac | |
| *T315I* | | |
| Lig Oligo WT | gggttccctaagggttgga**ggagcccccgttctatatcatcac** | 70 |
| Lig Oligo Mut | gggttccctaagggttgga*tcattt***ggagcccccgttctatatcatcat** | |
| Hyb Oligo | 5′Phos **tgagttcatgacctacgggaacctc**tctagattggatcttgctggcac | |
| *F317-C* | | |
| Lig Oligo WT | gggttccctaagggttgga**cccccgttctatatcatcactgagtt** | 70 |
| Lig Oligo Mut | gggttccctaagggttgga*attatct***ccccccgttctatatcatcactgagtg** | |
| Hyb Oligo | 5′Phos **catgacctacgggaacctcctg**tctagattggatcttgctggcac | |
| *F317-I* | | |
| Lig Oligo WT | gggttccctaagggttgga**gccccccgttctatatcatcactgagt** | 70 |
| Lig Oligo Mut | gggttccctaagggttgga*attattg***gccccccgttctatatcatcactgaga** | |
| Hyb Oligo | 5′Phos **tcatgacctacgggaacctcctg**tctagattggatcttgctggcac | |

**Table 1** (*Continued*)

| *LD-system* | Primer tag sequence *Stuffer sequence* **Target hybridization sequence** | *Hybridization temperature (C°)* |
|---|---|---|
| *F317L-A* | | |
| Lig Oligo WT | gggttccctaagggttgga**gcccccgttctatatcatcactgagttc** | 70 |
| Lig Oligo Mut | gggttccctaagggttgga*cttatc***gcccccgttctatatcatcactgagtta** | |
| Hyb Oligo | 5′Phos **atgacctacgggaacctcctgga**tctagattggatcttgctggcac | |
| *F317L-G* | | |
| Lig Oligo WT | gggttccctaagggttgga**cccccgttctatatcatcactgagttc** | 70 |
| Lig Oligo Mut | gggttccctaagggttgga*cttatc***cccccgttctatatcatcactgagttg** | |
| Hyb Oligo | 5′Phos **atgacctacgggaacctcctgga**tctagattggatcttgctggcac | |
| *F317-V* | | |
| Lig Oligo WT | gggttccctaagggttgga**gcccccgttctatatcatcactgagt** | 70 |
| Lig Oligo Mut | gggttccctaagggttgga*attattg***gcccccgttctatatcatcactgagg** | |
| Hyb Oligo | 5′Phos **tcatgacctacgggaacctcctg**tctagattggatcttgctggcac | |
| *M351T* | | |
| Lig Oligo WT | gggttccctaagggttgga**ccactcagatctcgtcagccat** | 70 |
| Lig Oligo Mut | gggttccctaagggttgga*gatgtt***ccactcagatctcgtcagccac** | |
| Hyb Oligo | 5′Phos **ggagtacctggagaagaaaaacttcatcc**tctagattggatcttgctggcac | |

[a]LD-system designed in a reverse complementary fashion.

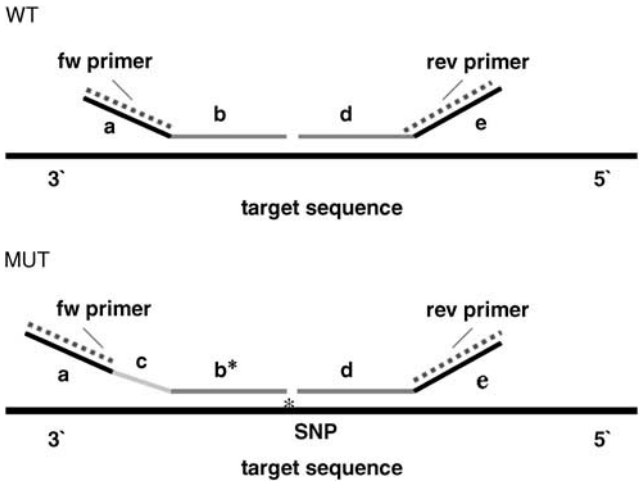


**Figure 1** LD–PCR assay for the detection and quantification of wild-type (WT) and point-mutated (MUT) sequences. The principle of LD–PCR is a modification of the MLPA technology.[12] The LD–PCR reaction contains three different probes: (1) The wild-type ligation probe (Lig-WT) contains a section complementary to the WT target sequence (**b**) and a tag sequence for the forward primer (**a**). (2) The ligation probe for the mutant sequence (Lig-MUT) (**b***) differs from the Lig-WT probe by a nucleotide at the 3′ terminal position complementary to a specific point mutation. This probe carries the same tag sequence (**a**) for the forward primer, but contains an additional stuffer sequence of six non-homologous nucleotides (**c**). (3) The common hybridization (Hyb) probe contains a section complementary to its target sequence directly adjacent to that of the ligation probes (**d**) and a tag sequence for the reverse primer (**e**). Upon specific hybridization to the target sequence, the probes are fused under conditions described in the text, permitting the ligation only in the presence of perfect match to the target sequence. In a subsequent step, the ligated probes are amplified competitively in a PCR reaction with a single set of primers binding to the tag sequences (**a** + **e**). Owing to the difference in length between the WT- and MUT-derived products, the amplicons can be readily separated and quantified by fluorescent capillary electrophoresis.

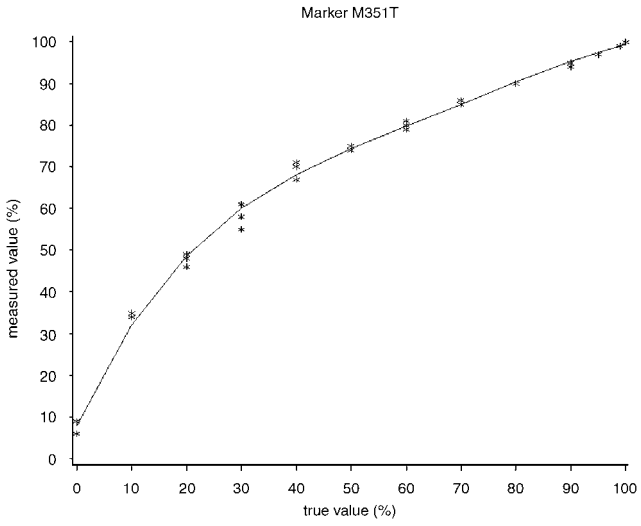


**Figure 2** Calibration curve for LD–PCR analysis. An exemplary standard curve (mutation M351T) for quantitative analysis by LD–PCR and fluorescent capillary electrophoresis showing the relation between measured values (*y*-axis) and true values (*x*-axis) is displayed. On the basis of individual standard curves, a computer program permitting calculation of the size of mutant clones from measured values was established for all mutations included in the current panel.

To obtain positive controls for specific mutations in the *BCR–ABL* TK domain and to establish calibration curves for quantitative analysis, plasmids containing the point mutations of interest were generated. A *BCR–ABL* TK domain fragment of about 1 kb was amplified and cloned into a pGEMt vector (Promega, Mannheim, Germany). Presence of the wild-type *BCR–ABL* sequence was confirmed by direct sequencing in both directions. This plasmid served as a basis for specific mutagenesis within the *ABL* TK domain using the QuikChange II Site–Directed Mutagenesis Kit (Stratagene, CA, USA). Mixtures of wild-type plasmids and mutant plasmids were used to generate dilution series including the following dilution steps: 0, 1, 5, 10, 20, 30, 40, 50, 60, 70, 80, 90 and 100%. Individual dilution series were analyzed in triplicates as a basis for the establishment of standard curves. An exemplary standard curve is shown in Figure 2. The standard curves were used to convert the values measured by LD–PCR to percentages of cells displaying a

specific mutation, to account for the differences between measured and true values. A statistical program specifically designed for the present study was employed for the evaluation of measurements in CML patients. Initial statistical evaluation was based on independent analysis of LD–PCR detection systems for three different mutations (T315I, E250G, Y253F). For each detection system, three dilution series $d_k$ were produced at levels $x = 0,0.1,0.2,0.3,0.4,0.5,0.6,0.7,0.8,0.9$, 0.95, 0.99 and 1. For each dilution series, three LD–PCR analyses $l_{j(k)}$ were conducted independently and each LD–PCR assay was subjected to two independent measurements by fluorescent capillary electrophoresis $a_{i(j(k))}$. Denoting the measurements with y, the following model was applied: $y_{ijk} = f(x) + d_k + l_{j(k)} + a_{i(j(k))} + \varepsilon_{ijk}$, where $f(x)$ is a non-linear function, the factors $d_k$, $l_{j(k)}$ and $a_{i(j(k))}$ are nested, and $\varepsilon_{ijk}$ is the error term. Analysis was restricted to polynomial regression, where $f(x)$ is a polynomial of maximal degree four. To assess the influence of factors possibly affecting quantitative measurements, we performed analysis of covariance using SAS PROC GLM (SAS Institute Inc., SAS 9.1.3 Help and Documentation, Cary, NC, USA: SAS Institute Inc., 2000–2004). After ensuring that neither the dilution series $d_k$ nor the fragment analysis $a_{i(j(k))}$ exert significant effects, we took the average over measurements by fluorescent capillary electrophoresis and then considered the simplified model $y = f(x,\beta) + \varepsilon$, where the term $\varepsilon$ contains all random errors due to dilution series and LD–PCR. Based on our analysis, the error resulting from dilution series can be regarded as negligible compared to the error derived from the LD–PCR. The computation of confidence intervals of $x$ was performed in Matlab using polynomial regression as described.[13] Biostatistical calculation of a total of 648 data points generated for the three mutations indicated, identified the LD–PCR itself as the only statistically relevant variable affecting quantitative analysis. Based on the evaluation of this model, the standards for quantitative analysis of all other mutations were established according to a statistical design based on the remaining variable determined as relevant. Hence, for every other mutation, 36 data points were collected to establish standards for quantification.

The LD–PCR reactions were performed using the thermocycler AB-9600 (Applied Biosystems(AB), Foster City, USA). For LD–PCR, the following reaction components were mixed on ice: 0.5 μl probe mix (0.8 μl from 1 μM concentrations of each Lig-WT probe, Lig-MUT probe and Hyb probe in 200 μl TE buffer), 1.5 μl of MLPA buffer (MRC Holland, Amsterdam, The Netherlands) and 50 ng of the *BCR–ABL* PCR product (determined by photometric measurement). The *BCR–ABL* products were derived from patient specimens (see below) or from calibration plasmid samples generated by one or two rounds of PCR amplification.[14] To prevent formation of secondary structures within the target or probe sequences and self-hybridization of the probes, which might affect the efficiency of the assay, the reactions were subjected to a hot-start at 98 °C for 5 min. For specific binding of the Lig and Hyb probes, the reaction was cooled down to the appropriate hybridization temperature (Table 1). In contrast to the original MLPA technology, the hybridization time of the LD–PCR was shortened from 16 hours to one minute. This change allowed rapid processing and accurate quantification of mutated cell clones in patient samples, while the sensitivity of detection remained unaffected. Subsequently, the reactions were placed at 54 °C for the addition of ligation reagents: 32 μl of ligation components including 3 μl Ligase-65 buffer A, 3 μl Ligase-65 buffer B, 1 μl Ligase 65 (all MRC Holland) and 25 μl water were added to the reaction. The ligase reactions were performed for 15 min at 54 °C, followed by inactivation of the enzyme for 5 min at 98 °C and cooling of the samples to 4 °C. Ten μl of this reaction were mixed with 4 μl 10 × SALSA PCR buffer (MRC Holland) and 26 μl sterile water. After heating to 60 °C to prevent non-specific primer annealing, the reaction was supplemented with 10 μl of the PCR-mix containing 2 μl FAM-labelled SALSA PCR primers, 2 μl SALSA enzyme dilution buffer, 0.5 μl SALSA polymerase (all MRC Holland) and 5.5 μl sterile water. Subsequently, the appropriate amplification program was performed, as described.[12] The possible occurrence of false-positive LD–PCR results was controlled (and successfully excluded) by testing of multiple *BCR–ABL* products lacking mutations in the *ABL* TK domain.

Quantitative analysis was performed on the ABI PRISM 3100-Avant Genetic Analyzer (AB). The PCR product obtained from the LD–PCR reaction was diluted with sterile water at 1:50, and 1 μl of the dilution was mixed with 0.3 μl GeneScan-500 ROX Size Standard (AB) and 9 μl Hi-Di Formamide (AB). Denaturation was performed at 94 °C for 3 min, and the reaction was subsequently cooled to 4 °C. The sample was injected into a 36 cm capillary column containing the high performance polymer POP-4 (AB) (10 s injection time, 1 kV injection voltage and 15 kV electrophoresis voltage).

Results were analyzed using the ABI PRISM GeneScan Analysis software 3.7 (AB). The PCR amplicons of the WT and MUT products differed in length by 6 bp. Peak heights of the WT and the MUT products were determined, and the ratio calculated by the following formula: % MUT = (peak height of MUT product/$\sum$ peak heights of MUT + WT products) × 100. For each mutation, calibration curves were established by preparing dilution series of quantified plasmids containing WT and MUT sequences, as indicated above.

All LD–PCR systems established were tested for the limits of detection and quantitative accuracy by using the appropriate plasmid dilution series. For several LD–PCR detection systems, the lowest dilution step analyzed (1%) could be reproducibly detected and clearly differentiated from the WT sample. However, as indicated by initial testing, reliable distinction between WT and MUT targets at levels below 5% has been difficult for some of the mutations included in the current panel, because of the presence of cross-reactivity inherent in individual detection systems. The observation of cross-reactivity was apparently related to the nucleotide composition at and near the mutant site. For example, mutations representing a G/C substitution tended to show a higher potential for non-specific binding to the target sequence than other non-matching bases. In some instances, problems associated with the target sequence could be overcome by designing LD–PCR systems targeting the opposite DNA strand, as performed for example, for the mutations Q252H-C and Q252H-T (Table 1). In practice, most detection systems lacking cross-reactivity actually reach a detection limit of 1%, while the assays displaying the highest levels of cross-reactivity observed only permit reliable identification of mutant cells at levels of $\geqslant 5\%$. Hence, the overall limit of detection for the mutations included in the study can be regarded as being in the range between 1–5%. The detection assays are highly reproducible, with an s.d. of ±2%. The confidence intervals (95% CI) of quantitative analysis were calculated on the basis of serial testing of plasmid standards (see above) and were shown to be in a range of ±5%. We propose that two subsequent measurements of mutant clones in a patient, indicating an increasing or decreasing clone size, may be regarded as a true change if the confidence intervals of the measured values do not overlap. The application of this extremely stringent criterion should prevent the

**Table 2** Mutations and sizes of mutant clones in clinical specimens

| *Patient* | *Result direct sequencing* | *Nucleotide changes* | *Result LD–PCR (%MUT)* |
|---|---|---|---|
| 1 | G250E | GGG→GAG | 100 |
| 2 | Y253H | TAC→CAC | 100 |
| 3 | G250E | GGG→GAG | 100 |
| 4 | M351T | ATG→ACG | 14 |
| 5 | M244V | ATG→GTG | 97 |
| 6 | G250E | GGG→GAG | 51 |
| 7 | M351T | ATG→ACG | 100 |

Displayed are the types of mutation detected by sequence analysis in seven CML patients with suboptimal response to treatment with imatinib and the relative sizes of mutant clones determined at individual time points by LD–PCR and fluorescent capillary electrophoresis.

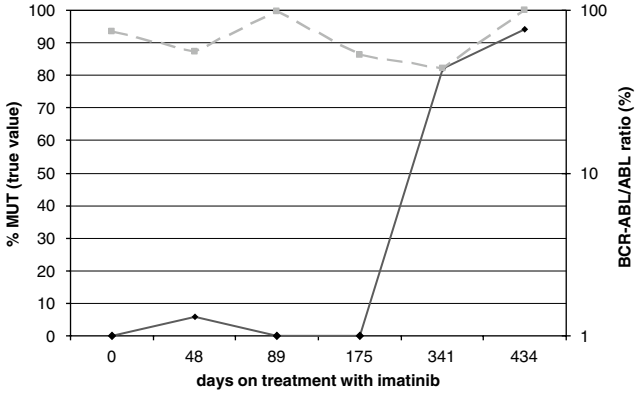


**Figure 3** Kinetics of a mutant clone during treatment with imatinib. Serial LD–PCR analysis of peripheral blood (PB) specimens in a CML patient carrying a *BCR–ABL* clone with the mutation M351T is shown (solid curve). The analysis revealed rapid proliferation and ultimate dominance of the mutant clone starting approximately 1 year after initiation of treatment with imatinib. The levels of *BCR–ABL* transcripts in PB at corresponding time points are shown (dashed curve).

misinterpretation of variability inherent in the technique. According to this restriction and the confidence intervals calculated for individual LD–PCR detection systems, it is possible to consider elevations or decreases by 10% as true changes in the size of mutant clones. A computer program based on an algorithm for the calculation of confidence intervals for all LD–PCR detection systems has been established. The program permits automated quantitative assessment of mutant clones on the basis of values measured by LD–PCR. The implementation of this tool greatly facilitates the analysis of clinical specimens. The program is available upon request (Sandra.Preuner@ccri.at).

After careful standardization of all LD–PCR assays using appropriate plasmid constructs, applicability of the technique in the clinical setting was assessed in a pilot study. Peripheral blood specimens derived from 30 CML patients with suboptimal response and seven control patients with adequate response to treatment with imatinib were tested. All patients studied were initially screened for the presence of mutations in the entire TK domain by direct bidirectional sequencing of appropriate PCR products, as described.[14] The results served as a basis for subsequent quantitative analysis by LD–PCR. Seven patients with suboptimal response to imatinib revealed four different mutations including M244V, Y253H, G250E and M351T (Table 2). Other specimens analyzed had no evidence of mutations in the TK domain at the sensitivity level of the sequencing method. LD–PCR analysis confirmed the findings and facilitated assessment of the proportion of mutant cells in peripheral blood specimens (Table 2). To determine the applicability of LD–PCR analysis to the monitoring of the proliferation kinetics of mutant clones, six consecutive peripheral blood samples of a CML patient carrying a M351T mutation were analyzed. In this proof of principle experiment, serial LD–PCR analysis revealed expansion of the mutant clone during the course of treatment (Figure 3).

It should be pointed out that the LD–PCR method was not designed for broad mutational screening. The technique is appropriate for rapid search for a limited number of specific mutations of interest, and for quantitative monitoring of cell clones carrying one or more known mutations. It appears that the method presented may be particularly useful in the following clinical circumstances:

(a) In the screening for individual mutations of interest. For example, in patients resistant to imatinib, where the presence of a particular mutation (for example, the T315I), should be excluded prior to switching to a second generation inhibitor.
(b) In the screening for a limited number of specific mutations in patients treated with a second generation TK inhibitor, in whom the spectrum of relevant mutations appears to be restricted.
(c) In the quantitative surveillance of the size of mutant clones during treatment with any TK inhibitor in patients in whom the presence of a mutation had been detected by other approaches (for example, sequencing). The LD–PCR would then allow the monitoring of the response of individual mutant clones to current treatment.

The results of the pilot study performed indicate that the LD–PCR technique presented has the potential to be instrumental in the clinical setting. The detection assays are robust and provide rapid quantitative assessment of mutant clones. The current LD–PCR detection panel covering 18 common mutations can be easily extended to any other mutation of interest. Prospective testing of the LD–PCR technique is required to assess the possible benefit of molecular monitoring of mutant clones in the clinical management of CML patients.

S Preuner[1], D Denk[1], F Frommlet[2], M Nesslboeck[1] and T Lion[1]
[1]*Division of Molecular Microbiology and Development of Genetic Diagnostics, Children's Cancer Research Institute (CCRI), Vienna, Austria and*
[2]*Department of Statistics and Decision Support, University of Vienna, Austria*
*E-mail: Thomas.Lion@ccri.at*

## References

1 Quintas-Cardama A, Kantarjian H, Cortes J. Flying under the radar: the new wave of BCR-ABL inhibitors. *Nat Rev Drug Discov* 2007; **6**: 834–848.
2 Hehlmann R, Hochhaus A, Baccarani M. Chronic myeloid leukaemia. *Lancet* 2007; **370**: 342–350.
3 Hochhaus A, Kantarjian HM, Baccarani M, Lipton JH, Apperley JF, Druker BJ *et al.* Dasatinib induces notable hematologic and cytogenetic responses in chronic-phase chronic myeloid leukemia after failure of imatinib therapy. *Blood* 2007; **109**: 2303–2309.
4 Shah NP, Tran C, Lee FY, Chen P, Norris D, Sawyers CL. Overriding imatinib resistance with a novel ABL kinase inhibitor. *Science* 2004; **305**: 399–401.
5 Soverini S, Gnani A, Colarossi S, Castagnetti F, Palandri F, Giannoulia P *et al.* Philadelphia chromosome-positive leukemia

patients who harbour imatinib-resistant mutations have a higher likelihood of developing additional mutations associated with resistance to novel tyrosine kinase inhibitors. *Blood* 2007; **110** abstract [322].
6 Soverini S, Martinelli G, Rosti G, Bassi S, Amabile M, Poerio A *et al*. ABL mutations in late chronic phase chronic myeloid leukemia patients with up-front cytogenetic resistance to imatinib are associated with a greater likelihood of progression to blast crisis and shorter survival: a study by the GIMEMA Working Party on Chronic Myeloid Leukemia. *J Clin Oncol* 2005; **23**: 4100–4109.
7 Hughes T, Deininger M, Hochhaus A, Branford S, Radich J, Kaeda J *et al*. Monitoring CML patients responding to treatment with tyrosine kinase inhibitors: review and recommendations for harmonizing current methodology for detecting BCR-ABL transcripts and kinase domain mutations and for expressing results. *Blood* 2006; **108**: 28–37.
8 Willis SG, Lange T, Demehri S, Otto S, Crossman L, Niederwieser D *et al*. High-sensitivity detection of BCR-ABL kinase domain mutations in imatinib-naive patients: correlation with clonal cytogenetic evolution but not response to therapy. *Blood* 2005; **106**: 2128–2137.
9 Khorashad JS, Anand M, Marin D, Saunders S, Al-Jabary T, Iqbal A *et al*. The presence of a BCR-ABL mutant allele in CML does not always explain clinical resistance to imatinib. *Leukemia* 2006; **20**: 658–663.
10 Vivante A, Amariglio N, Koren-Michowitz M, Ashur-Fabian O, Nagler A, Rechavi G *et al*. High-throughput, sensitive and quantitative assay for the detection of BCR-ABL kinase domain mutations. *Leukemia* 2007; **21**: 1318–1321.
11 Nardi V, Raz T, Cao X, Wu CJ, Stone RM, Cortes J *et al*. Quantitative monitoring by polymerase colony assay of known mutations resistant to ABL kinase inhibitors. *Oncogene* 2008; **27**: 775–782, .
12 Schouten JP, McElgunn CJ, Waaijer R, Zwijnenburg D, Diepvens F, Pals G. Relative quantification of 40 nucleic acid sequences by multiplex ligation-dependent probe amplification. *Nucleic Acids Res* 2002; **30**: e57.
13 Lundberg E, De Mare J. Interval estimates in the spectroscopy calibration problem. *Scand J Statistics* 1980; **7**: 40–42.
14 Branford S, Hughes T. Detection of BCR-ABL mutations and resistance to imatinib mesylate. *Methods Mol Med* 2006; **125**: 93–106.